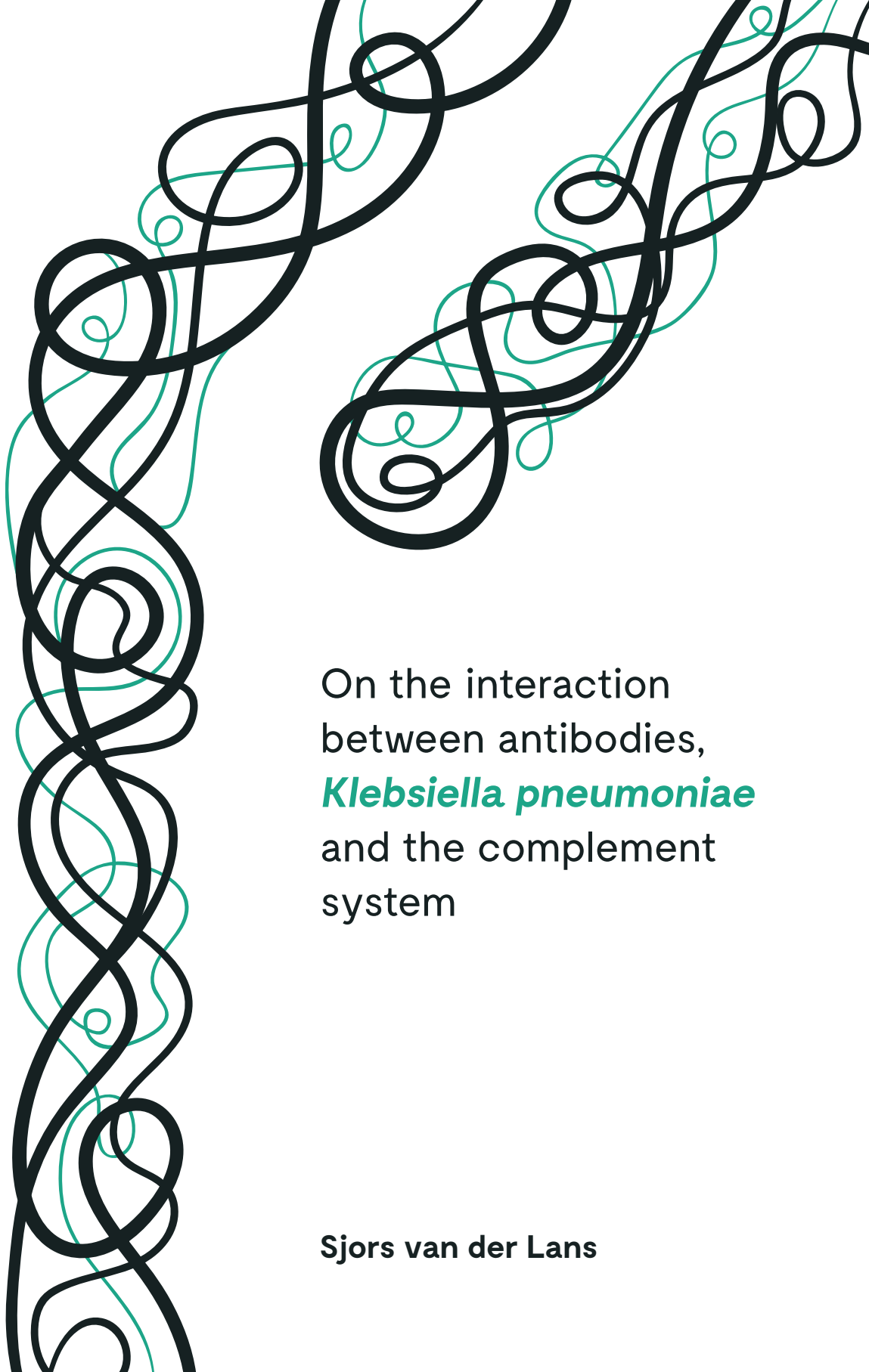

On the interaction between antibodies, *Klebsiella pneumoniae* and the complement system

Sjors van der Lans

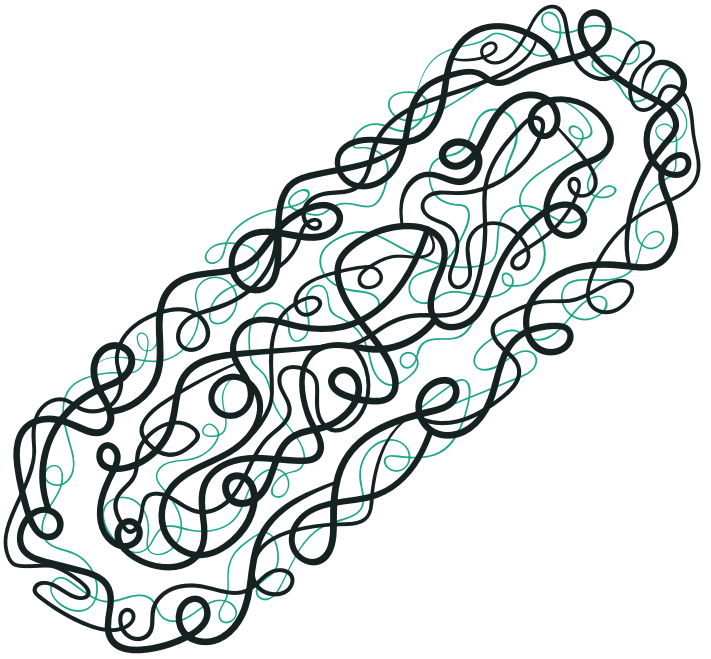

On the interaction between antibodies, *Klebsiella pneumoniae* and the complement system

Recognition is key

Sjors van der Lans

On the interactions between antibodies, Klebsiella pneumoniae and the complement system

PhD thesis, Utrecht University, the Netherlands

ISBN: 978-90-393-7624-9
DOI: 10.33540/2111

Author:	Sjors van der Lans
Cover design:	Jens Weidenaar
Layout and design:	Erwin Timmerman (persoonlijkproefschrift.nl) & Jens Weidenaar
Printing:	Ridderprint

Financial support for the printing costs of this thesis was kindly provided by Genmab B.V, Hycult Biotechnology B.V, the Netherlands Society of Medical Microbiology (NVMM) and the Royal Netherlands Society for Microbiology (KNVM), and Infection & Immunity Utrecht.

On the interactions between antibodies, *Klebsiella pneumoniae* and the complement system

Recognition is key

Over de interactie tussen antilichamen, *Klebsiella pneumoniae* en het complementsysteem

Herkenning is cruciaal

(met een samenvatting in het Nederlands)

Proefschrift

ter verkrijging van de graad van doctor aan de
Universiteit Utrecht op gezag van de
rector magnificus, prof. dr. H.R.B.M. Kummeling,
ingevolge het besluit van het college voor promoties
in het openbaar te verdedigen op

dinsdag 13 februari 2024 des middags te 4.15 uur

door

George Petrus Antonius van der Lans

geboren op 20 januari 1995
te Eindhoven

Promotoren
Prof. dr. S.H.M. Rooijakkers
Prof. dr. A.J.R. Heck

Copromotor
Dr. B.W. Bardoel

Beoordelingscommissie
Dr. A.J. McCarthy
Prof. dr. L.A. Trouw
Prof. dr. G. Vidarsson (voorzitter)
Prof. dr. R.J.L. Willems
Prof. dr. H.A.B. Wösten

Dit proefschrift werd mededmogelijk gemaakt met financiële steun van de Nederlandse Organisatie voor Wetenschappelijk Onderzoek (NWO) met een TTW-NACTAR beurs (nummer 16442, toegekend aan G.P.A. van der Lans, prof. dr. S.H.M. Rooijakkers en prof. dr. A.J.R. Heck) in samenwerking met Genmab B.V. (Utrecht, Nederland) en Hycult Biotechnology B.V (Uden, Nederland).

“...trúðu á mátt sinn ok **megin**...”

Hrólfs saga Kraka

...they put their trust in their own might and main...

From The Saga of King Hrolf Kraki, translated by prof. dr. Jesse L. Byock

Paranimfen:
G. Korsten, MSc
Dr. L. Aguinagalde Salazar

Table of content

Chapter 1

General Introduction

Sjors van der Lans

Klebsiella pneumoniae

Klebsiella pneumoniae is a Gram-negative bacterium that has been recognized as an important opportunistic human pathogen. *K. pneumoniae* primarily infects individuals with an impaired immune system such as neonates, elderly and immunocompromised patients[1–3], and may cause various types of infections including urinary tract infections, pneumonia, surgical-site infections and bloodstream infection. These infections are mostly nosocomial, as *K. pneumoniae* is able to spread between patients in hospitals via medical devices, e.g. catheters and ventilators, as well as via healthcare personnel [4]. Furthermore, *K. pneumoniae* can colonize the gastrointestinal tract, from where it can spread to other parts of the body to cause infection [5,6]. Besides hospital acquired infections, *K. pneumoniae* strains have emerged that are able to cause community acquired infections in adults with no apparent underlying diseases [7,8]. Infections with these hypervirulent *K.* pneumoniae strains often lead to pyogenic liver abscesses, endophthalmitis, meningitis and bloodstream infections [7–9]. These infections have a relatively fast disease progression, and high mortality and morbidity rates [10–12]. Hypervirulent strains are characterized by producing large amounts of extracellular polysaccharides resulting in a hypermucoviscous phenotype, and their strong ability to sequester iron [13–19]. Although most hypervirulent *K. pneumoniae* infections occur in South-East Asia, strains have been spreading to the rest of the world [20].

K. pneumoniae is notorious for the development and spread of antibiotic resistance. It has been reported that in 2021 over a third of all strains reported to the European Center for Disease Prevention and Control were resistant to at least one antibiotic, although large variation exists between countries (0% to 73.7%) [21]. *K. pneumoniae* strains have developed resistance to all major classes of antibiotics, and can employ various resistance mechanisms[21,22]. Most concerning has been the resistance to β-lactam antibiotics due to the expression of extended spectrum β-lactamases (ESBL), and development of carbapenem resistance [23]. Resistance genes are often plasmid-encoded, leading to rapid spread of antibiotic resistance. For example, between 2005-2015 carbapenem resistance increased from virtually non-existing to 40-60% of the clinical isolates being resistant in several European countries [23]. Plasmid carriage also makes it easy to accumulate resistance genes, as is exemplified by the report of a strain that carried over ten different β-lactamase genes [24]. Even more worrisome is the spread of antibiotic resistance from *K. pneumoniae* to other species, such as *Escherichia coli* [23,25]. *K. pneumoniae* strains that are (multi)drug resistant have to be treated with last-resort antibiotics, but unfortunately, resistance against compounds

such as colistin, and tigecycline has been observed as well [26–28]. Multidrug resistant strains are virtually impossible to treat, leading to high mortality and morbidity rates [29], and it has been reported that *K. pneumoniae* caused over 700.000 antibiotic resistance related deaths in 2019 alone [30]. The development of multidrug resistance among hypervirulent strains is of great concern, as such strains have been emerging in the last decade [31–33].

K. pneumoniae has several characteristics that allow it to cause infection. The ability to adhere itself to its extracellular environment plays a crucial role in both initiating and maintaining infections[34–36]. *K. pneumoniae* produces various adhesins that are used to attach itself to synthetic surfaces of medical devices, which facilitates the entrance of bacteria into patient's bodies [36]. After *K. pneumoniae* has entered the body, adhesins are involved in establishing infection by aiding in biofilm formation and promote adherence to epithelial surfaces [34,36,37]. During infections *K. pneumoniae* produces siderophores to sequester iron, which is essential for the metabolism of *K. pneumoniae*. Almost all strains can produce enterobactin, but humans are able to counteract this siderophore by producing lipocalin-2 as part of their innate immune defense [38]. Other siderophores such as yersiniabactin, salmochelin and aerobactin, have evolved to overcome such defenses. The importance of these siderophores for virulence is exemplified by the observation that hypervirulent strains express many more siderophores compared to non-infectious strains [14–19].

Evading recognition and activation by the immune system is very important for the infectious biology of *K. pneumoniae*, in which both lipopolysaccharides (LPS) and capsule, two major polysaccharide surface structures, play a crucial role (fig. 1). LPS is part of the outer leaflet of the outer membrane of Gram-negative bacteria, and is formed by membrane-embedded lipid A to which a long polysaccharide O-antigen chain is attached. The capsule forms a thick protective layer that protect the cell from antibacterial compounds [39–42]. The importance of both LPS O-antigen and capsule have been illustrated in murine infection models, where loss of either of these structures can substantially reduce the pathogenicity of *K. pneumoniae* [43–45]. In addition, genes involved in capsule expression, such as *rmpA* and *magA*, are strongly associated with hypervirulence of *K. pneumoniae* [46–48].

K. pneumoniae can express various O-antigens (O-types) and capsule polysaccharides (K-types). Over eight O-types have been described, and of these O1-, O2- and O3-

antigens are most associated with infections in human [49]. Strikingly, the over 70% of all ESBL-carrying strains belong to O1- and O2-strains, and over half of the carbapenem resistant strains express an O2-antigen [50]. Additionally, the majority of the hypervirulent strains express an O1 antigen [49]. *K. pneumoniae* is known to express over seventy different K-types, and many more have been predicted based on gene diversity [49]. The majority of the hypervirulent *K. pneumoniae* strains expresses either the K1 or K2 capsule, but no preference in capsule type has been observed among the non-hypervirulent clinical isolates[13,19,51–55]. Both the LPS O-antigen and capsule play an important role in the protection against the human complement system and phagocytes.

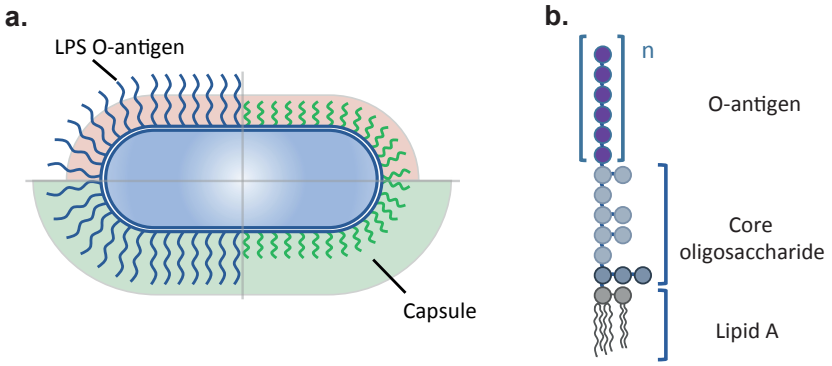

Figure 1| Major surface polysaccharides of *K. pneumoniae*

(**a**) *K. pneumoniae* expresses two major surface polysaccharides: lipopolysaccharide (LPS) O-antigen and capsule. The outer membrane of *K. pneumoniae* mainly consists of LPS, with the O-antigen extending to the extracellular environment. Capsule forms a thick polysaccharide matrix around the bacterial cell. Both the O-antigen and capsule can protect *K. pneumoniae* from the immune system by forming a barrier layer around the bacterium. *K. pneumoniae* can express various O-antigen (O) and capsule (K) types (indicated by variation in colors), that differ both in their molecular composition as well in their length and thickness. (**b**) LPS consists of a membrane embedded lipid A decorated with a core oligosaccharide and a long O-antigen polysaccharide chain consisting of repeating sugar moieties. Depending on the O-type and strain, the number of repeats my vary.

Classically, *K. pneumoniae* has been concerned to be a stealth pathogen, but in the last decades it has become apparent that *K. pneumoniae* has evolved mechanisms that actively interfere with the immune response. Studies in mice have revealed *K. pneumoniae* is able to manipulate cellular signal transduction pathways to reduce

the expression of NF-κB, leading to a decreased production of defensins and pro-inflammatory interleukins [56]. In addition, *K. pneumoniae* can enhance the production of the anti-inflammatory interleukin IL-10, thereby dampening the immune response [57]. Strikingly, capsule expression by *K. pneumoniae* seemed to be required in both NF-κB downregulation and IL-10 upregulation, as capsule mutants were no longer able to influence expression. Furthermore, *K. pneumoniae* has been described to infect and survive inside human macrophages by inducing the formation of intracellular compartments that do not fuse with lysosomes [57–59]. Finally, there is evidence that *K. pneumoniae* can attract monocytic myeloid-derived suppressor cells to the site of infection, which suppress inflammation, thereby preventing clearance of *K. pneumoniae* from the body [60].

The main immune evasion strategy of *K. pneumoniae* consists of preventing immune activation and recognition. To overcome these defenses, it is key that the immune system recognize *K. pneumoniae* once it enters the body. Antibodies play a major role in this process.

Antibody and B cell development

Antibodies, or immunoglobulins, play a key role in the immune recognition of bacteria, as they can bind to bacteria via their Fragment antibody binding (Fab) arms, and interact with the immune system via their Fragment crystallizable (Fc) tail. Antibodies consist of four polypeptide chains, two heavy (H) and two light (L) chains, that together form a heterotetrameric Y-shaped molecule (fig. 2a). The light chain consists of a variable (VL) and a constant (CL) domain, whereas the heavy chains consist of a variable (VH) and multiple constant domains (CH_1 CH_n). Antibodies have two Fab arms, each of which is formed by pairing of the VL and CL of a light chain with the VH and CH_1 of a heavy chain, which are connected via electrostatic interactions and disulfide bonds. Within this Fab arm the VH and VL both contain three complementarity-determining regions (CDRs) that together form the antigen binding site. The Fc domain is formed by pairing the remaining CH domains of the heavy chain with the CH domains of a second heavy-light chain pair. The two heavy chains are also connected via electrostatic interactions, as well as multiple disulfide bonds in the hinge region of the antibody, which separates the CH_1 from the CH_2 and the other CH domains. The constant domain sequences of the heavy chain determine the isotype of an antibody, which can be switched during B cell development. There are several isotypes (IgG1-G4, IgM, IgA-A2, IgD, and IgE),

which interact with different parts of the immune system, thereby determining the antibody's functionality.

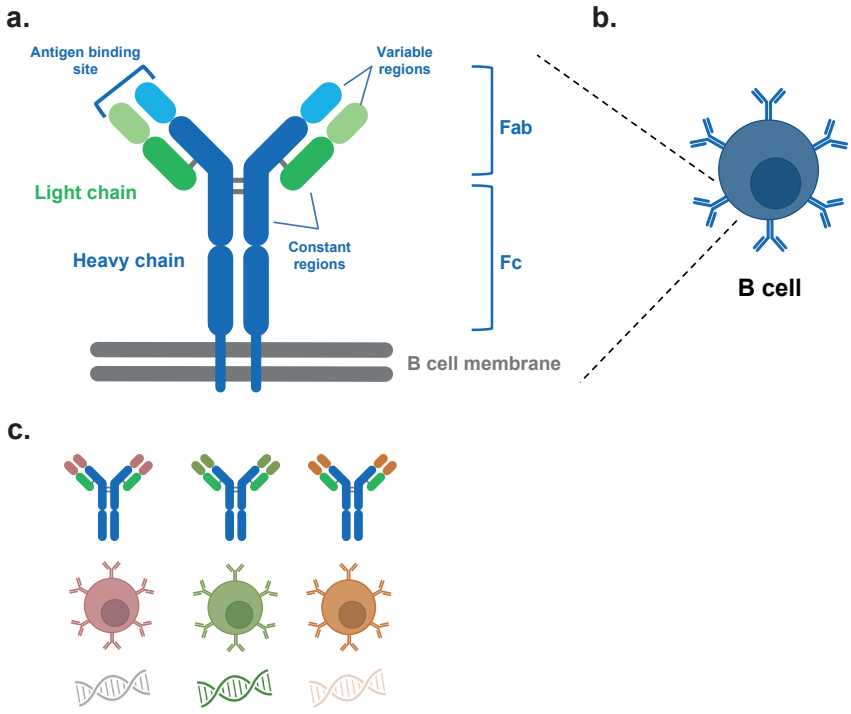

Figure 2| Antibody and B cell

(a) Antibodies consist of two heavy and light chains linked by disulfate bonds (gray). Both the heavy and light chain contain constant and variable regions. The variable regions of a heavy and light chain are unique for each antibody clone, and together form the antigen binding site. The paired heavy and light chains together form a single Fab arm. The constant regions of the heavy chains are shared between different antibodies of the same isotype and form the Fc region, which can be recognized by the immune system. **(b)** B cells can express membrane anchored antibodies on their surface as B cell receptors (BCR). B cells can bind their antigens via their BCRs, which leads to B cell activation. **(c)** During B cell development, genetic rearrangements occur in the DNA sequences coding for the variable region, leading to the formation of a unique variable region for each B cell clone. This results in antibodies with different antigen binding site, and different antigen specificities. Fab: Fragment antigen binding; Fc: Fragment crystallizable

The human body can generate a large variety of antibodies that recognize different antigens, as well as various antibodies that target the same antigen. This is achieved by varying the amino acid composition of the antigen binding site in the variable regions. This variation, as well as isotype switching, is generated during B cell development. B cell development starts in the bone marrow, where hematopoietic stem cells enter a process that leads to differentiation into a B cell [61]. During this process, the antibody's variable domains are formed by genetic rearrangement of variable (V), diversity (D), and joining (J) gene segments of the heavy chain, and V and J segments of the light chain. For the heavy chains 50 V, 27 D and 6 J segments can be recombined into a variable region. Light chains are encoded on two loci (κ and λ), of which one is selected during antibody development. For the κ-light chains, 44 V and 5 J segments can be recombined, and for λ-light chains 33 V and 5 J segments. During genetic recombination, one of each of these segments is selected, and fused to each other to form an antibody with a specific VDJ-VJ combination [62,63]. Based on V(D)J recombination alone, over three million different variable domains can be expressed, allowing the generation of antibodies recognizing a wide variety of antigens (fig. 2c) [61]. When the antibody is successfully recombined, the still immature B cell expresses the antibody bound to its surface as a B cell receptor (BCR; fig. 2b) and migrates from the bone marrow to the spleen. Here it finishes maturation to become a mature naïve B cell that expresses its germline encoded naïve antibody as both IgM and IgD BCRs, and re-enters circulation.

Naïve BCRs have an inherent affinity for certain antigens, and during a bacterial infection, some naïve B cells are able to recognize bacterial antigens via their BCR. Due to the diversity in BCRs, various bacterial antigens can be recognized by different B cells clones. Antigen recognition leads to activation of these B cells, resulting in a polyclonal B cell response. Activated B cells migrate to the lymph nodes, where they undergo initial clonal expansion. Some of the B cell clones become IgM secreting plasma cells, whereas others migrate to germinal centers. In these germinal centers, several genetic recombinations of the antibody take place. Antibodies can switch isotype via class switch recombination, in which the CH domain sequences of one isotype are replaces for those of another isotype, resulting is the expression of a different Fc tail. Furthermore, an antibody's affinity for its antigen can be increased by affinity maturation, a process during which the sequences of the antigen binding sites of the variable regions are randomly altered through somatic hyper mutations. These mutations primarily occur in the CDR regions, which are essential for antigen binding. Subsequently, B cells expressing antibodies with greater affinity are selected [64,65].

This leads to an increase in antibody affinity, as well as diversification of the antibody repertoire. After these processes have taken place, some of the B cells develop into plasmablasts specialized in producing antibodies in large quantities, whereas others develop into memory B cells [66]. Most plasmablasts are short lived but some migrate to the bone marrow where they can remain for extended periods of time as long-lived plasma cells that produce protective antibodies. In contrast to plasmablasts and -cells, memory B cells do not secrete antibodies, but instead express them as surface-bound BCRs. Memory B cells keep circulating throughout the body, and during a re-infection can bind their bacterial antigen upon a second encounter. This leads to activation, proliferation, and differentiation of the memory B into antibody secreting plasmablasts, allowing a fast antibody response [61].

Complement and neutrophil activation by antibodies that recognize *K. pneumoniae*

Antibodies play an important role in the immune response by activating the complement system and neutrophils[67,68]. The complement system is part of the innate immune system and consists of a family of soluble proteins that form a protective cascade in blood and other body fluids. Complement can be activated via three distinct routes on bacteria: the classical pathway (fig. 3a), the lectin pathway and the alternative pathway. Although these pathways are initiated via different mechanisms, they all lead to the formation of surface-bound C3convertases that cleave C3 into C3a and C3b. The C3a peptide is released, whereas C3b covalently attaches to the bacterial cell surface. When the local surface densities of C3b are high enough, C3b associates with the C3-convertases to form C5-convertases. The cleavage of C5 leads to the release of the C5a peptide, and the formation of the membrane attack complex (MAC) by association of C5b with C6, C7, C8 and multiple C9 proteins. MAC can form a pore in the outer membrane of Gram-negative bacteria, leading to direct killing of bacteria[69].

The classical pathway can be activated by IgG and IgM antibodies (fig. 3a). After binding, these antibodies recruit the classical pathway C1 complex, which can interact with the Fc-domains of IgG and IgM. This leads to C1 activation, initiating the formation of C3-convertases and starting the complement cascade. Importantly, the C1 complex has six Fc-binding domains that can interact with six Fc domains [70–72]. In the last decade, it has become apparent that antibodies need to form multimeric binding platforms for efficient C1 binding and complement activation (fig. 3b) [71]. IgM does this naturally, as it is expressed as a covalently linked pentamer onto which C1 can

efficiently dock, making IgM a very potent complement activator [70]. IgG is expressed as a monomer but upon binding of a bacterial surface, six IgG molecules can associate to form a hexameric C1 binding platform [71,72]. Hexamerization efficiency differs per IgG subclass, resulting in differences in complement activation potential between different IgG subtypes[71–73].

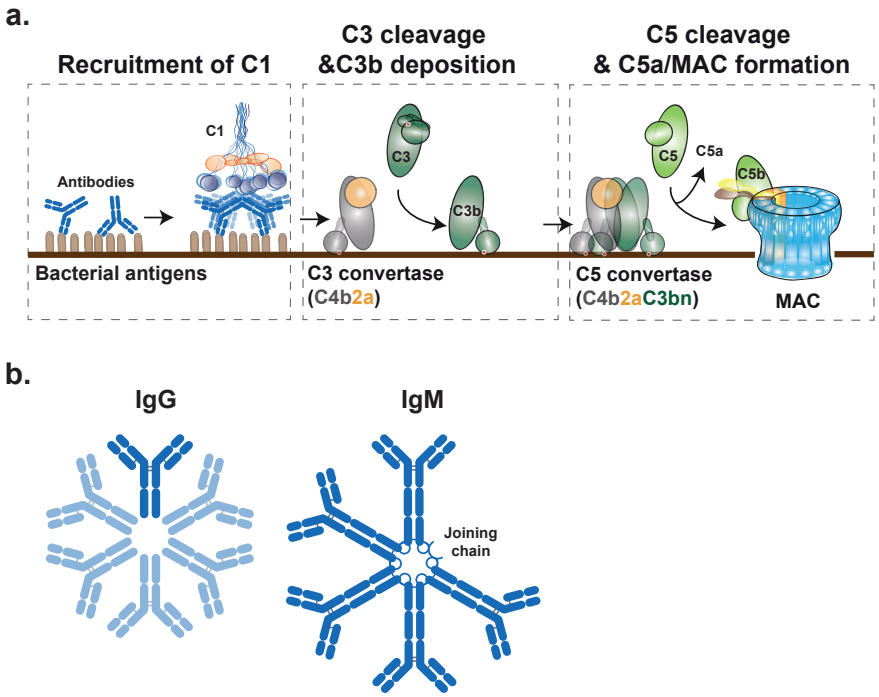

Figure 3| The classical complement pathway

(**a**) To initiate complement activation, bacteria need to be recognized by the complement system. This can occur via the classical pathway, when bacteria are bound by IgG or IgM antibodies. These antibodies can be recognized by the C1 complex, leading to the initiation of the complement pathways and the formation of C3-convertases that convert C3 into membrane bound C3b and soluble C3a. Once the density of C3b is high enough, C3b associates with C3-convertases to form C5-convertases. These convert C5 into C5b and C5a, which is released. Generation of C5b initiates the formation of the membrane attack complex (MAC), which can form lethal pores in the outer membrane of Gram-negative bacteria (**b**) IgG is expressed as a monomer whereas IgM is expressed as a covalently linked pentamer. Upon binding of a bacterial surface, six IgG molecules can associate to form a hexamer. Surface-bound IgG hexamers and IgM pentamers can interact with the six Fc-binding domains of the C1 complex for efficient C1 binding.

Antibodies also play a prominent role in the activation of neutrophils, which form an important part of the cellular immune defense against invading pathogens. These highly abundant leukocytes circulate through the bloodstream, from where they can rapidly migrate to the site of infection[74]. Recognition of bacteria by neutrophils leads to the induction of various effector responses, such as degranulation to release antimicrobial compounds and reactive oxygen species, as well as phagocytic uptake and intracellular killing of bacteria (fig. 4) [68,74]. Both antibody binding and antibody-mediated complement deposition aids in recognition of bacteria by neutrophils, as neutrophils express Fc-receptors as well as complement receptors (CR) that recognize antibodies and complement components, respectively, on the bacterial surface [68,74,75]. Neutrophils are also able to recognize C3a and C5a, which are released during complement activation on bacteria. These cleavage product function as strong chemoattractants, guiding neutrophils to the site of infection. Recognition of C5a also primes neutrophils to respond quickly as soon as bacteria are encountered. This involves morphological changes, upregulation of surface expression of CR3, and preparing for degranulation and phagocytosis [75–77]. The interactions between neutrophils and bacteria have been reviewed in detail elsewhere [74,78].

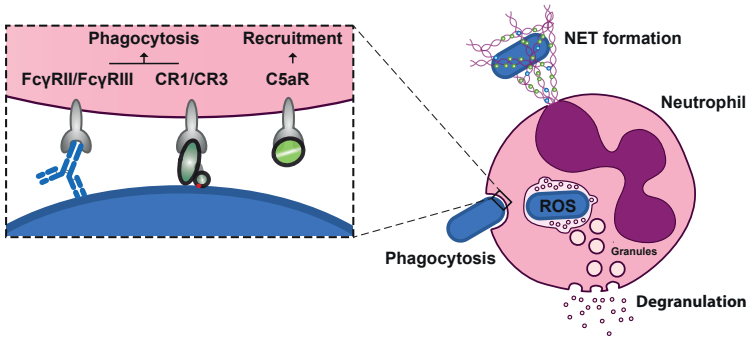

Figure 4| Neutrophil activation and effector functions

Neutrophils are able to recognize bacteria that are opsonized with antibodies and complement components via their Fc-receptors and complement receptors, respectively. Furthermore, released C5a during complement activation on bacteria activates neutrophils and stimulates them to migrate to the site of infection. Once neutrophils encounter and recognize a bacterium, various effector mechanisms can be initiated, such as degranulation to release antimicrobial compounds in the extracellular environment, as well as phagocytosis and intercellular killing of bacteria.

Both complement and neutrophils play an important role in clearance of *K. pneumoniae*. Complement and neutrophil deficient mice are more susceptible to *K. pneumoniae* [45,79], and patients with neutropenia have increased risk to *K. pneumoniae* infection [80,81]. However, virulent *K. pneumoniae* strains have developed mechanisms to counteract both complement and neutrophils, in which the LPS O-antigen and capsule play a prominent role. The protective properties of the O-antigen against complement have been shown in *K. pneumoniae* strains the lack the O-antigen. Genetic deletion of the O-antigen can lead to increased complement deposition on the bacterial surface, and sensitized *K. pneumoniae* mutants to MAC-mediated killing [82–84]. The length of the O-antigen is important for the protection against complement, with longer O-antigen being more protective [84]. As the O-antigen polysaccharide extends from the bacterial membrane, it can shield underlying surface structures from recognition by complement components, thereby preventing complement activation on *K. pneumoniae* [85,86]. Furthermore, activation of complement at the extremities of long O-antigen chains leads to incorrect localization of C3b [82,87]. This can prevent the MAC from reaching the bacterial outer membrane, and even cause release of MAC components from the bacterium [82,88]. The O-antigens of the various O-types differ can differ both in length and composition, which can influence complement sensitivity. It has been shown that strains expressing the O1-antigen, which is longer than the O2-antigen, are more resistant to complement-mediated killing compared to O2-antigen expressing *K. pneumoniae* [50,84]. Other modifications of the O-antigen may influence the complement sensitivity as well [89], but unfortunately this is still an understudied topic.

Capsule has also been shown to protect against complement, as loss of capsule can sensitize complement resistant *K. pneumoniae* to MAC-mediated killing [44,46,90,91]. Capsule can play various roles in the protection. It has been shown to prevent complement components from reaching the bacterial membrane after complement has been activated, whereas in other cases capsule prevents recognition by the complement system altogether [82]. These differences could be attributed to variations in capsule composition. Several capsule (K-)types have repeatedly been reported to promote serum resistance, including K1, K10 and K16 [92–94]. For other types, the relation to complement resistance is not always clear. For instance, K2, K7 and K21 were protective against complement [95], whereas in other studies they were not [94]. This suggests that other factors besides capsule type might be at play as well, such as the amount of capsule produced by individual bacteria. This is supported by the observations that *K. pneumoniae* strains that produce less capsule show an

increased C3b deposition on their surfaces [91,96]. A thicker capsule can better shield the bacterial outer membrane and its associated antigens. Chemical repression of capsule production demonstrated that decreased capsule production enhanced monoclonal antibody binding to the LPS core or O-antigen in a dose-dependent manner [92,93]. Similar results have been obtained for *K. pneumoniae* strains which had a reduced capsule production due to genetic modifications [82,95]. The capsule can also shield surface-bound antibodies and complement components from recognition by neutrophils, thereby preventing their activation. This has been highlighted by the various observations that loss of capsule leads to increased phagocytosis by neutrophils [46,97,98] and that highly capsulated strains are more resistant against phagocytosis[46,99]. Capsule can also more actively interfere with neutrophil activation, as sialic acid present in the capsule polysaccharide of some K-types can activate the SIGLEC9 inhibitory immune receptor, thereby preventing neutrophil activation and subsequent phagocytosis [100].

Besides providing protection, LPS and capsule are also prominent targets for antibodies and complement. Antibodies targeting the capsule or the O-antigen can induce opsonophagocytosis [50,101–104]. Furthermore, it has been described that MAC-mediated killing and phagocytosis works best in the presence of both surface targeting antibodies and the complement system [102,103,105,106]. Various studies that have focused on the contribution of antibodies to complement and neutrophil activation, have shown that LPS and capsule can be drivers of activation as well as defense mechanisms. Other surface structures, such as fimbriae, could also serve as targets, although differences in recognition have been observed between different strains [107,108]. These differences might be due to variations in capsule and O-antigen expression between *K. pneumoniae* strains. Another key factor is that most studies use either isolated polyclonal antibodies or immune sera as their antibody source [86,91,92,94,97,100–102,105,109–111]. Due to the polyclonal nature of these sources their antibody composition can vary tremendously. Furthermore, using animal-derived antibodies to study human immune activation can have its complications. Therefore, it would be better to study interaction between antibodies, *K. pneumoniae* and the immune system by using human monoclonal antibodies. This would not only broaden our current understanding but might also pave the way towards the development of therapeutic antibodies to treat *K. pneumoniae* infections.

Discovery of antibodies against *K. pneumoniae*

Several methods have been developed to obtain monoclonal antibodies. Some of these utilize the B cell's ability to produce antibodies. B cells can be stimulated to produce antibodies *ex vivo* but can only be kept in culture for a short period of time. Various solutions to this problem have been developed. One of the first methods to obtain monoclonal antibodies has been the generation of hybridomas, where B cells are fused with immortal myeloma cells, resulting in an immortal antibody producing hybrid cell [112]. Clones that produce antibodies with the correct characteristics can be selected and cultured for extended periods of time. Several other techniques have been developed to immortalize B cells, including Epstein-Barr virus-induced immortalization, as well as genetic manipulation of B cells [113,114]. The disadvantage of these techniques, however, is the relatively low efficiency.

Artificial screening methods, such as phage display and yeast display, have been developed to screen for interesting antibodies on a large scale [115,116]. These techniques are based on generating large libraries of vector organisms that express many different antibodies on their surfaces, which can be used to screen antibody sequences from libraries of sequenced human antibody repertoires, as well as further develop a known antibody by screening various sequence variants. Although these screening methods are very powerful, they require the expression of antibodies by microorganisms in which antibody folding and post-translational modifications are not always correct[117].

In the last decade it has become possible to extract antibody sequences directly from primary material. During this process, it is essential to keep the heavy and light chain information paired since these are both needed to form the antigen binding site. This can be achieved by single cell sorting of B cells and processing them individually. Sorted plasmablasts, for instance, can be stimulated to produce antibodies on a small scale [118,119]. Cells that produce antibodies with the correct specificities can be selected and sequenced via reverse transcription (RT-) PCR [120]. In this process the mRNA coding for the heavy and light chains is converted into complementary (c)DNA, which is amplified and can be sequenced. Furthermore, the cDNA can be cloned into expression vectors for recombinant antibody expression. Selecting antibodies from plasmablast can be laborious, as only a small fraction of all cultures plasmablast will produce the desired antibody. Therefore, it is advantage to first select antigen-specific B cells. In contrast to plasmablast, memory B cells express their antibodies on their surfaces as B cell receptors (BCR), and memory B cells that bind fluorescently labelled

antigens via their BCRs can be single cell sorted [121]. Subsequently, via RT-PCR, cloning, sequencing, and recombinant expression, antibodies can be tested for their antigen specificity as well as functionality.

Several human monoclonal antibodies targeting *K. pneumoniae* have been identified, via various approaches. The majority of these antibodies have been selected using isolated O-antigen polysaccharides, which has resulted in various high affinity antibodies that target the O1-, O2, or O3-antigen [50,121]. Some of these antibodies can activate the immune system. But to get a better understanding of the interaction between antibodies, *K. pneumoniae* and the immune system, additional antibodies that target other antigens need to be studied as well. This would require identification of new antibodies with other antigenic targets. And as complement activation needs to occur on the bacterial surface, identification should be focused on antibodies that recognize surface antigens. But the surface of *K. pneumoniae* contains many different antigens, and it remains largely unknown which of these antigens serves as a good target for complement activating antibodies. In order to determine what makes certain antibodies potent immune activators, it is important to select antibodies without having a bias towards a preselected antigen.

Aim of this thesis

In this thesis, we aimed to investigate the human immune responses against *K. pneumoniae*, focusing on antibody-dependent complement activation induced by antibodies on *K. pneumoniae*. We wanted to study how complement is activated by antibodies generated by healthy individuals, and explore antibody responses in patients that suffered *K. pneumoniae* infections. Studying antibody-mediated complement activation using polyclonal antibodies can be complicated due a large variety in antibody clones. For that reason, we developed a novel approach to identify human monoclonal antibodies that recognize *K. pneumoniae* surface antigens to study antibody-mediated complement activation in detail.

References

1. Boyd, A. R. & Orihuela, C. J. Dysregulated inflammation as a risk factor for pneumonia in the elderly. *Aging and Disease* **2** (2011)
2. Afroza, S. Neonatal sepsis-a global problem: an overview. *Mymensingh medical journal* **15** (2006).
3. Krawczyk, B., Wysocka, M., Michalik, M. & Gołębiewska, J. Urinary tract infections caused by *K. pneumoniae* in kidney transplant recipients – epidemiology, virulence and antibiotic resistance. *Frontiers in Cellular and Infection Microbiology* **12** (2022).
4. Jarvis, W. R., Munn, V. P., Highsmith, A. K., Culver, D. H. & Hughes, J. M. The epidemiology of nosocomial infections caused by *Klebsiella pneumoniae*. *Infection Control* **6** (1985).
5. Siu, L. K., Yeh, K. M., Lin, J. C., Fung, C. P. & Chang, F. Y. *Klebsiella pneumoniae* liver abscess: A new invasive syndrome. *The Lancet Infectious Diseases* **12** (2012).
6. Gorrie, C. L. *et al.* Gastrointestinal carriage is a major reservoir of *klebsiella pneumoniae* infection in intensive care patients. *Clinical Infectious Diseases* **65** (2017).
7. Liu, Y. C., Cheng, D. L. & Lin, C. L. *Klebsiella pneumoniae* liver abscess associated with septic endophthalmitis. *Arch. Intern. Med.* **146** (1986).
8. Cheng, D. L., Liu, Y. C., Yen, M. Y., Liu, Y. C. & Wang, R. S. Septic metastatic lesions of pyogenic liver abscess: their association with *Klebsiella pneumoniae* bacteremia in diabetic patients. *Arch. Intern. Med.* **151** (1991).
9. Fang, C. T. *et al. Klebsiella pneumoniae* genotype K1: An emerging pathogen that causes septic ocular or central nervous system complications from pyogenic liver abscess. *Clinical Infectious Diseases* **45** (2007).
10. Wang, J. H. *et al.* Primary liver abscess due to *Klebsiella pneumoniae* in Taiwan. *Clinical Infectious Diseases* **26** (1998).
11. Liu, Y. M. *et al.* Clinical and molecular characteristics of emerging hypervirulent *Klebsiella pneumoniae* bloodstream infections in mainland China. *Antimicrob. Agents Chemother.* **58** (2014).
12. Ko, W. C. *et al.* Community-acquired *Klebsiella pneumoniae* bacteremia: Global differences in clinical patterns. *Emerg. Infect. Dis.* **8** (2002).
13. Shon, A. S., Bajwa, R. P. S. & Russo, T. A. Hypervirulent (hypermucoviscous) *Klebsiella pneumoniae*: A new and dangerous breed. *Virulence* **4** (2013).
14. Hsieh, P. F., Lin, T. L., Lee, C. Z., Tsai, S. F. & Wang, J. T. Serum-induced iron-acquisition systems and TonB contribute to virulence in *Klebsiella pneumoniae* causing primary pyogenic liver abscess. *Journal of Infectious Diseases* **197** (2008).
15. Bachman, M. A. *et al. Klebsiella pneumoniae* yersiniabactin promotes respiratory tract infection through evasion of lipocalin 2. *Infect. Immun.* **79** (2011).
16. Podschun, R., Sievers, D., Fischer, A. & Ullmann, U. Serotypes, hemagglutinins, siderophore synthesis, and serum resistance of *Klebsiella* isolates causing human urinary tract infections. *Journal of Infectious Diseases* **168** (1993).
17. El Fertas-Aissani, R., Messai, Y., Alouache, S. & Bakour, R. Virulence profiles and antibiotic susceptibility patterns of *Klebsiella pneumoniae* strains isolated from different clinical specimens. *Patho. Bio.* **61** (2013).
18. Vernet, V. *et al.* Virulence factors (aerobactin and mucoid phenotype) in *Klebsiella pneumoniae* and *Escherichia coli* blood culture isolates. *FEMS Microbiol. Lett.* **130** (1995).
19. Yu, W. L. *et al.* Comparison of prevalence of virulence factors for *Klebsiella pneumoniae* liver abscesses between isolates with capsular K1/K2 and non-K1/K2 serotypes. *Diagn. Microbiol. Infect. Dis.* **62** (2008).
20. Fierer, J., Walls, L. & Chu, P. Recurring *Klebsiella pneumoniae* pyogenic liver abscesses in a resident of San Diego, California, due to a K1 strain carrying the virulence plasmid. *J. Clin. Microbiol.* **49** (2011).

21. European Centre for Disease Prevention and Control. *Antimicrobial resistance in the EU/EEA (EARS-Net) - Annual Epidemiological Report 2021*. https://atlas.ecdc.europa.eu/ (2022).
22. Li, Y., Kumar, S., Zhang, L. & Wu, H. *Klebsiella pneumonia* and its antibiotic resistance: a bibliometric analysis. *BioMed. Research International* (2022)
23. Navon-Venezia, S., Kondratyeva, K. & Carattoli, A. *Klebsiella pneumoniae*: A major worldwide source and shuttle for antibiotic resistance. *FEMS Microbiology Reviews* **41** (2017).
24. Moland, E. S., Seong, G. H., Thomson, K. S., Larone, D. H. & Hanson, N. D. *Klebsiella pneumoniae* isolate producing at least eight different β-lactamases, including AmpC and KPC β-lactamases. *Antimicrobial Agents and Chemotherapy* **51** (2007).
25. León-Sampedro, R. *et al.* Pervasive transmission of a carbapenem resistance plasmid in the gut microbiota of hospitalized patients. *Nat. Microbiol.* **6** (2021).
26. Jernigan, M. G., Press, E. G., Nguyen, M. H., Clancy, C. J. & Shields, R. K. The combination of doripenem and colistin is bactericidal and synergistic against colistin-resistant, carbapenemase-producing *Klebsiella pneumoniae*. *Antimicrob. Agents Chemother.* **56** (2012).
27. van Duin, D. *et al.* Tigecycline therapy for carbapenem-resistant *Klebsiella pneumoniae* (CRKP) bacteriuria leads to tigecycline resistance. *Clinical Microbiology and Infection* **20** (2014).
28. Shields, R. K. *et al.* Emergence of ceftazidime-avibactam resistance due to plasmid-borne blaKPC-3 mutations during treatment of carbapenem-resistant *Klebsiella pneumoniae* infections. *Antimicrob. Agents Chemother.* **61** (2017).
29. CDC. Vital Signs: Carbapenem-Resistant Enterobacteriacae. *Morbidity and Mortality Weekly Report* **62**, (2013) https://www.cdc.gov/mmwr/preview/mmwrhtml/mm6209a3.htm
30. Murray, C. J. *et al.* Global burden of bacterial antimicrobial resistance in 2019: a systematic analysis. *The Lancet* **399**, 629–655 (2022).
31. Yao, H., Qin, S., Chen, S., Shen, J. & Du, X. D. Emergence of carbapenem-resistant hypervirulent *Klebsiella pneumoniae*. *The Lancet Infectious Diseases* **18** (2018).
32. Zhang, Y. *et al.* Emergence of a hypervirulent carbapenem-resistant *Klebsiella pneumoniae* isolate from clinical infections in China. *Journal of Infection* **71** (2015).
33. Gu, D. *et al.* A fatal outbreak of ST11 carbapenem-resistant hypervirulent *Klebsiella pneumoniae* in a Chinese hospital: a molecular epidemiological study. *Lancet Infect. Dis.* **18** (2018).
34. Struve, C., Bojer, M. & Krogfelt, K. A. Identification of a conserved chromosomal region encoding *Klebsiella pneumoniae* type 1 and type 3 fimbriae and assessment of the role of fimbriae in pathogenicity. *Infect. Immun.* **77** (2009).
35. Rosen, D. A. *et al.* Molecular variations in *Klebsiella pneumoniae* and *Escherichia coli* FimH affect function and pathogenesis in the urinary tract. *Infect. Immun.* **76** (2008).
36. Schroll, C., Barken, K. B., Krogfelt, K. A. & Struve, C. Role of type 1 and type 3 fimbriae in *Klebsiella pneumoniae* biofilm formation. *BMC Microbiol.* **10** (2010).
37. Jagnow, J. & Clegg, S. *Klebsiella pneumoniae* MrkD-mediated biofilm formation on extracellular matrix- and collagen-coated surfaces. *Microbiology* **149** (2003).
38. Smith, K. D. Iron metabolism at the host pathogen interface: Lipocalin 2 and the pathogen-associated iroA gene cluster. *International Journal of Biochemistry and Cell Biology* **39** (2007).
39. Kostina, E. *et al.* Noncapsulated *Klebsiella pneumoniae* bearing mannose-containing O antigens is rapidly eradicated from mouse lung and triggers cytokine production by macrophages following opsonization with surfactant protein D. *Infect. Immun.* **73** (2005).
40. Kabha, K. *et al.* SP-A enhances phagocytosis of *Klebsiella* by interaction with capsular polysaccharides and alveolar macrophages. *Am. J. Physiol. Lung Cell Mol. Physiol.* **272** (1997).

41. Ofek, I. *et al.* Surfactant protein D enhances phagocytosis and killing of unencapsulated phase variants of *Klebsiella pneumoniae*. *Infect. Immun.* **69** (2001).

42. Campos, M. A. *et al.* Capsule polysaccharide mediates bacterial resistance to antimicrobial peptides. *Infect. Immun.* **72** (2004).

43. Lawlor, M. S., Hsu, J., Rick, P. D. & Miller, V. L. Identification of *Klebsiella pneumoniae* virulence determinants using an intranasal infection model. *Mol. Microbiol.* **58** (2005).

44. Lin, J. C. *et al.* High prevalence of phagocytic-resistant capsular serotypes of *Klebsiella pneumoniae* in liver abscess. *Microbes. Infect.* **6** (2004).

45. Shankar-Sinha, S. *et al.* The *Klebsiella pneumoniae* O antigen contributes to bacteremia and lethality during murine pneumonia. *Infect. Immun.* **72** (2004).

46. Fang, C. T., Chuang, Y. P., Shun, C. T., Chang, S. C. & Wang, J. T. A Novel Virulence Gene in Klebsiella pneumoniae Strains Causing Primary Liver Abscess and Septic Metastatic Complications. *Journal of Experimental Medicine* **199**, (2004).

47. Chuang, Y. P., Fang, C. T., Lai, S. Y., Chaing, S. C. & Wang, J. T. Genetic determinants of capsular serotype K1 of *Klebsiella pneumoniae* causing primary pyogenic liver abscess. *Journal of Infectious Diseases* **193** (2006).

48. Holt, K. E. *et al.* Genomic analysis of diversity, population structure, virulence, and antimicrobial resistance in *Klebsiella pneumoniae*, an urgent threat to public health. *Proc. Natl. Acad. Sci. USA* **112** (2015).

49. Lam, M. M. C., Wick, R. R., Judd, L. M., Holt, K. E. & Wyres, K. L. Kaptive 2.0: updated capsule and lipopolysaccharide locus typing for the *Klebsiella pneumoniae* species complex. *Microb. Genom.* **8**, (2022).

50. Pennini, M. E. *et al.* Immune stealth-driven O2 serotype prevalence and potential for therapeutic antibodies against multidrug resistant Klebsiella pneumoniae. *Nat. Commun.* **8**, 1–12 (2017).

51. Chung, D. R. *et al.* Emerging invasive liver abscess caused by K1 serotype *Klebsiella pneumoniae* in Korea. *Journal of Infection* **54** (2007).

52. Fung, C. P. *et al.* A global emerging disease of *Klebsiella pneumoniae* liver abscess: Is serotype K1 an important factor for complicated endophthalmitis? *Gut* **50** (2002).

53. Follador, R. *et al.* The diversity of *Klebsiella pneumoniae* surface polysaccharides. *Microb. Genom.* **2**, (2016).

54. Mbelle, N. M. *et al.* Pathogenomics and evolutionary epidemiology of multi-drug resistant clinical *Klebsiella pneumoniae* isolated from Pretoria, South Africa. *Sci. Rep.* **10** (2020).

55. Zhang, Z. Y. *et al.* Capsular polysaccharide and lipopolysaccharide o type analysis of *Klebsiella pneumoniae* isolates by genotype in China. *Epidemiol. Infect.* (2020)

56. Regueiro, V. *et al. Klebsiella pneumoniae* subverts the activation of inflammatory responses in a NOD1-dependent manner. *Cell Microbiol.* **13** (2011).

57. Dolgachev, V. A. *et al.* Interleukin 10 overexpression alters survival in the setting of Gram-negative pneumonia following lung contusion. *Shock* **41** (2014).

58. Ohama, H. *et al.* M2b macrophage elimination and improved resistance of mice with chronic alcohol consumption to opportunistic infections. *American Journal of Pathology* **185** (2015).

59. Tsuchimoto, Y. *et al.* M2b monocytes provoke bacterial pneumonia and gut bacteria–associated sepsis in alcoholics. *The Journal of Immunology* **195** (2015).

60. Ahn, D. *et al.* Acquired resistance to innate immune clearance promotes *Klebsiella pneumoniae* ST258 pulmonary infection. *JCI Insight* **1**, (2016).

61. Lebien, T. W. & Tedder, T. F. B lymphocytes: How they develop and function. *Blood* **112** (2008).

62. ALT, F. W., Blackwell, T. K., Depinho, R. A., Reth, M. G. & Yancopoulos, G. D. Regulation of genome rearrangement events during lymphocyte differentiation. *Immunol. Rev.* **89** (1986).

63. Brack, C., Hirama, M., Lenhard-Schuller, R. & Tonegawa, S. A complete immunoglobulin gene is created by somatic recombination. *Cell* **15** (1978).

64. Kelsoe, G. Life and death in germinal centers. *Immunity* **4** (1996).

65. Jacob, J., Kelsoe, G., Rajewsky, K. & Weiss, U. Intraclonal generation of antibody mutants in germinal centres. *Nature* **354** (1991).

66. Bernasconi, N. L., Traggiai, E. & Lanzavecchia, A. Maintenance of serological memory by polyclonal activation of human memory B cells. *Science* **298** (2002).

67. Lu, L. L., Suscovich, T. J., Fortune, S. M. & Alter, G. Beyond binding: Antibody effector functions in infectious diseases. *Nature Reviews Immunology* **18** (2018).

68. Malech, H. L., Deleo, F. R. & Quinn, M. T. The role of neutrophils in the immune system: An overview. *Methods in Molecular Biology* **1124** (2014).

69. Heesterbeek, D. A. C., Angelier, M. L., Harrison, R. A. & Rooijakkers, S. H. M. Complement and bacterial infections: from molecular mechanisms to therapeutic applications. *Journal of Innate Immunity* **10** (2018).

70. Sharp, T. H. *et al.* Insights into IgM-mediated complement activation based on *in situ* structures of IgM-C1-C4b. *Proc. Natl. Acad. Sci. USA* **116** (2019).

71. Diebolder, C. A. *et al.* Complement is activated by IgG hexamers assembled at the cell surface. *Science* **343** (2014).

72. Abendstein, L. *et al.* Complement is activated by elevated IgG3 hexameric platforms and deposits C4b onto distinct antibody domains. *Nat. Commun.* **14** (2023).

73. Vidarsson, G., Dekkers, G. & Rispens, T. IgG subclasses and allotypes: From structure to effector functions. *Front Immunol* **5** (2014).

74. Kobayashi, S. D., Malachowa, N. & DeLeo, F. R. Neutrophils and bacterial immune evasion. *Journal of Innate Immunity* **10** (2018).

75. Metzemaekers, M., Gouwy, M. & Proost, P. Neutrophil chemoattractant receptors in health and disease: double-edged swords. *Cellular and Molecular Immunology* **17** (2020).

76. Sun, D. *et al.* Real-time imaging of interactions of neutrophils with *Cryptococcus neoformans* demonstrates a crucial role of complement C5a-C5aR signaling. *Infect. Immun.* **84** (2015).

77. Denk, S. *et al.* Complement c5a-induced changes in neutrophil morphology during inflammation. *Scand. J. Immunol.* **86** (2017).

78. de Vor, L., Rooijakkers, S. H. M. & van Strijp, J. A. G. Staphylococci evade the innate immune response by disarming neutrophils and forming biofilms. *FEBS Letters* **594** (2020).

79. Xiong, H. *et al.* Distinct contributions of neutrophils and CCR2+ monocytes to pulmonary clearance of different *Klebsiella pneumoniae* strains. *Infect. Immun.* **83** (2015).

80. Satlin, M. J. *et al.* Emergence of carbapenem-resistant Enterobacteriaceae as causes of bloodstream infections in patients with hematologic malignancies. *Leuk. Lymphoma* **54** (2013).

81. Valdez, J. M., Scheinberg, P., Young, N. S. & Walsh, T. J. Infections in patients with aplastic anemia. *Semin. Hematol.* **46** (2009).

82. Merino, S., Camprubi, S., Alberti, S., Benedi, V.-J. & Tomas, J. M. Mechanisms of *Klebsiella pneumoniae* resistance to complement-mediated killing. *Infection and Immunity* **60** (1992).

83. Ciurana, B. & Tomas, J. M. Role of lipopolysaccharide and complement in susceptibility of *Klebsiella pneumoniae* to nonimmune serum. *Infect. Immun.* **55** (1987).

84. McCallum, K. L., Schoenhals, G., Laakso, D., Clarke, B. & Whitfield, C. A high-molecular-weight fraction of smooth lipopolysaccharide in *Klebsiella* serotype O1:K20 contains a unique O-antigen epitope and determines resistance to nonspecific serum killing. *Infect. Immun.* **57**, (1989).

85. Merino, S., Camprubi, S., Alberti, S., Benedi, V. J. & Tomas, J. M. Mechanisms of *Klebsiella pneumoniae* resistance to complement-mediated killing. *Infect. Immun.* **60** (1992).

86. Alberti, S. *et al.* C1q binding and activation of the complement classical pathway by *Klebsiella pneumoniae* outer membrane proteins. *Infect. Immun.* **61**, (1993).

87. Albertí, S. *et al.* Analysis of complement C3 deposition and degradation on *Klebsiella pneumoniae*. *Infect. Immun.* **64**, (1996).

88. Doorduijn, D. J. *et al.* Soluble MAC is primarily released from MAC-resistant bacteria that potently convert complement component C5. *Elife* **11** (2022).

89. Szijártó, V. *et al.* Both clades of the epidemic KPC-producing *Klebsiella pneumoniae* clone ST258 share a modified galactan O-antigen type. *International Journal of Medical Microbiology* **306** (2016).

90. Clements, A. *et al.* The major surface-associated saccharides of *Klebsiella pneumoniae* contribute to host cell association. *PLoS One* **3** (2008).

91. Álvarez, D., Merino, S., Tomás, J. M., Benedí, V. J. & Albertí, S. Capsular polysaccharide is a major complement resistance factor in lipopolysaccharide O side chain-deficient *Klebsiella pneumoniae* clinical isolates. *Infect. Immun.* **68** (2000).

92. Domenico, P., Tomas, J. M., Merino, S., Rubires, X. & Cunha, B. A. Surface antigen exposure by bismuth dimercaprol suppression of *Klebsiella pneumoniae* capsular polysaccharide. *Infect. Immun.* **67** 664–669 (1999).

93. Salo, R. J. *et al.* Salicylate-enhanced exposure of *Klebsiella pneumoniae* subcapsular components. *Infection* **23**, 371–377 (1995).

94. Tomas, J. M., Camprubi, S., Merino, S., Davey, M. R. & Williams, P. Surface exposure of O1 serotype lipopolysaccharide in *Klebsiella pneumoniae* strains expressing different K antigens. *Infect. Immun.* **59**, (1991).

95. Held, T. K., Jendrike, N. R. M., Rukavina, T., Podschun, R. & Trautmann, M. Binding to and opsonophagocytic activity of O-antigen-specific monoclonal antibodies against encapsulated and nonencapsulated *Klebsiella pneumoniae* serotype O1 strains. *Infect. Immun.* **68**, 2402–2409 (2000).

96. De Astorza, B. *et al.* C3 Promotes Clearance of Klebsiella pneumoniae by A549 Epithelial Cells. *Infect. Immun.* **72** (2004).

97. Domenico, P., Salo, R. J., Cross, A. S. & Cunha, B. A. Polysaccharide capsule-mediated resistance to opsonophagocytosis in *Klebsiella pneumoniae*. *Infect. Immun.* **62** (1994).

98. Sahly, H., Keisari, Y. & Ofek, I. Manno(rhamno)biose-containing capsular polysaccharides of *Klebsiella pneumoniae* enhance opsono-stimulation of human polymorphonuclear leukocytes. *J. Innate Immun.* **1** (2009).

99. van der Geest, R. *et al.* Phagocytosis is a primary determinant of pulmonary clearance of clinical *Klebsiella pneumoniae* isolates. *Front. Cell Infect. Microbiol.* **13** (2023).

100. Lee, C. H., Chang, C. C., Liu, J. W., Chen, R. F. & Yang, K. D. Sialic acid involved in hypermucoviscosity phenotype of *Klebsiella pneumoniae* and associated with resistance to neutrophil phagocytosis. *Virulence* **5** (2014).

101. Lepper, P. M., Möricke, A., Held, T. K., Schneider, E. M. & Trautmann, M. K-antigen-specific, but not O-antigen-specific natural human serum antibodies promote phagocytosis of *Klebsiella pneumoniae*. *FEMS Immunol. Med. Microbiol.* **35**, 93–98 (2003).

102. Kobayashi, S. D. *et al.* Antibody-mediated killing of carbapenem-resistant ST258 *Klebsiella pneumoniae* by human neutrophils. *mBio* **9** (2018).

103. Serushago, B. A., Mitsuyama, M., Handa, T., Koga, T. & Nomoto, K. Role of antibodies against outer-membrane proteins in murine resistance to infection with encapsulated *Klebsiella pneumoniae*. *J. Gen. Microbiol.* **135**, 2259–2268 (1989).

104. Rollenske, T. *et al.* Cross-specificity of protective human antibodies against *Klebsiella pneumoniae* LPS O-antigen. *Nat. Immunol.* **19**, 617–624 (2018).

105. DeLeo, F. R. *et al.* Survival of carbapenem-resistant *Klebsiella pneumoniae* sequence type 258 in human blood. *Antimicrob. Agents Chemother.* **61** (2017).

106. Krieger, A. K. *et al.* Porcine iucA+ but rmpA- *Klebsiella pneumoniae* strains proliferate in blood of young piglets but are killed by IgM and complement dependent opsonophagocytosis when these piglets get older. *Vet. Microbiol.* **266** (2022).

107. Qun, W. *et al.* Target-agnostic identification of functional monoclonal antibodies against *Klebsiella pneumoniae* multimeric MrkA fimbrial subunit. *Journal of Infectious Diseases* **213** (2016).

108. Wang, Q. *et al.* Anti-MrkA monoclonal antibodies reveal distinct structural and antigenic features of MrkA. *PLoS One* **12** (2017).

109. Kobayashi, S. D. *et al.* Phagocytosis and killing of carbapenem-resistant ST258 *Klebsiella pneumoniae* by human neutrophils. *Journal of Infectious Diseases* **213** (2016).

110. Albertí, S. *et al.* Interaction between complement subcomponent C1q and the *Klebsiella pneumoniae* porin OmpK36. *Infect. Immun.* **64** (1996).

111. Garbett, N. D., Munro, C. S. & Cole, P. J. Opsonic activity of a new intravenous immunoglobulin preparation: Pentaglobin compared with Sandoglobulin. *Clin. Exp. Immunol.* **76**, 8–12 (1989).

112. Smith, S. A. & Crowe, Jr., J. E. Use of human hybridoma technology to isolate human monoclonal antibodies. *Microbiol. Spectr.* **3** (2015).

113. Corti, D. & Lanzavecchia, A. Efficient methods to isolate human monoclonal antibodies from memory b cells and plasma cells. *Microbiol. Spectr.* **2** (2014).

114. Kwakkenbos, M. J. *et al.* Generation of stable monoclonal antibody-producing B cell receptor-positive human memory B cells by genetic programming. *Nat. Med.* **16** (2010).

115. Frenzel, A., Schirrmann, T. & Hust, M. Phage display-derived human antibodies in clinical development and therapy. *mAbs* **8** (2016).

116. DeKosky, B. J. *et al.* Functional interrogation and mining of natively-paired human VH:VL antibody repertoires. *The Journal of Immunology* **200** (2018).

117. Spadiut, O., Capone, S., Krainer, F., Glieder, A. & Herwig, C. Microbials for the production of monoclonal antibodies and antibody fragments. *Trends in Biotechnology* **32** (2014).

118. Huang, J. *et al.* Broad and potent neutralization of HIV-1 by a gp41-specific human antibody. *Nature* **491** (2012).

119. Huang, J. *et al.* Isolation of human monoclonal antibodies from peripheral blood B cells. *Nat. Protoc.* **8** (2013).

120. Tiller, T. *et al.* Efficient generation of monoclonal antibodies from single human B cells by single cell RT-PCR and expression vector cloning. *J. Immunol. Methods* **329** (2008).

121. Rollenske, T. *et al.* Cross-specificity of protective human antibodies against Klebsiella pneumoniae LPS O-antigen. *Nature Immunology* **19**, 617–624 (2018).

Chapter 2

Colistin resistance mutations in phoQ can sensitize *Klebsiella pneumoniae* to IgM-mediated complement killing

Sjors P. A. van der Lans[1], Manon Janet-Maitre[2,3], Maartje Ruyken[1], Frerich M. Masson[1], Kimberly A. Walker[4], Dennis J. Doorduijn[1], Axel B. Janssen[1,5], Willem van Schaik[1,6], Ina Attrée[2], Suzan H. M. Rooijakkers[1] and Bart W. Bardoel[1]*

[1]Department of Medical Microbiology, University Medical Center Utrecht, Utrecht University, The Netherlands.
[2]Bacterial Pathogenesis and Cellular Responses group, UMR5075, Institute of Structural Biology, University Grenoble Alpes, France.
[3]Department of Molecular Microbiology, Washington University School of Medicine, St. Louis, USA
[4]Department of Microbiology and Immunology, University of North Carolina, USA.
[5]Department of Fundamental Microbiology, University of Lausanne, Switzerland.
[6]Institute of Microbiology and Infection, College of Medical and Dental Sciences, University of Birmingham, United Kingdom.
*Corresponding author: B.W.Bardoel-2@umcutrecht.nl

Published in : Scientific reports 13 12618 (2023)

Abstract

Due to multi-drug resistance, physicians increasingly use the last-resort antibiotic colistin to treat infections with the Gram-negative bacterium *Klebsiella pneumoniae.* Unfortunately, *K. pneumoniae* can also develop colistin resistance. Interestingly, colistin resistance has dual effects on bacterial clearance by the immune system. While it increases resistance to antimicrobial peptides, colistin resistance has been reported to sensitize certain bacteria for killing by human serum. Here we investigate the mechanisms underlying this increased serum sensitivity, focusing on human complement which kills Gram-negatives via membrane attack complex (MAC) pores. Using *in vitro* evolved colistin resistant strains and a fluorescent MAC-mediated permeabilization assay, we showed that two of the three tested colistin resistant strains, Kp209_CSTR and Kp257_CSTR, were sensitized to MAC. Transcriptomic and mechanistic analyses focusing on Kp209_CSTR revealed that a mutation in the *phoQ* gene locked PhoQ in an active state, making Kp209_CSTR colistin resistant and MAC sensitive. Detailed immunological assays showed that complement activation on Kp209_CSTR in human serum required specific IgM antibodies that bound Kp209_CSTR but did not recognize the wild-type strain. Together, our results show that developing colistin resistance affected recognition of Kp209_CSTR and its killing by the immune system.

Introduction

Infections with antibiotic-resistant bacteria form a serious threat for public health. Among the most concerning bacteria is the Gram-negative bacterium *Klebsiella pneumoniae*, which caused nearly 1 million antibiotic resistance associated deaths in 2019 alone [1]. In the past decades, the number of antibiotic resistant *K. pneumoniae* has risen dramatically for several classes of antibiotic [2–4]. Propagation of antibiotic resistance often occurs in nosocomial settings, where antibiotic resistant strains are transferred between patients and antibiotic resistance genes can spread between *K. pneumoniae* lineages [5]. To treat infections caused by antibiotic resistant *K. pneumoniae*, clinicians increasingly need to use last resort antibiotics such as colistin. Colistin, a membrane-targeting antibiotic, is attracted to the Gram-negative cell envelope via electrostatic interactions [6]. The Gram-negative cell envelope consists of a thin peptidoglycan cell wall in between an outer and an inner membrane, with negatively charged lipopolysaccharides (LPS) being present in the outer leaflet of the outer membrane. The positively charged colistin is attracted to these negative charges in the cell envelope, causing colistin to insert into the membranes. This will subsequently destabilise and disrupt both the outer and inner membrane, ultimately leading to cell death [7].

Previously, it was shown that development of colistin resistance in Gram-negative bacteria has a negative impact on bacterial fitness and virulence *in vivo* [8–10]. Intriguingly, various different effects have been observed *in vitro*. While antimicrobial peptides and lysozyme were less effective against colistin resistant strains [9,11], killing of *K. pneumoniae* and *Escherichia coli in vitro* by human serum was more efficient in colistin resistant strains [8,12]. Although human serum contains several antimicrobial components, the main antimicrobial effector in serum is the complement system, a protein network that can directly kill Gram-negative bacteria via the formation of the membrane attack complex (MAC). MAC formation is initiated after bacteria are recognized by the complement system, which leads to sequential deposition of complement proteins on the bacterial surface. This ultimately results in the formation of the MAC, a multi-protein complex that forms a pore in the outer membrane, leading to inner membrane destabilization and bacterial killing [13].

In this study, we aimed to investigate how colistin resistance affects bacterial sensitivity to human complement. Using a sensitive fluorescent MAC assay and a panel of *in vitro* evolved colistin resistant *K. pneumoniae* strains [9], we identified two isogenic

strain pairs, Kp209 / Kp209_CSTR and Kp257 / Kp257_CSTR, in which the colistin resistant (CSTR) mutant exhibited increased sensitivity to MAC. Transcriptomic and mutational analysis of Kp209_CSTR reveal that a mutation locking PhoQ in an active state made this strain resistant to colistin and sensitive to MAC at the same time. Detailed immunological assays show that bacterium-specific IgMs mediate enhanced MAC sensitivity in the colistin-resistant Kp209_CSTR.

Results

Inner membrane damage correlates with MAC-mediated killing of *K. pneumoniae*

To study the relation between colistin resistance and MAC sensitivity, we first established an *in vitro* assay system to quantify MAC-mediated killing of *K. pneumoniae* in microplates. Previously, we showed that fluorescent DNA dyes can be used as a proxy for MAC-dependent killing of *E. coli*. Specifically, we used Sytox DNA dyes that can only stain Gram-negative bacteria when both the outer and inner membrane are damaged [13]. We observed that MAC-mediated inner membrane damage of *K. pneumoniae* in human serum correlated with bacterial killing on plate [13]. To determine if this assay can be used for *K. pneumoniae* clinical isolates, we analysed the MAC-mediated membrane permeabilization and killing of ten clinical *K. pneumoniae* strains. Bacteria were incubated with 10% normal human serum (NHS) containing both complement and naturally occurring antibodies. Inner membrane permeabilization was monitored by measuring fluorescence over time and compared to bacterial survival that was assessed by counting colony forming unites (CFU) on plate (fig. 1ab).

First, we observed that four out of ten tested isolates were resistant to MAC-mediated killing (Kp570, Kp444, Kp879 and Kp307), as these strains showed no decrease in survival (fig. 1a). No or a minimal increase in inner membrane damage for these three MAC resistant isolates was seen (fig. 1ab, supplementary fig. 1). Furthermore, the strain that was most sensitive to MAC-mediated killing (Kp193) showed the strongest membrane permeabilization (fig. 1a). Inner membrane damage started after 20 minutes in Kp193, after which the signal quickly increased and reached a plateau after 40 minutes (fig. 1b). Five strains showed a slow increase in membrane permeabilization (Kp365, Kp982, Kp709, Kp702 and Kp880) (fig. 1ab, supplementary fig. 1). Most of these strains showed only a minor reduction in survival. No inner membrane

permeabilization was observed when MAC formation was blocked by serum heat-inactivation or addition of a C5 cleavage inhibitor. Taken together, these data indicate that for *K. pneumoniae*, MAC activity can be quantified by measuring inner membrane damage via Sytox green.

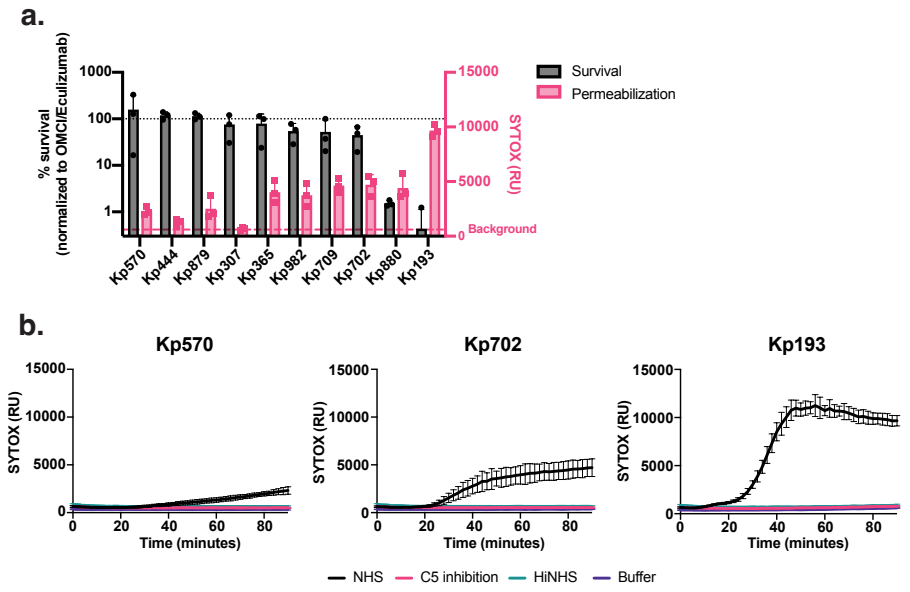

Figure 1| MAC-dependent inner membrane permeabilization correlates with reduced viability of *K. pneumoniae*

(**a**) Survival on plate and inner membrane permeabilization of clinical *K. pneumoniae* isolates after 90-minute incubation in 10% normal human serum (NHS) at 37 °C in the presence of 1 μM SYTOX green nucleic acid stain. Survival data was normalized to CFU counts in conditions where C5 conversion was inhibited by addition of 20 μg/ml OMCI and 20 μg/ml Eculizumab. Inner membrane permeabilization (SYTOX fluorescence intensity) was determined in a microplate reader. Red dotted line indicates background permeabilization signal (OMCI+ Eculizumab). (**b**) Inner membrane permeabilization of Kp570, Kp702 and Kp193 in the presence of 10% NHS, 10% NHS in which C5 conversion was inhibited by addition of 20 μg/ml OMCI and 20 μg/ml Eculizumab (C5 inhibition), or 10% heat inactivated NHS (HiNHS). Bacteria were incubated at 37 °C in the presence of 1 μM SYTOX green nucleic acid stain, and inner membrane permeabilization (SYTOX fluorescence intensity) was detected every 2 minutes for 90 minutes in a microplate reader. (A-B) Data represent mean ± standard deviation of three independent experiments.

Developing colistin resistance sensitizes *K. pneumoniae* Kp209 and Kp257 to MAC-mediated killing

Since previous studies demonstrated that colistin resistance can affect serum sensitivity of certain *K. pneumoniae* isolates [8,11,12], we wondered whether there was a role for MAC in this process. First, we used our fluorescent MAC activity assay to investigate the influence of colistin resistance on MAC-mediated killing of *K. pneumoniae.* To allow a direct comparison, we used three isogenic *K. pneumoniae* strain pairs that were previously selected during an *in vitro* evolution experiment, in which three colistin sensitive *K. pneumoniae* strains (Kp209, Kp257 and Kp040) were exposed to increasing concentrations of colistin to evolve colistin-resistant (CSTR) strains (Kp209_CSTR, Kp257_CSTR and Kp040_CSTR) [9]. Colistin resistance in Kp209_CSTR and Kp257_CSTR was linked to mutations in the *phoQ* gene (WAQRN-97-C and G385S, respectively). Kp040_CSTR had a IS5 insertion in the promoter region of *crrAB* and *crrC,* and a point mutation in the promoter region of *ecpR* or *phnC* [9]. Mutations in these genes have been associated with colistin resistance, which was attributed to a reduced negative charged of the outer membrane due to altered lipid A modifications [9,14–17].

In this study, we exposed these three isogenic strain pairs to NHS and quantified MAC-mediated membrane damage. While acquisition of colistin resistance increased the MAC-dependent permeabilization of Kp209_CSTR in 10% NHS, no effect was observed for Kp257_CSTR or Kp040_CSTR (fig. 2a). In concordance, colony enumeration experiments confirmed that Kp209_CSTR was killed more effectively by NHS than Kp209 (fig. 2b). Membrane damage of Kp209_CSTR was caused by MAC, as blocking complement activation via a C5 conversion inhibitor or heat inactivation of NHS prevents membrane permeabilization. Similar results were obtained using NHS composed of sera of a different pool of donors, and with sera from individual donors for Kp209 and Kp209_CSTR (supplementary fig. 2). As Kp257_CSTR has a mutation in the same gene (*phoQ*) as Kp209_CSTR, but was not sensitive to 10% NHS, we decided to increase the concentration of NHS. When measuring membrane permeabilization and serum survival in 50% NHS, we observed that Kp257_CSTR was permeabilized and killed, whereas Kp257 was not, indicating that acquisition of colistin resistance also increased serum sensitivity of Kp257_CSTR (fig. 2c&d). No permeabilization or killing was observed for Kp040 and Kp040_CSTR in 50% NHS (fig. 2c&d). Taken together these data confirm that developing colistin resistance can lead to increased MAC-sensitivity, although this does not happen for every *K. pneumoniae* strain.

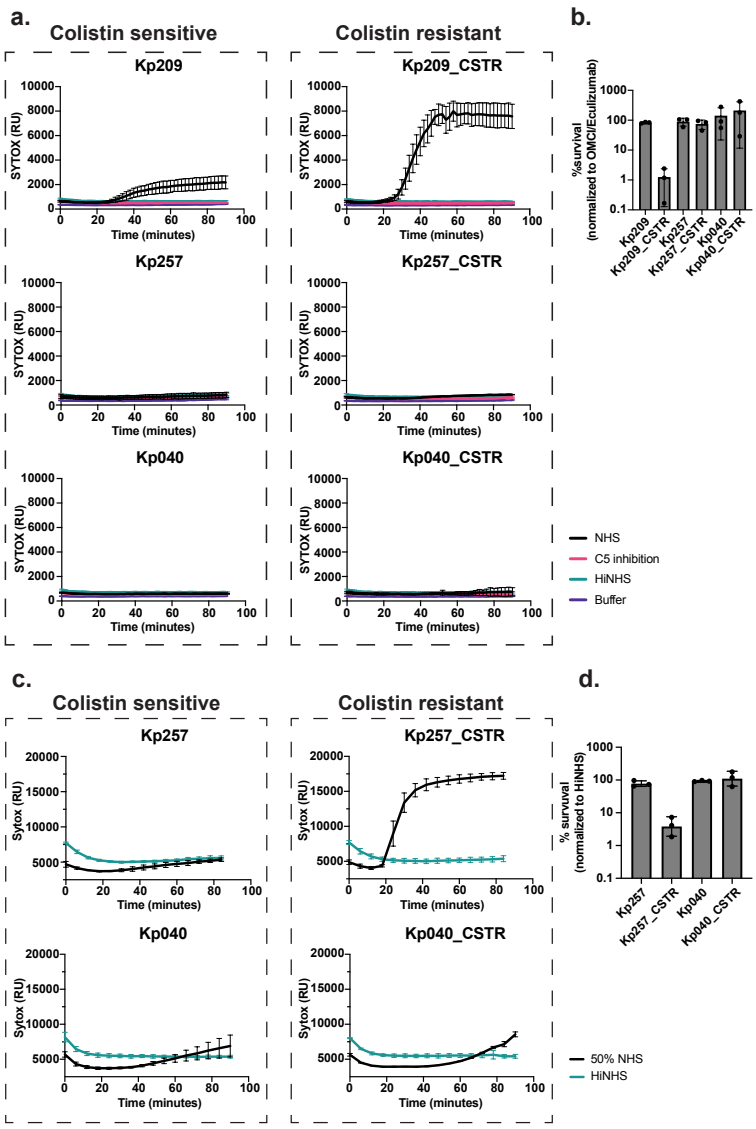

Figure 2| Colistin resistant Kp209_CSTR has been sensitized to MAC-mediated killing

(a) Inner membrane permeabilization of Kp209, Kp257 and Kp040, and their colistin resistant derived strains Kp209_CSTR, Kp257_CSTR and Kp040_CSTR in the presences of 10% NHS, 10% NHS in which C5 conversion was inhibited by addition of 20 µg/ml OMCI and 20 µg/ml Eculizumab (C5 inhibition), or 10% heat inactivated NHS (HiNHS). Bacteria were incubated at 37 °C in the presence of 1 µM SYTOX green nucleic acid stain, and inner membrane permeabilization (SYTOX fluorescence intensity) was detected every 2 minutes for 90 minutes in a microplate reader. **(b)** Survival on plate of Kp209, Kp257 and Kp040, and their colistin resistant derived strains Kp209_CSTR, Kp257_CSTR, and Kp040_CSTR after 90 minutes incubation in 10% NHS at 37 °C. Survival data is normalized

to CFU counts in conditions where the terminal complement pathway was blocked by inhibiting C5 conversion (20 µg/ml OMCI and 20 µg/ml Eculizumab). (**c**) Inner membrane permeabilization of Kp257, Kp257_CSTR, Kp040 and Kp040_CSTR in the presence of 50% NHS, or 50% HiNHS. Bacteria were incubated at 37 °C in the presence of 1 µM SYTOX green nucleic acid stain, and inner membrane permeabilization (SYTOX fluorescence intensity) was detected every 6 minutes for 90 minutes in a microplate reader. (**d**) Survival on plate of Kp257, Kp257_CSTR, Kp040 and Kp040_CSTR after 90 minutes incubation in 50% NHS at 37 °C. Survival data was normalized to CFU counts in 50% HiNHS. (a-d) Data represent mean ± standard deviation of three independent experiments

Overactivation of PhoQ sensitizes Kp209_CSTR to MAC-mediated membrane permeabilization

Genetic comparison of Kp209 and Kp209_CSTR revealed that Kp209_CSTR exclusively contains mutations in the *phoQ* gene [9], a sensor histidine kinase that is part of the PhoPQ two-component regulatory system [18]. More specifically, the *phoQ* gene of Kp209_CSTR contains a WAQRN-97-C deletion located in the sensory domain of PhoQ [9,19]. In *Salmonella*, it was shown that disruption of tryptophan residue at position 97 (W-97) locks PhoQ in an active state [20,21]. To investigate if PhoQ in Kp209_CSTR is locked in an active state, we compared the gene expression of Kp209 and Kp209_CSTR, which indicated increased transcriptional activation of the PhoPQ regulon in Kp209_CSTR (fig. 3a). 124 genes were significantly upregulated (Log2(FC)>1, Padj<0.05) in Kp209_CSTR, whereas 60 genes were downregulated (Log2(FC)<-1, Padj<0.05) (supplementary table 1). Of the upregulated genes, many are known to be dependent on PhoQ activity, such as genes coding for proteins involved in magnesium transport and LPS modifications[18,22]. To determine if PhoPQ regulated genes are also upregulated in Kp257_CSTR, which has a G385S mutation in the histidine kinase domain of PhoQ, we measured the relative expression of *arnD* and *mgtE* in Kp257 and Kp257_CSTR, as these genes were among the strongest upregulated genes in Kp209_CSTR. We observed an increased relative expression of 13.8-fold and 7.8-fold for *arnD* and *mgtE*, respectively, in Kp257_CSTR compared to Kp257 (supplementary fig. 3). This indicated that the *phoQ* colistin resistance mutation in Kp257_CSTR also promotes expression of PhoPQ regulated genes, similar to what we observed for Kp209_CSTR.

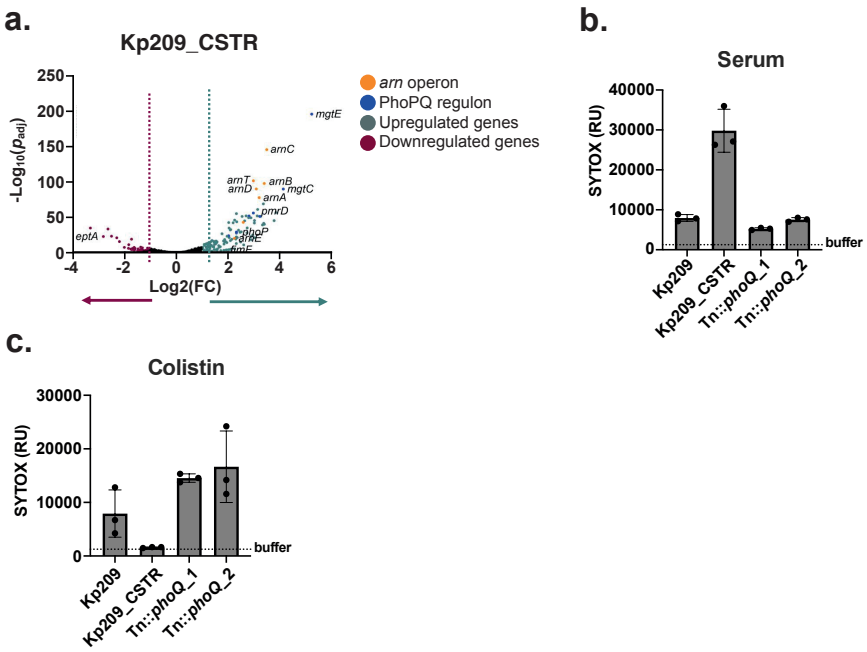

Figure 3| Colistin resistant Kp209_CSTR has been sensitized to MAC-mediated killing due to enhanced PhoQ activation

(**a**) RNA was isolated from log phase Kp209 and Kp209_CSTR, and their transcriptomes were analysed. The volcano plot depicts differential expressed genes in Kp209_CSTR compared to Kp209. In Kp209_CSTR 124 genes were upregulated and 60 downregulated. (**b-c**) Kp209_CSTR transposon (Tn) library was exposed to 16% normal human serum (NHS), followed by re-exposed to 32% NHS, and surviving colonies were selected. Two unique Tn mutants had a transposon insertion in *phoQ* (Tn::*phoQ*). (**b**) Inner membrane permeabilization of Kp209, Kp209_CSTR, and Kp209_CSTR Tn::*phoQ* mutants in the presence of 10% NHS. (**c**) Inner membrane permeabilization of Kp209, Kp209_CSTR, and Kp209_CSTR Tn::*phoQ* mutants in the presence of 1 µg/ml colistin. (**b-c**) Bacteria were incubated at 37 °C in the presence of 1 µM SYTOX green nucleic acid stain, and inner membrane permeabilization (SYTOX fluorescence intensity) was detected after 60 minutes in a microplate reader. Data represent mean ± standard deviation of three independent experiments.

To directly prove that PhoQ plays a role in MAC sensitivity of Kp209_CSTR, we generated a transposon (Tn) library of Kp209_CSTR and exposed it to human serum. The library was first challenged with 16% NHS, followed by re-exposure of surviving bacteria to 32% NHS. Out of the surviving bacteria, eight colonies were picked and the *phoQ* gene was analysed. This revealed that three out of the eight Tn mutants had a transposon insertion in *phoQ* (Tn::*phoQ*). Two of the three Tn::*phoQ* mutants were

clonally related as they had the same transposon at an identical insertion site. We analysed the MAC-mediated membrane permeabilization of the two unique Tn::*phoQ* mutants , which showed reduced membrane permeabilization compared to Kp209_CSTR (fig. 3b), indicating that loss of *phoQ* leads to decreased MAC sensitivity. We also assessed colistin sensitivity of the Tn::*phoQ* mutants. As colistin disrupts the bacterial cell envelop to kill bacteria, the membrane permeabilization assay could be used to compare colistin sensitivity between Kp209, Kp209_CSTR and the Tn::*phoQ* mutants (fig. 3c). Kp209_CSTR was not permeabilized by colistin, whereas the colistin sensitive Kp209 was. Both Kp209_CSTR Tn::*phoQ* mutants were permeabilized by colistin, indicating that loss of PhoQ function leads to increased colistin sensitivity of this strain. Taken together these data indicate that enhanced PhoQ activity, as a result of colistin resistance mutations, led to an increased MAC-sensitivity in Kp209_CSTR.

Capsule production is reduced in Kp209_CSTR

Enhanced PhoPQ activity due to colistin resistance mutations has been linked to decreased capsule production in *K. pneumoniae*[11,12]. Therefore, we tested capsule production of Kp209_CSTR, and found that it was reduced compared to Kp209 (supplementary fig. 4). This reduction was the result of the constitutively active PhoQ, as disrupting this gene by transposon insertion restored capsule production to level of Kp209 (supplementary fig. 4). The LPS O-antigen, the other major extracellular polysaccharide of *K. pneumoniae* was not different in length and abundance between Kp209 and Kp209_CSTR (supplementary fig. 4).

Classical pathway activation is crucial for killing of Kp209_CSTR

To study the mechanism that caused increased MAC-mediated killing of Kp209_CSTR, we first analysed which complement pathway was responsible for MAC-dependent permeabilization. The complement system can be activated via three distinct pathways (classical, lectin and alternative pathway) which are activated via different mechanisms, but all lead to the formation of MAC on Gram-negative bacteria. Both the classical and the lectin pathway depend on complement protein C2, therefore we used C2 depleted serum to determine the involvement of these pathways. We observed that depletion of C2 resulted in the complete loss of membrane permeabilization of Kp209_CSTR (fig. 4a). This effect was restored by adding back C2 to physiological levels, which indicated that C2 was crucial for complement-mediated membrane damage of Kp209_CSTR. Similarly, factor B (fB) depleted serum was used to determine the role of the alternative pathway. Depletion of fB did not influence inner membrane permeabilization

of Kp209_CSTR (fig. 4b). These data suggest that killing of Kp209_CSTR is primarily driven by the classical and/or lectin pathway. To further distinguish between the classical and lectin pathway, we used inhibitors to specifically block the first steps of classical pathway activation. The initiation of the classical pathway starts when IgG or IgM antibodies bind the bacterial surface. Upon binding, these antibodies can recruit the large C1 complex, which is specific to the classical pathway. C1 consists of the recognition protein C1q and associated proteases C1r and C1s. To block C1 dependent complement activation, we simultaneously added both a monoclonal antibody that directly prevents C1q association to surface-bound antibodies, and the C1r inhibitor BBK32 [23–25]. Addition of these inhibitors to NHS prevented inner membrane damage of Kp209_CSTR (fig. 4c). In summary, these findings indicate that MAC-mediated membrane permeabilization of Kp209_CSTR in these conditions primarily depends on the classical pathway.

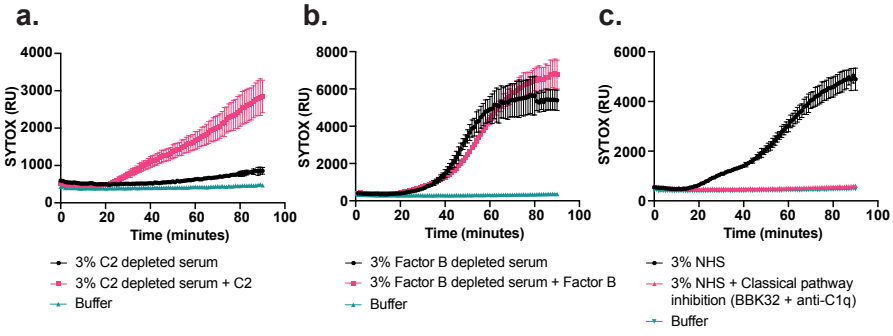

Figure 4| MAC-dependent inner membrane permeabilization of Kp209_CSTR is dependent on the classical pathway

(**a**) Inner membrane permeabilization of Kp209_CSTR in the presence of 3% C2 depleted serum or C2 depleted serum reconstituted with C2 to physiological concentrations (0.6 µg/ml in 3% serum). (**b**) Inner membrane permeabilization of Kp209_CSTR in the presence of 3% fB depleted serum or fB depleted serum reconstituted with fB to the physiological concentration (6 µg/ml in 3%). (**c**) Inner membrane permeabilization of Kp209_CSTR in the absence or presence of the classical pathway inhibitors anti-hu-C1q and BBK32 (both 10 µg/ml) in 3% normal human serum (NHS). (**a-c**) Bacteria were incubated at 37 °C in the presence of 1 µM SYTOX green nucleic acid stain, and inner membrane permeabilization (SYTOX fluorescence intensity) was detected every two minutes for 90 minutes in a microplate reader. Data represent mean ± standard deviation of three independent experiments.

IgM specific for Kp209_CSTR is responsible for MAC-mediated membrane permeabilization of Kp209_CSTR

The sensitivity of Kp209_CSTR to the classical complement pathway suggests a role for IgG or IgM in the increased MAC-dependent membrane permeabilization in NHS. We hypothesized that there might be increased binding of IgG or IgM to Kp209_CSTR in NHS, but incubation of Kp209 and Kp209_CSTR with NHS revealed that there was no major difference in total IgG or IgM binding to these strains (supplementary fig. 5). As IgG and IgM are polyclonal in NHS, we analysed if NHS contains antibodies that specifically recognize Kp209_CSTR, but not Kp209. A relative low concentration of Kp209_CSTR-specific antibodies could explain why we did not observe a difference in the total antibody binding between Kp209 and Kp209_CSTR. To investigate this hypothesis, we depleted antibodies from NHS using whole bacteria (fig. 5a). NHS was incubated with Kp209, Kp209_CSTR, or *E. coli* used as a control, at 4 °C to allow antibody binding without activating complement, followed by the removal of bacteria to collect NHS deprived of bacterium-specific antibodies. Three rounds of depletion where sufficient to remove most strain-specific antibodies (fig. 5b & supplementary fig. 5). Depleting NHS with Kp209 removed all IgG binding to Kp209_CSTR (fig. 5b), and *vice versa* (supplementary fig. 5), indicating that both strains were bound by the same IgGs in NHS. Depletion with Kp209_CSTR abolished IgM binding to Kp209 (supplementary fig. 5), showing that all the IgM that bound Kp209 also recognized Kp209_CSTR. However, although depletion with Kp209 strongly reduced IgM binding to Kp209_CSTR, considerable binding was still detectable, implying that NHS contains Kp209_CSTR-specific IgM (fig. 5b). We validated that antibodies were specifically removed from NHS by *K. pneumoniae* depletion, as they did not affect antibody binding to *E. coli* (supplementary fig. 5).

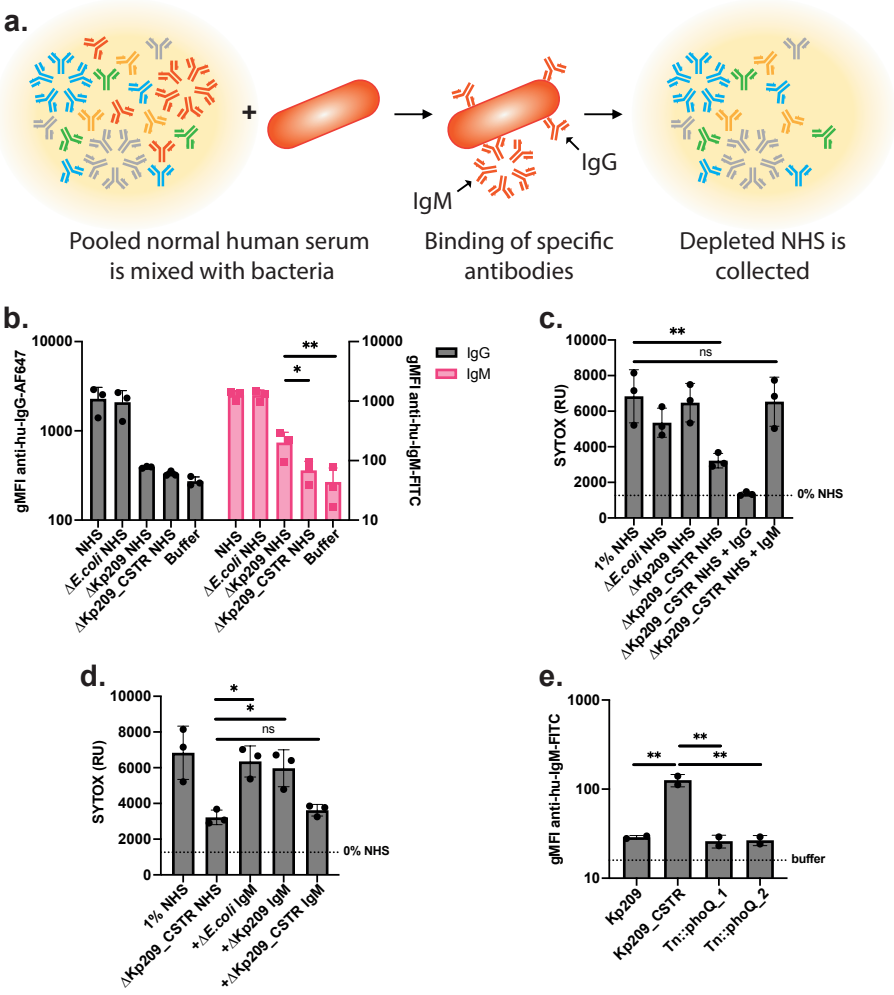

Figure 5| NHS contains Kp209_CSTR specific IgM that is vital for MAC-dependent inner membrane permeabilization

(**a**) Schematic representation of method to deplete bacterium specific antibodies from normal human serum (NHS). NHS was mixed with bacteria and incubated for 10 minutes at 4 °C to allow specific antibodies to bind. Bacteria were pelleted and discarded, and the depleted NHS was collected. Three rounds of depletion were performed. Image was created using Adobe Illustrator v27.7 (**b**) IgG and IgM binding to Kp209_CSTR in NHS, NHS depleted with *E. coli* MG1655, Kp209 or Kp209_CSTR (Δ*E. coli* NHS, ΔKp209 NHS, and ΔKp209_CSTR NHS, respectively (**c**) Inner membrane permeabilization of Kp209_CSTR in the presence of 1% NHS or NHS depleted using *E. coli* MG1655, Kp209 or Kp209_CSTR (Δ*E. coli* NHS, ΔKp209 NHS, and ΔKp209_CSTR NHS, respectively). ΔKp209_CSTR NHS was supplemented with physiological concentrations of IgG (+IgG; 125 µg/ml in 1% NHS) or IgM (+IgM; 15 µg/ml in 1% NHS) isolated from NHS. (**d**) Inner membrane permeabilization of Kp209_CSTR in the presence of 1% NHS depleted using Kp209_CSTR (ΔKp209_CSTR NHS), supplemented

with physiological concentrations of IgM isolated from NHS (15 µg/ml in 1% NHS), depleted using *E. coli* MG1655, Kp209 or Kp209_CSTR (+Δ*E. coli* IgM, +ΔKp209 IgM, and +ΔKp209_CSTR IgM, respectively). (**e**) IgM binding to Kp209, Kp209_CSTR, and Kp209_CSTR Tn::*phoQ* mutants in 10% NHS depleted using Kp209. Data represent mean ± standard deviation of 2 independent experiments. (**b&e**) IgG and IgM binding was performed in 0.3% and 10% (depleted) NHS, respectively. Binding was detected using anti-hu-IgG-AF647 or anti-hu-IgM-FITC by flow cytometry. Flow cytometry data are represented by geometric mean fluorescent intensity (gMFI) values of bacterial populations. (**c&d**) Bacteria were incubated at 37 °C in the presence of 1 µM SYTOX green nucleic acid stain, and inner membrane permeabilization (SYTOX fluorescence intensity) was detected after 60 minutes. (**b-d**) Data represent mean ± standard deviation of three independent experiments. (**b-e**) Statistical analysis was performed using a paired one-way ANOVA with a Tukey's multiple comparisons test on SYTOX fluorescence intensity (**c&e**) or Log_{10}-transformed gMFI data (**b&d**). Significance is shown as *p≤0.05; ** p≤0.005; ***p≤0.005, **** p≤0.0005.

The finding that NHS contained Kp209_CSTR-specific IgM raised the question whether IgM played a role in classical pathway activation. Therefore, we incubated Kp209_CSTR in Kp209_CSTR-depleted NHS and observed that membrane permeabilization was reduced (fig. 5c). Membrane permeabilization of *E. coli* was not altered in Kp209_CSTR-depleted NHS, indicating that the membrane permeabilizing potential was not affected by the depletion (supplementary fig. 5). To test if IgM was required for membrane permeabilization of Kp209_CSTR, we supplemented Kp209_CSTR-depleted NHS with polyclonal IgG or IgM purified from NHS and monitored bacterial membrane permeabilization. Addition of polyclonal IgM fully restored membrane permeabilization on Kp209_CSTR, whereas polyclonal IgG did not (fig. 5c). Similar results were obtained when Kp209_CSTR-depleted NHS was supplemented with isolated IgM of individual donors (supplementary fig. 5). NHS depletion using Kp209 or *E. coli* did not affect complement-mediated membrane damage on Kp209_CSTR, indicating that components required for complement activation on Kp209_CSTR were still present (fig. 5c). This suggested that KP209_CSTR-specific IgM was responsible for complement-mediated membrane damage.

To verify that Kp209_CSTR-specific IgM was responsible for classical pathway activation, we used the antibody depletion technique to deplete polyclonal IgM isolated form NHS. Similar to NHS, depletion of polyclonal IgM with Kp209 reduced the IgM binding to Kp209_CSTR but again residual binding was observed, confirming the presence of Kp209_CSTR-specific IgM (supplementary fig. 5). Depletion of polyclonal IgM using Kp209 or Kp209_CSTR did not affect binding to *E. coli* (supplementary fig. 5). Next, we supplemented NHS depleted with Kp209_CSTR with the different

preparations of IgM to study the effect on membrane permeabilization of Kp209_CSTR. IgM depleted with Kp209 or *E. coli* was able to restore membrane permeabilization on Kp209_CSTR, in contrast to IgM depleted with Kp209_CSTR (fig. 5d). This confirmed that Kp209_CSTR-specific IgM is crucial for antibody driven complement activation on Kp209_CSTR. As Kp209_CSTR has a constitutively active PhoQ, we were curious if Kp209_CSTR-specific IgM binding would be lost after *phoQ* disruption. To this end, we incubated the Kp209_CSTR Tn::*phoQ* mutants with Kp209-depleted NHS and measured IgM binding (fig. 5e). IgM binding to the Tn::*phoQ* mutants was comparable to the binding signal observed for Kp209. This indicates that PhoQ activity is required for Kp209_CSTR-specific IgM binding. In summary, we found that human serum contains IgM specific for Kp209_CSTR that induces MAC-mediated inner membrane damage.

Discussion

Membrane attack complex (MAC) insertion into the outer membrane is important for the direct killing of Gram-negative bacteria by the complement system. In the past, resistance against the membrane-targeting antibiotic colistin has been shown to influence sensitivity to serum in Gram-negative bacteria [8,12]. Here, we aimed to study the effect of developing colistin resistance on MAC-mediated killing of *K. pneumoniae*. Of the three colistin resistant strains tested, both Kp209_CSTR and Kp257_CSTR became more MAC-sensitive. The *phoQ* mutations responsible for colistin resistance in these strains enhanced expression of PhoQ regulated genes, indicating that a more active form of PhoQ leads to increased MAC-sensitivity. *Vice versa*, inactivation of *phoQ* in Kp209_CSTR decreased MAC-dependent membrane permeabilization and colistin resistance. Finally, we demonstrated that MAC-mediated membrane permeabilization of Kp209_CSTR in NHS was activated by IgM that specifically recognized Kp209_CSTR.

The finding that MAC-mediated membrane permeabilization of Kp209_CSTR is driven by Kp209_CSTR-specific IgM suggests that an epitope for IgM becomes exposed on Kp209_CSTR due to the mutation in *phoQ*. This epitope might be shielded by capsular polysaccharides on the wild-type Kp209, and becomes available on Kp209_CSTR due to the reduction in capsule production. A role for a thicker capsule in shielding bacterial outer membrane and associated antigens from recognition by antibodies was demonstrated in previous studies. For example, chemical repression of capsule

production by *K. pneumoniae* was demonstrated to lead to enhanced monoclonal antibody binding to the LPS [26,27]. Similarly, reduced capsule production due to genetic modifications changed the ability of the capsule to shield outer membrane proteins of *K. pneumoniae* [28,29].

NHS and IgM was isolated from healthy donors with no described prior exposure to *K. pneumoniae*. The question remains why NHS contained IgM that specifically recognized Kp209_CSTR. One possibility is that the IgM that targeted Kp209_CSTR was a natural antibody, which are defined as germline-encoded antibodies expressed without any known direct antigenic stimulus [30]. Natural antibodies targeting bacterial antigens have been found in mice, and are assumed to exist in humans as well [31]. On the other hand, *K. pneumoniae* is a human commensal residing in the gut microbiota and nasopharynx, and estimations of gastrointestinal carriage in the western world range from 5 to 45% [32,33]. It is therefore probable that the serum IgM binding to Kp209_CSTR is part of a specific antibody response against antigens originating from commensal *K. pneumoniae.* This is supported by reports that healthy individuals produce both IgM and IgG antibodies recognizing *K. pneumoniae* [34–38]. Furthermore, the antibodies of healthy donors recognizing *K. pneumoniae* antigens belonging to the IgG, IgA and IgM isotypes can be highly affinity-maturated [39,40].

Only a minority of IgMs that bound to the surface of Kp209_CSTR were essential for inducing MAC-mediated membrane permeabilization. A large part of the IgM that bound Kp209_CSTR also bound to Kp209, but only the Kp209_CSTR-specific IgM was crucial for triggering inner membrane permeabilization. This indicates that the IgM target is an important determinant for MAC-dependent membrane damaging effects. This difference might relate to the location of the target in relation to the outer membrane. For *K. pneumoniae* it has been reported that MAC deposition needs to occur close to the outer membrane to be bactericidal, and that localization of MAC far from the outer membrane prevents bacterial lysis [41]. This would suggest that the target of the bactericidal IgM would be located in close proximity to the outer membrane. However, it remains unclear which epitope the bactericidal IgM targets. Due to the large number of alternatively expressed genes, it was not possible to pinpoint a target using the transcriptomics data for Kp209_CSTR. We observed increased expression for several outer membrane proteins, fimbriae, porin, and efflux pump genes, as well as for genes involved in LPS modification, indicating that both surface proteins and LPS remain potential targets [26,42,43]. Further studies might elucidate which surface

structures are targeted, but this will be complicated due the polyclonal nature of IgM. For now, it remains unclear whether the Kp209_CSTR-specific IgM binding that specifically recognizes Kp209_CSTR is monoclonal and bind to one antigen, or a polyclonal mixture that targets multiple different epitopes.

We found that colistin resistance mutations in *phoQ* had an opposite effect on the MAC sensitivity of Kp209_CSTR and Kp257_CSTR. This might be explained by the different mode of action between colistin and MAC. Although colistin and MAC both interact with and destabilize bacterial membranes, their mechanisms are critically different. Colistin is a small amphipathic molecule attracted to the cell envelope via electrostatic interactions, where it inserts into and destabilizes the bacterial membranes [6]. Antibody-induced MAC deposition is initiated after specific recognition of bacterial surface structures by antibodies. This activates the classical complement cascade, resulting in sequential deposition of complement components on the bacterial surface. Only in the final stages of the complement cascade, when C5 convertases are being deposited, membrane piercing MAC pores can be formed [13]. As colistin and MAC both target bacterial membranes, but act via different mechanisms, becoming resistant to colistin could have a different effect on MAC sensitivity, which was the case for Kp209_CSTR and Kp257_CSTR.

In contrast to Kp209_CSTR and Kp257_CSTR, colistin resistance did not enhance MAC sensitivity of Kp040_CSTR under the tested conditions. This indicates that colistin resistance can occur without influencing MAC sensitivity. There have been two previous reports on *K. pneumoniae* and *E. coli* where it was shown that colistin resistant mutants were more serum sensitive compared to wild-type strains [8,12]. For *E. coli*, increased serum sensitivity was found in two of the three tested strains, indicating that also for *E. coli* colistin resistance not always leads to increases serum sensitivity [8]. The previous study on *K. pneumoniae* showed that all three tested strains became more serum sensitive [12]. These were all ST23, whereas strains tested in our study belong to different sequence types. This suggests that in different genetic backgrounds serum sensitivity can be affected differently after acquiring colistin resistance. Overall, there is a connection between colistin resistance and increased MAC-sensitivity, but variation between different strains remains to be explained.

Transcriptome analysis revealed that the WAQRN-97-C deletion in the sensory domain of PhoQ led to a constitutively active form of PhoQ in Kp209_CSTR [9,19]. The

tryptophan residue at position 97 (W-97) is essential to the sensory function of PhoQ in *S. enterica*, and its loss results in a constitutively active PhoQ [20,21]. In concordance with our own results, a deletion in the PhoQ sensory domain in one of previously reported *K. pneumoniae* ST23 led to upregulation of PhoPQ regulated genes, indicating that PhoQ was more active [12]. We found that PhoQ activity influences capsule production, which might play a role in binding of Kp209_CSTR-specific IgM. Transcriptomic analysis revealed that expression of capsule genes was not altered, suggesting that all the capsule producing machinery should be present in Kp209_CSTR. This suggests that capsule production was not affected on a transcriptional level, but at a later stage of capsule synthesis. It has been postulated that addition of 4-amino-4-deoxy-L-arabinose (L-Ara4N) to lipid A, one of the modifications observed for Kp209_CSTR, could influence capsule production [9,44]. The precursor of L-Ara4N, UDP-glucuronic acid, is also required for capsule production [44–46]. Increased L-Ara4N synthesis would limit the availability of UDP-glucuronic acid, thereby reducing capsule production. This is supported by reports that capsule production can be enhanced by mutating LPS synthesis genes in *E. coli* [45]. UDP-glucuronic acid is converted to L-Ara4N by the Arn pathway. In line with the hypothesis, genes of the Arn pathway, which is responsible for conversion of UDP-glucuronic adic into L-Ara4N, were strongly upregulated in Kp209_CSTR. The *arn* operon is under control the PmrAB two-component system, which is activated by PmrD [47]. The expression of *pmrD* is regulated by PhoPQ and was strongly upregulated in Kp209_CSTR as a result of the mutations in *phoQ* [18].

As the number of antibiotic resistant *K. pneumoniae* strains rises, infections with these bacteria becomes an increasing risk to human health. Studying how the complement system kills *K. pneumoniae* will reveal new insights in the infection biology of *K. pneumoniae*. Understanding the interaction between killing of *K. pneumoniae* by the immune system and antibiotics will help to improve treatment of *K. pneumoniae* infections.

Methods

Bacterial strains

Klebsiella pneumoniae clinical isolates were collected during routine diagnostics in the medical microbiology department in the University Medical Centre Utrecht, The Netherlands. *Klebsiella pneumoniae* Kp209, Kp257 and Kp040, and their colistin

resistant daughter strains were kindly provided by Axel Janssen (University Medical Centre Utrecht, The Netherlands; University of Lausanne, Switzerland;[9]). KPPR1S and KPPR1S*ΔwcaJ* were kindly provided by Kimberly Walker (University of North Carolina, USA;[48]). For the experiments with *Escherichia coli*, the laboratory strain MG1655 was used.

Serum preparation and reagents

Normal human serum (NHS) was prepared as described before [13]. In short, blood was drawn from healthy volunteers, allowed to clot, and centrifuged to separate serum from the cellular fraction. Serum of 15-20 donors was pooled and stored at -80 °C. Heat inactivation (Hi) of NHS was achieved by incubating NHS at 56 °C for 30 minutes. OMCI was produced and purified as previously described [49]. RPMI (ThermoFisher) supplemented with 0.05% human serum albumin (HSA, Sanquin), further referred to as RPMI buffer, was used in all experiments, unless otherwise stated. Eculizumab was kindly provided by Frank Beurskens, Genmab, Utrecht, The Netherlands. Sera deficient from factor B (fB) and complement component C2 were obtained from Complement Technology. Purified factor B and C2 were produced by U-protein express (Utrecht, The Netherlands). C1r protease inhibitor BBK32 was kindly provided by Brandon Garcia, Greenville, NC, USA. Monoclonal mouse anti-hu-C1q IgG1 4A4B11 was produced in house (ATCC HB-8327) [25,50].

Bacterial growth

For all experiments, bacteria were cultured on Lysogeny broth (LB) 1.5% agar plates at 37 °C, unless stated otherwise. Single colonies were picked and cultured overnight in liquid LB medium at 37 °C while shaking. The following day the bacteria were subcultured by diluting the overnight culture 1/100 in fresh medium and grown to OD_{600}= 0.4-0.5 at 37 °C while shaking. Bacteria were washed twice with RPMI buffer by centrifugation at 10,000 g for two minutes and resuspended to OD_{600}= 0.5 in RPMI buffer. For the Kp209_CSTR Tn mutants, both solid and liquid medium were supplemented with 30 µg/ml kanamycin.

Bacterial viability assay

Bacteria (OD_{600}= 0.05) were incubated in serum diluted in RPMI buffer. In the conditions where C5 conversion was blocked to prevent the initiation to the terminal complement pathway, 20 µg/ml OMCI + 20 µg/ml Eculizumab was added. After incubation at 37 °C, 10-fold serial dilutions in RPMI buffer were prepared and plated. Colony forming units

were determined on LB agar plates after culturing the bacteria on plate over night at 37 °C. Survival in NHS was normalized to NHS in which C5 conversion was inhibited ((#NHS/#C5 inhibition) *100%), or to NHS in which complement was heat inactivated ((#NHS/#HiNHS) *100%).

Membrane permeabilization

Bacteria (OD_{600}= 0.05) were incubated in serum or colistin diluted in RPMI buffer in the presence of 1 µM SYTOX Green Nucleic Acid stain (ThermoFisher). Bacteria were incubated at 37 °C under shaking conditions. Fluorescence was determined in a microplate reader (CLARIOstar, Labtech) using an excitation wavelength of 490-14 nm and an emission wavelength of 537-30 nm.

Antibody deposition

Bacteria (OD_{600}= 0.05) were incubated in HiNHS diluted in RPMI buffer for 30 minutes at 4 °C under shaking conditions. Bacteria were washed twice by centrifugation with RPMI buffer, resuspended 1 µg/ml goat anti-hu-IgG-AF647 (2040-31, SouthernBiotech) or 2 µg/ml goat anti-hu-IgM-FITC (202002, SouthernBiotech) for 30 minutes at 4 °C while shaking. Bacteria were washed twice with RPMI buffer and fixated in 1.5% paraformaldehyde in PBS for five minutes. Fluorescence was determined via flow cytometry (MACSQuant, Milteny Biotech), acquiring 10,000 events per condition. Flow cytometry data was analysed in FlowJo V.10. Bacteria were gated based on the forward and side scatter, and AF647 and FITC geometric mean fluorescence intensity was determined for the bacterial population.

Serum depletion with bacterium

Bacteria (OD_{600}= 1.0) were incubated in ice cold NHS (20% in RPMI buffer). After a 10minute incubation on ice while shaking, bacteria were pelleted in a cooled centrifuge (two minutes at 10.000 g) and the bacterium depleted NHS was collected. The depletion steps were preformed trice in total. Antibody depletion was verified via flow cytometry.

Polyclonal IgG and polyclonal IgM isolation from NHS

IgG and IgM were isolated from NHS as previously described [25]. In short, IgG was isolated using 5 ml HiTrap Protein G High Performance column (GE Healthcare), whereas IgM was isolated using POROS™ CaptureSelect™ IgM Affinity Matrix (ThermoScientific) in a XK column (GE Healtcare) using an ÄKTA FPLC system. After

capture antibodies were eluted according to the manufacturer's instructions. Collected antibodies were dialyzed overnight against PBS at 4 °C, and stored at -80 °C.

Transcriptome analysis

RNA extraction

Subcultures of Kp209 and Kp209_CSTR were grown to OD_{600}=0.5-0.6 at 37 °C while shaking. RNA was isolated using the hot phenol-chloroform method. Briefly, bacterial were incubated in hot phenol lysis solution (1% SDS, 2 mM EDTA, 40 mM sodium acetate in acid phenol (Invitrogen #15594-047)) for 45 minutes at 65 °C. Total RNA was purified by successive steps of phenol-chloroform extraction, followed by an extraction with cold chloroform. After ethanol precipitation, genomic DNA was digested by Turbo DNAse (Invitrogen #AM1907) treatment. Total RNA quantity and quality were assessed using an Agilent Bioanalyzer.

RNA-seq libraries construction.

Ribosomal RNAs (rRNAs) depletion was performed using Ribominus bacteria 2.0 transcriptome isolation kit (Invitrogen) according to manufacturer's instructions. Depletion efficacy was verified on an Agilent Bioanalyzer using RNA pico chips and remaining RNAs were concentrated using ethanol precipitation. The Collibri stranded RNA library prep kit for Illumina (Invitrogen) was used to build cDNA libraries for sequencing starting from 15 ng of RNA according to manufacturer's instructions. cDNA libraries quality and concentration were assessed using an Agilent Bioanalyzer High sensitivity DNA chip. RNA-seq was performed in biological triplicates.

Sequencing and data analysis.

Sequencing was performed by the Montpellier GenomiX platform (MGX, https://www.mgx.cnrs.fr/) using an Illumina Novaseq instrument. Following quality control, Bowtie2 was used for sequencing reads mapping [51,52] onto the genome of Kp209 available on the European Nucleotide Archive under accession number PRJEB29521 [9], previously annotated with Prokka. The read count per feature was calculated using Ht-seq count [53]. Finally, differential gene expression between the Kp209 and Kp209_CSTR strains was performed using DESeq2 [54].

RNA isolation, reverse transcription and real-time PCR

Subcultures of Kp257 and Kp257_CSTR were grown to OD_{600}=0.5 at 37 °C while shaking. Total RNA was isolated for three biological replicates per strain using the RNeasy Protect Bacteria Kit (74524, QIAGEN) the manufacturer's protocol, using lysozyme (L6876, Sigma-Aldrich) and proteinase K (19131, QIAGEN) to lyse the bacteria. DNA was digested on column using the RNase-Free DNase set (79254, QIAGEN), and isolated RNA was subsequently treated with RNase-free DNase I (M0303, New England BioLabs) to remove residual genomic DNA according to the manufacturer's protocols. RNA was converted to cDNA by reverse transcription using the iScript cDNA Synthesis Kit (1708890, BioRad) according to the manufacturer's protocols. Real-time PCR was performed using 2x FastStart Universal SYBER Green Master (Rox) (4913850001, Roche), with each primer at 300 nM and 0.5 ng cDNA input. Primers (supplementary table 2) for *arnD* and *rpoB* were selected from previous publications [12,55]. Primers for *mgtE* designed using the PrimerQuest tool available on the webserver of Integrated DNA technologies using the coding sequence of *mgtE* of Kp257 [9]. Reactions were performed in triplicate on a StepOnePlus Real-Time PCR System (ThermoFisher), activating the FastStart Taq DNA polymerase for 10 minutes at 95 °C, followed by 40 cycles of denaturation at 95 °C for 15 seconds, and quantifications at 56 °C for 1 minute. Melt-curve analysis was performed from 56 °C to 95 °C a ramp of 0.5 °C every 5 seconds to assess primer specificity. Relative expression of *arnD* and *mgtE* compared to *rpoB* was calculated.

Transposon library and serum exposure

Kp209_CSTR was mutagenized via conjugation using strain WM3064 carrying the pKMW7 vector with a barcoded Tn5 transposon library as described previously [56]. Bacteria with a transposon insertion were selected using LB supplemented with kanamycin and the library was stored (OD_{600}= 1) at -80 °C. For serum exposure experiments, transposon library was 10-fold diluted in LB medium and cultured to mid-log (OD_{600}= 0.6). Bacteria were pelleted and resuspended in RPMI buffer. Washed bacteria (OD_{600}= 0.05) were incubated with RPMI buffer or 16% NHS for 2 hours at 37 °C. Samples were diluted 10-fold in LB medium and incubated overnight at 37 °C. The overnight culture was diluted 100-fold in fresh LB medium and challenged with 32% NHS for 2 hours at 37 °C followed by serial dilutions in PBS and plating on LB agar. Surviving colonies were picked that survived the 32% NHS challenge for further analysis.

Capsule production analysis

Capsule production was assessed by measuring the uronic acid content as previously described [48]. Briefly, 500 µl stationary phase bacteria grown in LB medium added to 100 µl 1% Zwittergent 3-14 detergent in citric acid (100 mM pH 2.0) and incubated at 50 °C for 20 minutes. 300 µl supernatant was collected after centrifugation (five minutes 16,000 g), mixed with 1200 µl 100% ethanol, and incubated at 4 °C overnight. After centrifugation (five minutes 16,000 g), the pellet was dissolved in 200 µl distilled water and 1200 µl tetraborate (12.5 mM in sulfuric acid) was mixed in by vortexing. After a five-minute incubation at 100 °C, the samples were cooled and 20 µl 3-hydroxydiphenol (0.15% in 0.5% sodium hydroxide) was added. Absorbance was measured at 520 nm. Uronic acid amounts were calculated from a standard curve prepared with glucuronolactone and normalized to the culture density (OD_{600}).

LPS silver stain

LPS silver stain was performed as previously described [57]. Briefly, single bacterial colonies were scraped of agar plates, and heat-inactivated at 56 °C for one hour, followed by protein digestion using proteinase K (400 µg/ml) for 90 minutes at 60 °C. Samples were diluted in 2x Laemmli buffer with 0.7 M β-mercaptoethanol, ran over a 4-12% BisTris gel and fixed overnight in ethanol (40% v/v) + glacial acetic acid (4% v/v). The gel was oxidised for five minutes in ethanol (40% v/v) + glacial acetic acid (4% v/v) + periodic acid (0.6% m/v) and stained for fifteen minutes in silver nitrate (0.6% m/v in 0.125 M sodium hydroxide + 0.3% ammonium hydroxide v/v). The gel was developed for seven minutes in citric acid (0.25% m/v) + formaldehyde (0.2% v/v).

Data analysis and statistical testing

Unless stated otherwise data collected as three biological replicates and analysed using GraphPad Prism version 9.4.1 (458). Statistical analyses are further specified in the figure legends.

Ethics statement

Human blood was isolated after informed consent was obtained from all subjects in accordance with the Declaration of Helsinki. Approval was obtained from the medical ethics committee of the UMC Utrecht, The Netherlands.

Data availability

The RNA-seq data generated in this study were deposited on the NCBI Gene Expression Omnibus (GEO) and is publicly available under the GSE212413 accession number (https://www.ncbi.nlm.nih.gov/geo/query/acc.cgi?acc=GSE212413). The datasets generated during and/or analysed during the current study are available from the corresponding author on reasonable request.

References

1. Murray, C. J. *et al.* Global burden of bacterial antimicrobial resistance in 2019: a systematic analysis. *The Lancet* **399**, 629–655 (2022).
2. Laxminarayan, R. *et al.* Antibiotic resistance-the need for global solutions. *The Lancet Infectious Diseases* **13**, 1057–1098 (2013).
3. Bush, K. *et al.* Tackling antibiotic resistance. *Nature Reviews Microbiology* **9**, 894–896 (2011).
4. Lin, Z., Yu, J., Liu, S. & Zhu, M. Prevalence and antibiotic resistance of *Klebsiella pneumoniae* in a tertiary hospital in Hangzhou, China, 2006–2020. *Journal of International Medical Research* **50**, (2022).
5. León-Sampedro, R. *et al.* Pervasive transmission of a carbapenem resistance plasmid in the gut microbiota of hospitalized patients. *Nat. Microbiol.* **6**, (2021).
6. Andrade, F. F., Silva, D., Rodrigues, A. & Pina-Vaz, C. Colistin update on its mechanism of action and resistance, present and future challenges. *Microorganisms* **8**, 1–12 (2020).
7. Sabnis, A. *et al.* Colistin kills bacteria by targeting lipopolysaccharide in the cytoplasmic membrane. *Elife* **10**, (2021).
8. Choi, Y. *et al.* Comparison of fitness cost and virulence in chromosome- and plasmid-mediated colistin-resistant *Escherichia coli*. *Front. Microbiol.* **11**, 798 (2020).
9. Janssen, A. B. *et al.* Evolution of colistin resistance in the *Klebsiella pneumoniae* complex follows multiple evolutionary trajectories with variable effects on fitness and virulence characteristics. *Antimicrob. Agents Chemother.* **65**, (2021).
10. López-Rojas, R. *et al.* Impaired virulence and *in vivo* fitness of colistin-resistant *Acinetobacter baumannii*. *Journal of Infectious Diseases* **203**, 545–548 (2011).
11. Bray, A. S. *et al.* MgrB-dependent colistin resistance in *Klebsiella pneumoniae* is associated with an increase in host-to-host transmission. *mBio* **13**, (2022).
12. Choi, M. J. & Ko, K. S. Loss of hypermucoviscosity and increased fitness cost in colistin-resistant *Klebsiella pneumoniae* sequence type 23 strains. *Antimicrob. Agents Chemother.* **59**, 6763–6773 (2015).
13. Heesterbeek, D. A. *et al.* Bacterial killing by complement requires membrane attack complex formation via surface-bound C5 convertases. *EMBO J.* **38**, e99852 (2019).
14. Lacour, S., Bechet, E., Cozzone, A. J., Mijakovic, I. & Grangeasse, C. Tyrosine phosphorylation of the UDP-glucose dehydrogenase of *Escherichia coli* is at the crossroads of colanic acid synthesis and polymyxin resistance. *PLoS One* **3**, (2008).
15. Yang, T. Y. *et al.* Contributions of insertion sequences conferring colistin resistance in *Klebsiella pneumoniae*. *Int. J. Antimicrob. Agents* **55**, (2020).
16. Olaitan, A. O., Morand, S. & Rolain, J. M. Mechanisms of polymyxin resistance: Acquired and intrinsic resistance in bacteria. *Frontiers in Microbiology* **5**, (2014).
17. Poirel, L., Jayol, A. & Nordmanna, P. Polymyxins: Antibacterial activity, susceptibility testing, and resistance mechanisms encoded by plasmids or chromosomes. *Clinical Microbiology Reviews* **30**, (2017).
18. Groisman, E. A. The pleiotropic two-component regulatory system PhoP-PhoQ. *Journal of Bacteriology* **183**, 1835–1842 (2001).
19. Lemmin, T., Soto, C. S., Clinthorne, G., DeGrado, W. F. & Dal Peraro, M. Assembly of the transmembrane domain of *E. coli* PhoQ histidine kinase: implications for signal transduction from molecular simulations. *PLoS Comput. Biol.* **9**, e1002878 (2013).
20. Chamnongpol, S., Cromie, M. & Groisman, E. A. Mg2+ sensing by the Mg2+ sensor PhoQ of *Salmonella enterica*. *J. Mol. Biol.* **325**, 795–807 (2003).

21. García Véscovi, E. & Soncini, F. C. Mg2+ as an extracellular signal: environmental regulation of *Salmonella* virulence. *Cell* **84**, (1996).

22. Kato, A., Tanabe, H. & Utsumi, R. Molecular characterization of the PhoP-PhoQ two-component system in *Escherichia coli* K-12: Identification of extracellular Mg2+-responsive promoters. *J. Bacteriol.* **181**, 5516–5520 (1999).

23. McGonigal, R. *et al.* C1q-targeted inhibition of the classical complement pathway prevents injury in a novel mouse model of acute motor axonal neuropathy. *Acta. Neuropathol. Commun.* **4**, 23 (2016).

24. Garcia, B. L., Zhi, H., Wager, B., Höök, M. & Skare, J. T. *Borrelia burgdorferi* BBK32 inhibits the classical pathway by blocking activation of the C1 complement complex. *PLoS Pathog.* **12**, e1005404 (2016).

25. Zwarthoff, S. A. *et al.* C1q binding to surface-bound IgG is stabilized by C1r2s2 proteases. *Proc. Natl. Acad. Sci. USA* **118**, e2102787118 (2021).

26. Domenico, P., Tomas, J. M., Merino, S., Rubires, X. & Cunha, B. A. Surface antigen exposure by bismuth dimercaprol suppression of *Klebsiella pneumoniae* capsular polysaccharide. *Infect. Immun.* **67**, 664–669 (1999).

27. Salo, R. J. *et al.* Salicylate-enhanced exposure of *Klebsiella pneumoniae* subcapsular components. *Infection* **23**, 371–377 (1995).

28. Held, T. K., Jendrike, N. R. M., Rukavina, T., Podschun, R. & Trautmann, M. Binding to and opsonophagocytic activity of O-antigen-specific monoclonal antibodies against encapsulated and nonencapsulated Klebsiella pneumoniae serotype O1 strains. *Infect. Immun.* **68**, 2402–2409 (2000).

29. Merino, S., Camprubi, S., Alberti, S., Benedi, V. J. & Tomas, J. M. Mechanisms of *Klebsiella pneumoniae* resistance to complement-mediated killing. *Infect. Immun.* **60**, 2529–2535 (1992).

30. Holodick, N. E., Rodríguez-Zhurbenko, N. & Hernández, A. M. Defining natural antibodies. *Front. Immunol.* **8**, 872 (2017).

31. Zhou, Z. H. *et al.* The broad antibacterial activity of the natural antibody repertoire is due to polyreactive antibodies. *Cell Host Microbe* **1**, 51–61 (2007).

32. Lepuschitz, S. *et al.* Fecal *Klebsiella pneumoniae* carriage is intermittent and of high clonal diversity. *Front. Microbiol.* **11**, 2962 (2020).

33. Shimasaki, T. *et al.* Increased relative abundance of *Klebsiella pneumoniae* carbapenemase-producing *Klebsiella pneumoniae* within the gut microbiota is associated with risk of bloodstream infection in long-term acute care hospital patients. *Clinical Infectious Diseases* **68**, 2053–2059 (2019).

34. Lepper, P. M., Möricke, A., Held, T. K., Schneider, E. M. & Trautmann, M. K-antigen-specific, but not O-antigen-specific natural human serum antibodies promote phagocytosis of *Klebsiella pneumoniae*. *FEMS Immunol. Med. Microbiol.* **35**, 93–98 (2003).

35. DeLeo, F. R. *et al.* Survival of carbapenem-resistant *Klebsiella pneumoniae* sequence type 258 in human blood. *Antimicrob. Agents Chemother.* **61**, (2017).

36. Garbett, N. D., Munro, C. S. & Cole, P. J. Opsonic activity of a new intravenous immunoglobulin preparation: Pentaglobin compared with Sandoglobulin. *Clin. exp. Immunol.* **76**, (1989).

37. Rossmann, F. S. *et al. In vitro* and *in vivo* activity of hyperimmune globulin preparations against multiresistant nosocomial pathogens. *Infection* **43**, 169–175 (2015).

38. Kobayashi, S. D. *et al.* Antibody-mediated killing of carbapenem-resistant ST258 *Klebsiella pneumoniae* by human neutrophils. *mBio* **9**, (2018).

39. Rollenske, T. *et al.* Cross-specificity of protective human antibodies against *Klebsiella pneumoniae* LPS O-antigen. *Nature Immunology* **19**, 617–624 (2018).

40. Pennini, M. E. *et al.* Immune stealth-driven O2 serotype prevalence and potential for therapeutic antibodies against multidrug resistant *Klebsiella pneumoniae*. *Nat. Commun.* **8**, 1–12 (2017).

41. Jensen, T. S. *et al.* Complement mediated *Klebsiella pneumoniae* capsule changes. *Microbes. Infect.* **22**, 19–30 (2020).
42. Xin Wang-Lin, S. *et al.* The capsular polysaccharide of *Acinetobacter baumannii* is an obstacle for therapeutic passive immunization strategies. *IAI* **85**, (2017).
43. Serushago, B. A., Mitsuyama, M., Handa, T., Koga, T. & Nomoto, K. Role of antibodies against outer-membrane proteins in murine resistance to infection with encapsulated *Klebsiella pneumoniae*. *J. Gen. Microbiol.* **135**, 2259–2268 (1989).
44. Grangeasse, C. *et al.* Autophosphorylation of the *Escherichia coli* protein kinase Wzc regulates tyrosine phosphorylation of Ugd, a UDP-glucose dehydrogenase. *Journal of Biological Chemistry* **278**, 39323–39329 (2003).
45. Wang, C. *et al.* Colanic acid biosynthesis in *Escherichia coli* is dependent on lipopolysaccharide structure and glucose availability. *Microbiol. Res.* **239**, (2020).
46. Rodrigues, C., Sousa, C., Lopes, J. A., Novais, Â. & Peixe, L. A front line on *Klebsiella pneumoniae* capsular polysaccharide knowledge: fourier transform infrared spectroscopy as an accurate and fast typing tool. *mSystems* **5**, (2020).
47. Dalebroux, Z. D. & Miller, S. I. Salmonellae PhoPQ regulation of the outer membrane to resist innate immunity. *Current Opinion in Microbiology* **17**, 106–113 (2014).
48. Walker, K. A., Treat, L. P., Sepúlveda, V. E. & Miller, V. L. The small protein rmpd drives hypermucoviscosity in *Klebsiella pneumoniae*. *mBio* **11**, 1–14 (2020).
49. Nunn, M. A. *et al.* Complement inhibitor of C5 activation from the soft tick *Ornithodoros moubata*. *The Journal of Immunology* **174**, 2084–2091 (2005).
50. Reckel, R. P., Harris, J. L., Wellerson, R. J., Shaw, S. M. & Kaplan, P. M. Method for detecting immune complexes in serum. (1986).
51. Seemann, T. Prokka: rapid prokaryotic genome annotation. *Bioinformatics* **30**, 2068–2069 (2014).
52. Langmead, B. & Salzberg, S. L. Fast gapped-read alignment with Bowtie 2. *Nature Methods* **9**, 357–359 (2012).
53. Anders, S., Pyl, P. T. & Huber, W. HTSeq-A Python framework to work with high-throughput sequencing data. *Bioinformatics* **31**, 166–169 (2015).
54. Love, M. I., Huber, W. & Anders, S. Moderated estimation of fold change and dispersion for RNA-seq data with DESeq2. *Genome Biol* **15**, 1–21 (2014).
55. Patole, S., Rout, M. & Mohapatra, H. Identification and validation of reference genes for reliable analysis of differential gene expression during antibiotic induced persister formation in *Klebsiella pneumoniae* using qPCR. *J. Microbiol. Methods* **182**, (2021).
56. Wetmore, K. M. *et al.* Rapid quantification of mutant fitness in diverse bacteria by sequencing randomly bar-coded transposons. *mBio* **6**, 1–15 (2015).
57. Doorduijn, D. J. *et al.* Polymerization of C9 enhances bacterial cell envelope damage and killing by membrane attack complex pores. *PLoS Pathog.* **17**, e1010051 (2021).

Author contributions

S.P.A.vdL., S.H.M.R., B.W.B. conceived the project. S.P.A.vdL. and M.R. performed serum depletion with bacteria, the membrane permeabilization assays, bacterial viability assays and antibody deposition assays. D.J.D. performed the LPS silver stain. K.A.W. performed the capsule production analysis. B.W.B and F.M.M. created the Kp209_CSTR transposon library. B.W.B. selected the serum resistant Kp209_CSTR transposon mutants and performed the *phoQ* transposon insertion analysis. M.J.M and M.R. performed the RNA isolation, M.J.M. constructed the RNA-seq libraries, and performed the sequence and data analysis. S.P.A.vdL., S.H.M.R. and B.W.B. wrote the manuscript. D.J.D., A.B.J., W.S., F.M.M., M.J.M., I.A. and K.A.W. proofread the manuscript before submission.

Additional information

Acknowledgments

The authors would like to thank Frank Beurskens (Genmab) for providing Eculizumab, Brandon Garcia for providing BBK32, and Marieke Nuhn for assistance with the real-time PCR. Image fig. 5a was created by Sjors van der Lans using Adobe Illustrator v27.7.

Competing interests

The authors declare no competing interests.

Financial disclosure statement

This work was supported by the Netherlands Organization for Scientific Research (NWO) through a TTW-NACTAR Grant #16442 (to SvdL and SHMR) and the European Union's Horizon 2020 research programs 787 H2020-EU-ITN-EJD (CORVOS #860044 to FM and SHMR). The funders had no role in the study design, data collection and analysis, or preparation of the manuscript.

Supplementary information

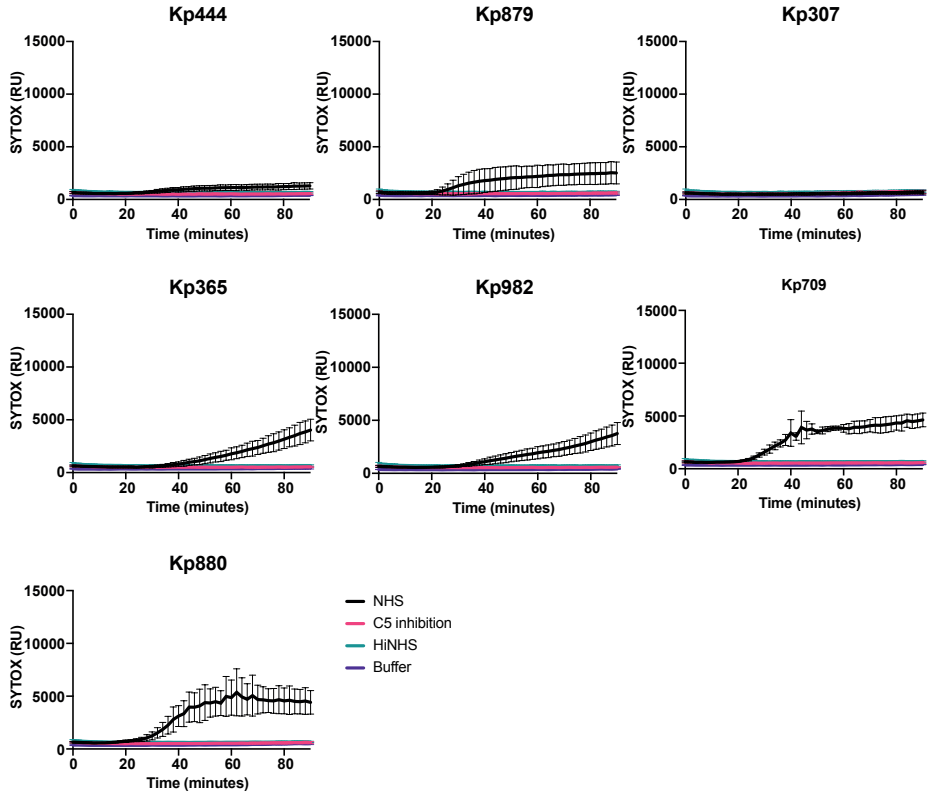

Supplementary figure 1

Inner membrane permeabilization of Kp444, Kp879, Kp307, Kp365, Kp982, Kp709 and Kp880 in time. Bacteria were incubated in the presence of 10% NHS, 10% NHS in which C5 conversion was inhibited by addition of 20 µg/ml OMCI and 20 µg/ml Eculizumab (C5 inhibition), or 10% heat inactivated NHS (HiNHS), at 37 °C in the presence of 1 µM SYTOX green nucleic acid stain, and inner membrane permeabilization (SYTOX fluorescence intensity) was detected every 2 minutes for 90 minutes in a microplate reader. Data represent mean ± standard deviation of three independent experiments.

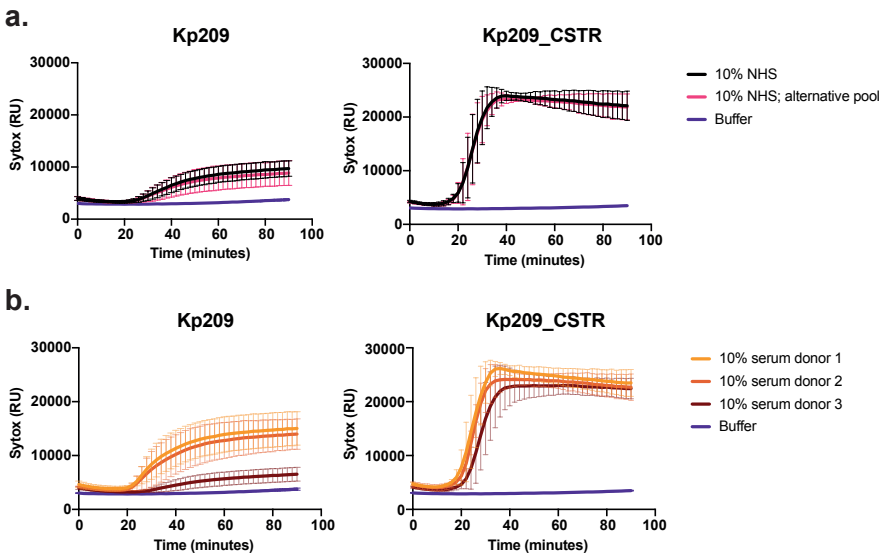

Supplementary figure 2

(**a**) Inner membrane permeabilization of Kp209 and Kp209_CSTR in the presences of (**a**) 10% NHS composed of sera from different pools of donors, or (**b**) 10% serum from different individual donors. (a&b) Bacteria were incubated at 37 °C in the presence of 1 µM SYTOX green nucleic acid stain, and inner membrane permeabilization (SYTOX fluorescence intensity) was detected every 2 minutes for 90 minutes in a microplate reader. Data represent mean ± standard deviation of three independent experiments.

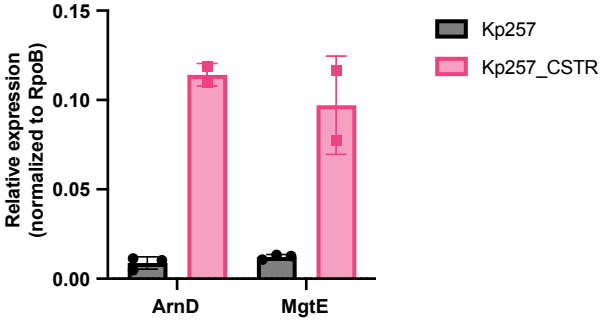

Supplementary figure 3

RNA was isolated from log phase Kp257 and Kp257_CSTR, and converted to cDNA. The relative expression of the *arnD* and *mgtE* genes compared to the *rpoB* control gene was determined by real-time PCR for both Kp257 and Kp257_CSTR. Real-time PCR was performed in triplicates. Data represent mean ± standard deviation of at least two independent biological replicates.

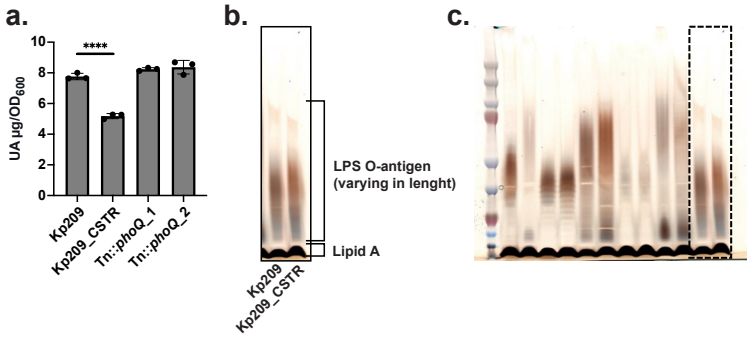

Supplementary figure 4

(**a**) Capsule production of Kp209 and Kp209_CSTR, and the Kp209_CSTR Tn::*phoQ* mutants was determined by measuring uranic acid content. Absorbance was measured at 520 nm, the uronic acid content calculated using a glucuronolactone standard curve and normalized to the culture density at 600 nm. Data represent mean ± standard deviation of three independent experiments. (F) Statistical analysis was performed using a paired one-way ANOVA with a Tukey's multiple comparisons test. Significance is shown as ****p≤0.0005. (**b**) SDS-PAGE silver stain of Kp209 and Kp209_CSTR LPS. Bacterial lysates were digested with protein K to remove all proteins and loaded on an SDS-PAGE gel. The LPS lipid A could, based on size, be distinguished from the O-antigen, which can have various lengths. Image is a representative of two independent experiments. Original gel is presented in supplementary figure S2c. (c) Original gel of the SDS-PAGE silver stain containing of Kp209 and Kp209_CSTR LPS, indicated with dashed lines.

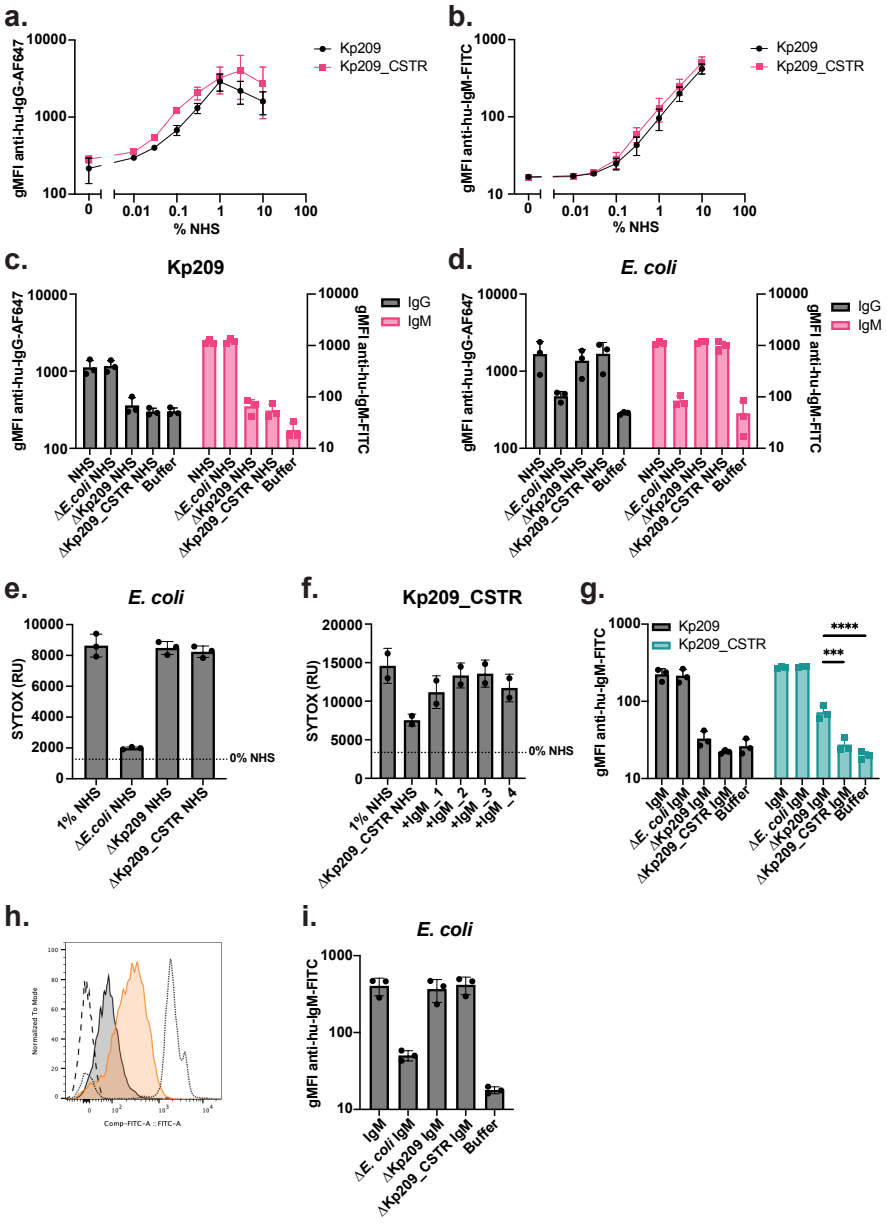

Supplementary figure 5

(**a&b**) Total IgG (**a**) and IgM (**b**) binding to Kp209 and Kp209_CSTR in normal human serum (NHS). (**c&d**) IgG and IgM binding to Kp209 (**c**) and *E. coli* MG1655 (**d**) in NHS depleted using *E. coli* MG1655, Kp209 or Kp209_CSTR (Δ*E. coli* NHS, ΔKp209 NHS, and ΔKp209_CSTR NHS, respectively). (**e&f**) Inner membrane permeabilization of *E. coli* MG1655 (**e**) and Kp209_CSTR (**f**) in the presence of 1% NHS, Δ*E. coli* NHS, ΔKp209 NHS, or ΔKp209_CSTR NHS (**f**) ΔKp209_CSTR NHS was supplemented with physiological concentrations of IgM (+IgM; 15 µg/ml in 1% NHS) isolated from individual serum

donors. (**g**) IgM binding to Kp209 and Kp209_CSTR in IgM isolated from NHS, or isolated IgM depleted using *E. coli* MG1655, Kp209 or Kp209_CSTR (Δ*E. coli* IgM, ΔKp209 IgM, and ΔKp209_CSTR IgM, respectively). (**h**) IgM binding to Kp209 and Kp209_CSTR with IgM isolated from NHS (dotted), IgM depleted with Kp209 (grey) or Kp209_CSTR (orange). Slitted line corresponds to the buffer control. Fluorescent intensity (gMFI) and number of events normalized to mode are depicted on the X- and Y-axis, respectively. The graph is representative for three independent repeats. (**i**) IgM biding to *E. coli* MG1655 in IgM isolated from NHS, Δ*E. coli* IgM, ΔKp209 IgM, or ΔKp209_CSTR IgM. (**a-d&g-i**) IgG binding was performed in 0.3% NHS. IgM binding was performed in 10% (depleted) NHS or 45 µg/ml (depleted) IgM isolated from NHS. Binding was detected using anti-hu-IgG-AF647 or anti-hu-IgM-FITC by flow cytometry. Flow cytometry data are represented by gMFI values of bacterial populations. Data represent mean ± standard deviation of three independent experiments. (**e&f**) Bacteria were incubated at 37 °C in the presence of 1 µM SYTOX green nucleic acid stain, and inner membrane permeabilization (SYTOX fluorescence intensity) was detected after (**e**) 60 or (**f**) 90 minutes. Data represents mean ± standard deviation of a minimal of two independent experiments. (**a&b**) Statistical analysis was performed using a nonlinear regression with a variable slope comparing the logEC50 via sum-of squares F test, (**c,d,g&i**) a paired one-way ANOVA with a Tukey's multiple comparisons on Log_{10}-transformed gMFI data, (**e**) or a paired one-way ANOVA with a Tukey's multiple comparisons test on SYTOX fluorescence intensity data.

Supplementary table 1| Differentially expressed genes in Kp209_CSTR compared to Kp209

Kpn209S ID	Name/prediction	Log_2(FC)	P_{adj}
Upregulated genes (Log_2(FC)>1, P_{adj}<0.05)			
Kpn209S_01234	*mgtE.1*	5.25	1.06E-195
Kpn209S_03326	*mgtC*	4.15	3.81E-90
Kpn209S_03165	-	3.87	3.69E-57
Kpn209S_03486	*iolT*	3.79	1.12E-45
Kpn209S_01244	*arnC*	3.51	9.15E-146
Kpn209S_03613	-	3.42	1.46E-40
Kpn209S_01243	*arnB*	3.42	5.53E-98
Kpn209S_01954	-	3.39	5.43E-42
Kpn209S_01095	*clcB*	3.38	2.77E-69
Kpn209S_03674	-	3.35	1.09E-39
Kpn209S_03723	*yabI*	3.28	1.08E-51
Kpn209S_00443	*mgtA*	3.24	1.48E-51
Kpn209S_01245	*arnA*	3.22	5.16E-78
Kpn209S_04650	*ctpF*	3.16	2.08E-61
Kpn209S_02782	-	3.15	2.28E-52
Kpn209S_01246	*arnD*	3.11	2.67E-90
Kpn209S_04711	*scrB*	3.04	1.29E-21
Kpn209S_04649	*mdtA*	3.04	7.99E-46

Supplementary table SI1 Differentially expressed genes in Kp209_CSTR compared to Kp209 *(continued)*

Kpn209S ID	Name/prediction	Log_2(FC)	P_{adj}
Kpn209S_04702	*btuF*	3.03	2.00E-42
Kpn209S_01247	*arnT*	3.00	8.63E-102
Kpn209S_02647	*pmrD*	3.00	1.73E-56
Kpn209S_03320	*mamB*	2.98	1.40E-25
Kpn209S_04708	*scrK*	2.91	9.08E-19
Kpn209S_03612	-	2.91	2.84E-23
Kpn209S_01631	*ribB*	2.91	1.21E-49
Kpn209S_04552	*pagP*	2.83	3.30E-52
Kpn209S_02224	-	2.81	9.56E-50
Kpn209S_04703	*hmuU*	2.76	1.72E-35
Kpn209S_00310	-	2.75	1.24E-28
Kpn209S_02223	-	2.72	2.16E-52
Kpn209S_02797	-	2.66	2.38E-45
Kpn209S_03487	*fruB*	2.62	1.69E-11
Kpn209S_01249	*arnF*	2.60	2.38E-43
Kpn209S_04337	*ybjG*	2.56	1.08E-51
Kpn209S_04704	*fhuC*	2.53	5.59E-30
Kpn209S_03568	-	2.50	1.38E-15
Kpn209S_02225	-	2.48	2.67E-29
Kpn209S_04648	*bepG*	2.42	3.12E-32
Kpn209S_04492	*kdpA*	2.38	8.00E-22
Kpn209S_02460	*apbE*	2.36	4.22E-44
Kpn209S_04416	*bioB*	2.34	4.79E-28
Kpn209S_04298	*macA*	2.34	1.63E-55
Kpn209S_04087	*phoP*	2.34	1.41E-29
Kpn209S_05121	-	2.34	1.16E-22
Kpn209S_02783	-	2.34	1.54E-13
Kpn209S_03672	*zntB*	2.32	1.10E-19
Kpn209S_02461	*ada*	2.27	1.97E-46
Kpn209S_01787	*fimA*	2.27	6.99E-06
Kpn209S_01248	*arnE*	2.27	9.90E-21
Kpn209S_03301	*maeA*	2.22	1.23E-42
Kpn209S_03166	*slyB*	2.17	2.38E-19
Kpn209S_01782	*fimH*	2.15	2.94E-05
Kpn209S_04297	*macB*	2.12	5.55E-33

Supplementary table SI1 Differentially expressed genes in Kp209_CSTR compared to Kp209 *(continued)*

Kpn209S ID	Name/prediction	Log_2(FC)	P_{adj}
Kpn209S_04415	*bioF*	2.11	1.50E-17
Kpn209S_00268	*mdoB*	2.11	1.69E-32
Kpn209S_04710	*sacX*	2.10	3.80E-05
Kpn209S_02462	*alkB*	2.06	9.26E-22
Kpn209S_03599	*speG*	2.06	2.33E-35
Kpn209S_00627	*nhaK*	2.05	5.59E-43
Kpn209S_01786	*fimC*	2.05	8.39E-05
Kpn209S_04088	*phoQ*	2.04	2.00E-24
Kpn209S_01785	*fimD*	2.03	9.59E-05
Kpn209S_04814	*yheI*	1.98	9.73E-24
Kpn209S_04414	*bioC*	1.98	9.80E-15
Kpn209S_01784	*fimF*	1.96	1.91E-04
Kpn209S_01788	*fim*	1.96	1.97E-04
Kpn209S_04709	*scrY*	1.95	2.35E-04
Kpn209S_03142	*mdtK*	1.93	3.93E-16
Kpn209S_02206	*pgpC*	1.89	4.07E-19
Kpn209S_04101	*dmdB*	1.88	2.68E-16
Kpn209S_04100	*betB*	1.87	8.48E-13
Kpn209S_01783	*fimG*	1.86	5.10E-04
Kpn209S_03183	*ydgT*	1.86	2.63E-17
Kpn209S_03598	-	1.85	5.05E-17
Kpn209S_00017	*yaeQ*	1.79	3.31E-27
Kpn209S_01781	-	1.74	1.55E-03
Kpn209S_02799	*ftsI*	1.72	5.67E-09
Kpn209S_04413	*bioD*	1.69	2.68E-08
Kpn209S_04493	*kdpB*	1.66	1.54E-10
Kpn209S_03300	-	1.61	5.59E-06
Kpn209S_04249	*dpaL*	1.60	7.22E-04
Kpn209S_03185	*ydgJ*	1.60	8.07E-16
Kpn209S_03327	*zapE*	1.58	1.39E-14
Kpn209S_00693	-	1.56	5.13E-17
Kpn209S_04813	*mdlB*	1.56	5.91E-14
Kpn209S_01938	*ppnN*	1.54	9.77E-13
Kpn209S_04677		1.52	9.18E-05
Kpn209S_04467	*ybgC*	1.50	3.59E-12

Supplementary table SI1 Differentially expressed genes in Kp209_CSTR compared to Kp209 *(continued)*

Kpn209S ID	Name/prediction	Log_2(FC)	P_{adj}
Kpn209S_03728	*ompN*	1.49	9.90E-05
Kpn209S_04757	*fetA*	1.49	3.69E-15
Kpn209S_01476	*mlaF*	1.48	1.74E-16
Kpn209S_03182	*ydgK*	1.47	1.84E-08
Kpn209S_03933	*pfeA*	1.44	6.22E-09
Kpn209S_01523	*osmY*	1.41	1.08E-17
Kpn209S_01538	*gatY*	1.40	8.90E-03
Kpn209S_04466	*tolQ*	1.38	6.13E-11
Kpn209S_01477	*mlaE*	1.36	3.59E-16
Kpn209S_03932	*yciB*	1.33	8.40E-10
Kpn209S_01121	-	1.33	2.00E-07
Kpn209S_04756	*fetB*	1.32	1.22E-12
Kpn209S_01524	*diaA*	1.31	9.16E-15
Kpn209S_02488	*lpxT*	1.31	9.59E-05
Kpn209S_00015	*nlpE*	1.30	6.10E-15
Kpn209S_01790	-	1.29	6.40E-09
Kpn209S_04812	*glnK*	1.25	2.66E-03
Kpn209S_00337	-	1.25	1.87E-08
Kpn209S_01636	*tolC*	1.25	7.20E-11
Kpn209S_04729	*lpxL*	1.24	6.57E-09
Kpn209S_01478	*mlaD*	1.24	6.74E-14
Kpn209S_04846	*yajR*	1.22	1.74E-07
Kpn209S_04464	-	1.20	4.50E-08
Kpn209S_02092	-	1.20	1.52E-05
Kpn209S_01480	*mlaB*	1.19	3.77E-13
Kpn209S_04338	*deoR*	1.19	1.50E-08
Kpn209S_04465	*tolR*	1.18	5.96E-08
Kpn209S_00016	*arfB*	1.18	6.49E-13
Kpn209S_03847	-	1.17	1.63E-02
Kpn209S_04469	*cydX*	1.12	1.16E-02
Kpn209S_00761	*tatA*	1.11	8.31E-11
Kpn209S_03299	-	1.11	4.30E-02
Kpn209S_05125	*umuC*	1.11	1.37E-03
Kpn209S_01479	*mlaC*	1.11	2.31E-12
Kpn209S_04468	-	1.08	7.62E-05

Supplementary table SI1 Differentially expressed genes in Kp209_CSTR compared to Kp209 *(continued)*

Kpn209S ID	Name/prediction	Log_2(FC)	P_{adj}
Kpn209S_04470	*cydB*	1.05	1.10E-07
Kpn209S_01122	-	1.04	1.31E-05
Kpn209S_00758	*tatD*	1.04	4.59E-08
Kpn209S_04712	*cra_*	1.03	1.59E-07
Down regulated genes Log_2(FC)<-1, P_{adj}<0.05)			
Kpn209S_04410	-	-3.28	2.33E-35
Kpn209S_04407	*eptA*	-2.78	2.52E-23
Kpn209S_02806	*yoaE*	-2.60	7.03E-34
Kpn209S_00354	-	-2.47	7.68E-24
Kpn209S_00355	-	-2.26	1.78E-21
Kpn209S_04408	*pmrA*	-2.16	3.29E-16
Kpn209S_00356	-	-1.97	4.50E-08
Kpn209S_02517	*oprB*	-1.81	1.16E-06
Kpn209S_04409	*pmrB*	-1.80	7.02E-12
Kpn209S_04419	*proY*	-1.72	1.04E-05
Kpn209S_04252	*yedS*	-1.70	1.25E-19
Kpn209S_04420	*hutH*	-1.69	8.22E-05
Kpn209S_03684	*cycA*	-1.67	2.39E-05
Kpn209S_00357	-	-1.66	1.30E-06
Kpn209S_04421	*hutU*	-1.64	2.94E-05
Kpn209S_02966	*rutC*	-1.60	7.18E-04
Kpn209S_02520	*bglB*	-1.59	4.59E-08
Kpn209S_01312	*feoA*	-1.57	8.04E-05
Kpn209S_02514	*yohK*	-1.57	6.19E-05
Kpn209S_00358	*ufaA*	-1.56	9.23E-07
Kpn209S_03046	-	-1.46	3.37E-03
Kpn209S_02515	-	-1.44	5.42E-06
Kpn209S_03019	-	-1.42	2.42E-03
Kpn209S_03686	*astB*	-1.40	1.28E-03
Kpn209S_03685	*astE*	-1.38	4.42E-03
Kpn209S_02519	*bglF*	-1.34	2.49E-08
Kpn209S_01311	*feoB*	-1.33	2.72E-03
Kpn209S_02189	*grcA*	-1.32	4.25E-03
Kpn209S_02830	*dadX*	-1.32	5.04E-05
Kpn209S_00849	*zinT*	-1.30	2.80E-06

Supplementary table SI1 Differentially expressed genes in Kp209_CSTR compared to Kp209 *(continued)*

Kpn209S ID	Name/prediction	Log_2(FC)	P_{adj}
Kpn209S_03595	*por*	-1.30	7.66E-03
Kpn209S_04342	-	-1.28	1.74E-02
Kpn209S_03687	*astD*	-1.28	7.21E-03
Kpn209S_03635	*ttdT*	-1.27	2.02E-03
Kpn209S_01194	-	-1.27	1.74E-07
Kpn209S_00616	*acs*	-1.25	7.97E-04
Kpn209S_02967	*dadA*	-1.24	9.09E-03
Kpn209S_02984	-	-1.18	7.67E-03
Kpn209S_00254	-	-1.18	1.80E-02
Kpn209S_01240	*nikA*	-1.16	7.75E-04
Kpn209S_00625	*cidA*	-1.16	9.95E-04
Kpn209S_02511	*mglC*	-1.14	8.95E-03
Kpn209S_02084	*nrdH*	-1.13	9.03E-03
Kpn209S_03634	*namA*	-1.11	2.34E-03
Kpn209S_05120	*scrK*	-1.10	4.96E-04
Kpn209S_04178	*putA*	-1.10	5.78E-04
Kpn209S_02491	*uxuA*	-1.09	5.87E-04
Kpn209S_02422	*nuoG*	-1.08	5.10E-07
Kpn209S_02421	*nuoF*	-1.08	5.66E-05
Kpn209S_05135	-	-1.08	9.26E-06
Kpn209S_01195	*bcsQ*	-1.07	4.63E-04
Kpn209S_00362	-	-1.07	1.05E-02
Kpn209S_05141	-	-1.06	5.51E-03
Kpn209S_01175	*kdgK*	-1.06	3.85E-02
Kpn209S_04476	*sdhB*	-1.06	7.56E-03
Kpn209S_03607	*bioD*	-1.05	9.26E-03
Kpn209S_02450	*glpQ*	-1.05	1.37E-04
Kpn209S_04789	*ykgO*	-1.05	6.90E-03
Kpn209S_03594	*uspG*	-1.01	2.78E-02
Kpn209S_02049	*srlE*	-1.01	1.79E-02

Supplementary table SI2. Real-time PCR primers

Primer	Sequence (5'→ 3')	T_M (°C)	Amplicon size (bp)	Reference
arnD-F	AACTACTGACCATGGCGGCG	61.5	116	12*
arnD-R	GCCAGCCAGTTCACCACGAA	62.5		12*
mgtE-F	TGGTGTGCATTACCCTGTG	57.0	100	This study
mgtE-R	ATAAACGGCGCGGAAACTA	56.3		This study
rpoB-F	GATCCGTGGCGTGACTTATT	55.0	118	54
rpoB-R	GCCCATGTAGACTTCTTGTTCT	54.6		54

*Reference 12 used the alternative gene name *pgbP* for *arnD*

Chapter 3

Unbiased selection of B cell using intact bacteria identified novel antibodies against *Klebsiella pneumoniae* that synergistically stimulate a potent complement response

Sjors P. A. van der Lans[1], Priscilla F. Kerkman[1], Maartje Ruyken[1], Carla J.C. de Haas[1], Stan Baijens[1], Remy M. Muts[1], Lisette M. Scheepmaker[1], Piet C. Aerts[1], Marije F. L. van 't Wout[1], Frank J. Beurskens[2], Janine Schuurman[2], Bart W. Bardoel[1], Suzan H. M. Rooijakkers[1]

[1]Department of Medical Microbiology, University Medical Center Utrecht, The Netherlands

[2]Genmab, Utrecht, The Netherlands

Manuscript in preparation

Abstract

Infections and antibiotic resistance associated deaths caused by the Gram-negative bacterium *K. pneumoniae* have increased worldwide. Antibodies that boost the host immune system provide an attractive novel treatment option. To efficiently induce bacterial killing, antibodies should bind the bacterial surface and activate the human complement system. It remains poorly understood why some antibodies are effective in complement activation and others are not. To obtain detailed insights into differences between antibodies, we developed an approach to identify and characterize antibody panels recognizing whole bacterial cells. Instead of using purified antigens, we employed an antigen-agnostic approach to stain and single cell sort human IgG memory B cells recognizing intact *K. pneumoniae*. B cell selection was performed using two clinical *K. pneumoniae* strains (*Kpn*O2 and *Kpn*O1), and the 641 sorted B cells yielded 69 *K. pneumoniae*-specific antibodies of which 29 were unique. Using transposon screening, we revealed that most antibodies targeted the O-antigen, and that three antibodies recognized the capsule of the *Kpn*O2 strain. All anti-O2-antibodies could activate complement on *Kpn*O2, in contrast to the anti-capsule antibodies. This suggests that the capacity of these antibodies to activate the complement system depends on their antigenic target. For the *Kpn*O1 strain, all antibodies targeted the O1-antigen and 13 out of 17 antibodies activated the complement system. Complement activation did not correlate to antibody binding, as complement activating and non-activating antibodies had similar binding dynamics. We showed that complement activating antibodies also triggered phagocytosis and killing of both *Kpn*O2 and *Kpn*O1 by human neutrophils. Finally, this panel of antibodies allowed us to study mixtures of different antibody clones. Surprisingly, we revealed that combining two inactive anti-capsule antibodies enables strong synergistic complement activation and phagocytosis of *K. pneumoniae.* In summary, using an unbiased selection approach we show that the antigenic target on the bacterial surface critically determines complement activation and that some antibodies can act synergistically. Altogether, this work contributes to a better understanding of antibody-mediated complement activation on bacterial cells, which accelerates the development of effective immune therapies against bacterial infections.

Introduction

The human complement system plays a key role in the first lines of defense against invading bacteria. It is part of the innate immune system and consists of a family of soluble proteins that form a protective cascade in blood and other body fluids. Although complement can be triggered by innate recognition, the complement reaction is much more efficient in the presence of specific antibodies. Antibody-dependent complement activation starts when component C1 binds to antigen-antibody complexes on bacterial surfaces. Six surface-bound IgG1 monomers can cluster via Fc-Fc interactions to form a hexamer[1,2]. This hexamer serves as a platform onto which C1 can dock via its six Fc-binding domains, leading to C1 activation and the start of the complement reaction. Complement activation on bacteria results in deposition of the opsonin C3b and the release of anaphylatoxin C5a, which promote phagocytic uptake and killing by human phagocytes[3–5]. Furthermore, complement activation induces the formation of lethal membrane attack complex (MAC) pores in the outer membrane of Gram-negative bacteria. Although anti-bacterial antibodies can trigger complement activation, it remains poorly understood why certain antibodies activate complement but other do not. For instance, it is not clear which bacterial surface structures are good targets for an effective complement response. Understanding the molecular basis of effective complement activation by monoclonals or combining antibodies to mimic a polyclonal response could greatly help to boost the development of antibody-based therapies against problematic infections.

Klebsiella pneumoniae is an important opportunistic human pathogen that frequently causes hospital acquired infections [6]. Of major concern is the strong increase in antibiotic resistance observed among *K. pneumoniae* clinical isolates, making treatment of infections more difficult [7–10]. In 2019 alone, *K. pneumoniae* caused over 700.000 antibiotic resistance associated deaths worldwide, making it the third leading cause of antibiotic resistance associated deaths [11]. As for all Gram-negative bacteria, the outer membrane of *K. pneumoniae* mainly consists of lipopolysaccharide (LPS), which is comprised of membrane-anchored lipid A decorated with a long O-antigen polysaccharide chain consisting of repeating sugar moieties. The O-antigen can protect *K. pneumoniae* against the complement system by preventing recognition of underlying surface structures, as well as hindering proper MAC formation [12,13]. *K. pneumoniae* can express various O-antigens (O-) types, which differ in molecular composition. The clinically most relevant O-types are the O1, O2 and O3, representing over 80% of

the clinical isolates [14]. In addition, the majority of antibiotic resistant and hypervirulent strains express either the O1 or O2-antigen [14,15]. Another important and highly diverse surface structure of *K. pneumoniae* is the polysaccharide capsule. The capsule plays an important role during infection of *K. pneumoniae*, as it is described to protect against antibody recognition, the complement system and phagocytosis [16–21]. Over 70 different capsule (K-) types have been described to be expressed by *K. pneumoniae*, and many more K-types have been predicted based on genetic diversity of the capsule locus (KL) [14]. *K. pneumoniae* can cause various types of infections, and primarily infects individuals with impaired immune systems [6,22]. However, these immuno-compromised patients frequently retain a functioning complement system, which provides an opportunity to boost the complement system using *K. pneumoniae* specific antibodies. Thus, improving our understanding of antibody-mediated complement activation on *K. pneumoniae* is crucial for the development of therapeutic strategies.

Prior efforts to identify human monoclonal antibodies against bacteria have mainly been focused on antibodies that target a single pre-determined antigen. In case of *K. pneumoniae,* human memory B cells have been used as a source to discover novel antibodies targeting purified O-antigens [15,23]. Although successful for identification of high-affinity antibodies, these approaches were biased towards a single antigen and potent antibodies against other surface targets were missed. We hypothesize that antibodies directed to different antigens and epitopes might activate the complement system in a different way. The density and exact location of antigens could influence complement activation as well. To study how differences antigens influence complement activation, we need a large panel of antibodies that are selected in an unbiased way. Only with such a larger panel of diverse antibodies in hand, we can close the current knowledge gap in understanding antibody-mediated bacterial killing, either via complement or via a combination of complement and neutrophils. Furthermore, combining various antibodies that bind to the same strain would allow us to mimic a natural infection where bacterial cells are targeted by multiple different antibodies.

In this study we aimed to develop an antigen-agnostic approach to identify a large panel of monoclonal antibodies recognizing the surface of *K. pneumoniae*. Since we do not know which surface antigens trigger potent complement activation, we decided not to pre-select a certain antigen but rather stain B cells with whole bacterial cells, keeping bacterial antigens in their natural context. With this method we successfully identified 29 unique antibodies against two clinical *K. pneumoniae* strains. Using

transposon and deletion mutants we identified the bacterial targets of our antibodies. Functional analyses suggests that the capacity of these antibodies to activate the complement system depends on their antigenic target. Also, our study shows that certain antibody combinations can act synergistically to activate complement on *K. pneumoniae.*

Results

Dual staining of human B cells using intact bacteria identifies 29 novel antibodies against *K. pneumoniae*

To identify human antibodies that target *K. pneumoniae,* we selected human B cells that recognized fluorescently labelled *K. pneumoniae* via their B cell receptor (BCR). Click chemistry was used to couple fluorescent dyes to lipopolysaccharide (LPS), a conserved cell envelope component of Gram-negative bacteria (fig. 1a & supplementary fig. 1a). This was achieved by growing bacteria in the presence of azide-carrying KDO which incorporates into the LPS and provided a handle for 'clicking' to cyclooctyne-labeled fluorophores. STORM microscopy (fig. 1a) and flow cytometry (supplementary fig. 1b) demonstrated successful surface labeling of *K. pneumoniae*. Next, we examined whether fluorescently labelled *K. pneumoniae* could be used to identify *K. pneumoniae* specific B cells, focusing on B cells from healthy individuals. B cells were stained by incubating them with a mix of two fluorescently labelled bacteria preparations, and B cells that bound bacteria were detected via flow cytometry. We identified single-positive B cells that bound either ATTO-488 or Cy5 labelled *K. pneumoniae* (fig. 1b, supplementary fig. 1c). In addition, approximately 0.05% of the B cells were double-positive for bacterium binding (fig. 1b). Adding an excess of unlabeled *K. pneumoniae* competed primarily with binding of fluorescent *K. pneumoniae* in the double-positive population (supplementary fig. 1d). This suggests that the dual staining approach helped to enrich for bacterium-specific B cells. Importantly, the double-positive B cell population was strongly enriched for memory B cells ($CD27^+$), whereas no enrichment was observed within the single-positive populations (fig. 1b). Together, this suggests that dual staining of B cells with fluorescently labelled intact bacteria allows for the enrichment of *K. pneumoniae*-specific memory B cells.

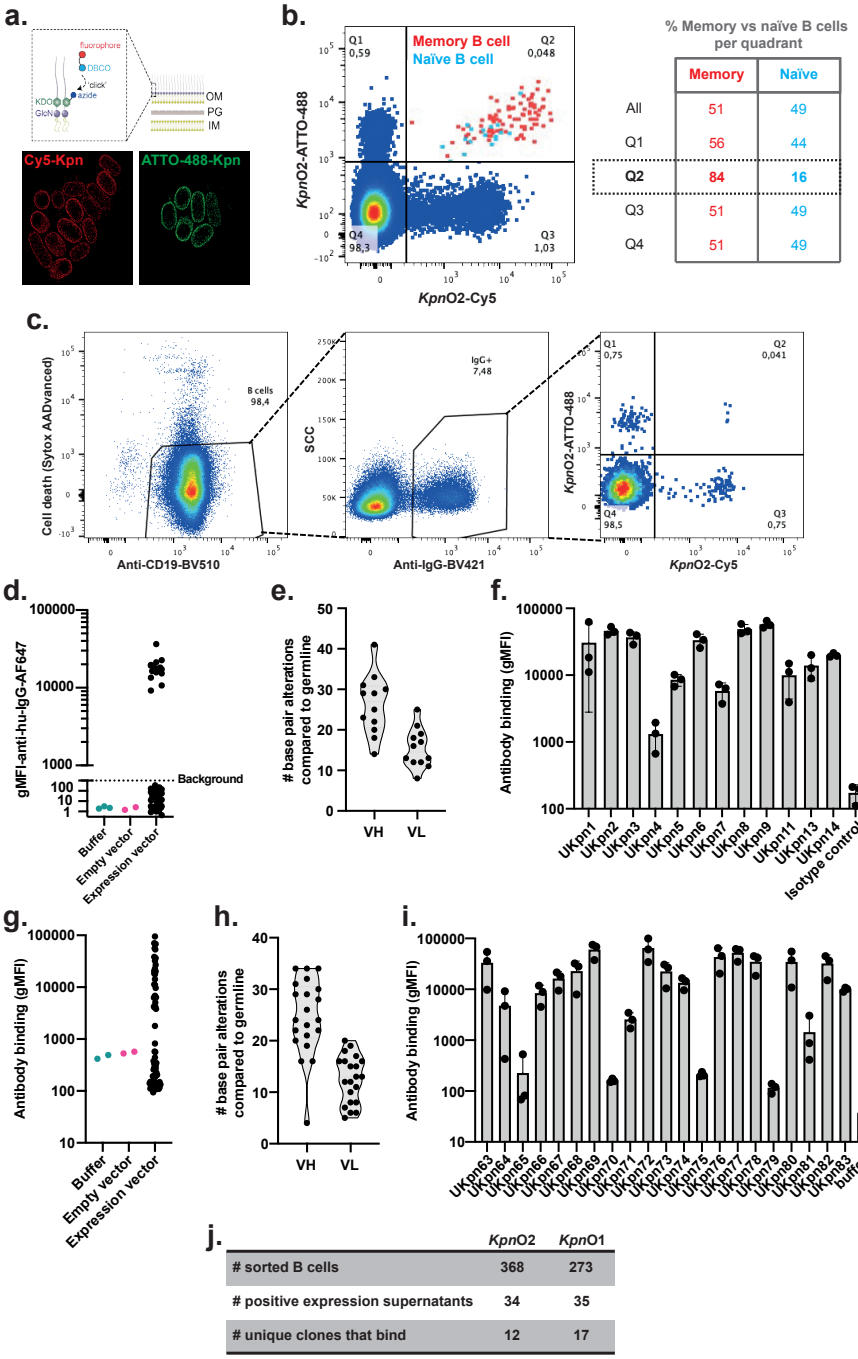

j.

	*Kpn*O2	*Kpn*O1
# sorted B cells	368	273
# positive expression supernatants	34	35
# unique clones that bind	12	17

Figure 1| Dual staining of human B cells with whole bacterial cells identifies 29 novel IgGs against *K. pneumoniae*

(a) Fluorescent labeling of the outer membrane of *K. pneumoniae* via click-chemistry. *K. pneumoniae* was cultured overnight in the presence of KDO-azide (2 μM), which was metabolically incorporated into the LPS core. Cyclooctyne-labelled fluorophores (50 μM) were added, which "clicked" to the azide handles. Fluorescent labeling of *Kpn*O2 with cy5 or ATTO-488 was assessed via dStorm microscopy. **(b&c)** Human B cell isolated from healthy donors were incubated with *Kpn*O2-ATTO-488 and *Kpn*O2-Cy5 (MOI of 0.5 per fluorophore). **(b) *B cells (CD19$^+$)*** that bound both *Kpn*O2-ATTO-488 and *Kpn*O2-Cy5 were detected by flow cytometry. Percentage of single-bacterium-positive (Q1: ATTO-488$^+$ Cy5$^-$; Q3: ATTO-488$^-$ Cy5$^+$), and the double-bacterium-positive (Q2: ATTO-488$^+$ Cy5$^+$) B cells in the total population was determined (0.59%, 1.03% and 0.048%, respectively). The distribution memory (CD27$^+$) verses naïve (CD27$^-$) B cells was calculated for the unstained, single stained and dual stained B cell compartments. **(c)** Gating strategy to sort *K. pneumoniae*-specific B cells. Alive B cells (CD19$^+$, death-cell-marker$^-$) that expressed IgG and bound both *Kpn*O2-ATTO-488 and *Kpn*O2-Cy5 were single cell sorted (Q2, right panel). **(d-i)** Single cell sorting of *K. pneumoniae*-specific B cells was performed using *Kpn*O2 **(d-f)** and *Kpn*O1 **(g-i**). The heavy and light variable regions (VH and VL, respectively) of single sorted B cells were amplified via RT-PCR and cloned into expression vectors to recombinantly express the antibodies as IgG1 in EXPI293F cells. Expression supernatants were screened for antibodies that bound to the selection bacteria by incubating *Kpn*O2 **(d)** and *Kpn*O1 **(h)** with 10-fold diluted expression supernatant to detect antibody binding. The VH and VL sequences of the *K. pneumoniae* binding antibodies were analyzed to determine unique clones and the number of base pair alteration in the sequences of the VH and VL of the antibodies recognizing *Kpn*O2 **(e)** and *Kpn*O1 **(h).** The unique antibodies were re-expressed and purified. Binding of the purified antibodies to *Kpn*O2 (1 μg/ml) **(f)** and *Kpn*O1 (2 μg/ml) **(i)** was determined. **(d,g,h,j)** IgG1 binding was detected by flow cytometry using anti-hu-IgG-AF647. Flow cytometry data are represented by geometric mean fluorescent intensity (gMFI) values of bacterial populations. **(f&i)** Data represent mean ± standard deviation of three independent experiments. **(j)** Summary of number of sorted cells, supernatants containing bacterium specific antibodies and unique purified antibody clones that were used for further analysis.

To proof that the dual staining selects for *K. pneumoniae*-specific B cells, we used single-cell sorting to isolate double-positive B cells, focusing on IgG expressing cells (fig. 1c; Q2). Next, the VH/VL regions of the sorted B cells were amplified via RT-PCR and cloned into IgG1 expression vectors. For initial screening of antibodies, recombinant IgG1 expression in HEK-293-F cells was performed on a small-scale. To analyze whether expression supernatants contained *K. pneumoniae*-specific antibodies, the supernatants were incubated with *K. pneumoniae*, and antibody binding was assessed by flow cytometry (fig. 1d, supplementary fig. 1e). Separate B cell selection rounds were performed with two clinical *K. pneumoniae* isolates: *Kpn*O2 (O2; KL110) and *Kpn*O1 (O1; KL114), which represent the two most dominant O-types among multidrug-resistant *K. pneumoniae* [15].

For *Kpn*O2, a total of 368 double-positive B cells were isolated by single-cell sorting. Screening of expression supernatants revealed 34 positive clones (9.2% success rate) (fig. 1d). VH/VL sequencing revealed that 14 out of 34 antibody clones had a unique CDR3 (fig. 1e, supplementary fig. 2a). All 14 unique clones had undergone somatic hypermutations in both the VH and VL, indicating affinity maturation (fig. 1e, supplementary fig. 2a). Of the 14 unique monoclonal antibodies, 12 bound to *Kpn*O2 after large-scale expression and IgG1 purification (fig. 1f&j). For *Kpn*O1, a total of 273 double-positive B cells were sorted, yielding 35 expression supernatants that contained antibodies against *Kpn*O1 (12.8% success rate) (fig. 1g). Out of these, 21 VH/VL sequences were unique (supplementary fig. 2b) and had undergone somatic hypermutation (fig. 1h). Finally, we confirmed that 17 unique monoclonal antibodies bound to *Kpn*O1 as purified IgG1s (fig. 1i&j). In conclusion, we developed a B cell staining approach to specifically select and clone human B cells recognizing entire *K pneumoniae* bacteria. Using this method, we identify 29 unique human antibodies recognizing two clinically relevant *K. pneumoniae* strains.

Antibodies targeting O2 antigen but not the capsule drive complement activation on *Kpn*O2

Next, we compared the newly identified anti-*K. pneumoniae* antibodies, first focusing on the antibodies recognizing *Kpn*O2. Measuring antibody binding to *Kpn*O2 revealed that the binding efficiency varied up to 100-fold between the identified antibodies (fig. 2a). Next, we investigated whether antibodies could induce surface deposition of C3b molecules, a central step in the complement cascade. To this end, *Kpn*O2 was incubated with isolated antibodies and normal human serum (NHS) as a source of complement, and surface deposition of C3b was quantified by flow cytometry. Although most antibodies against *Kpn*O2 triggered C3b deposition on this strain in a dose-dependent manner, for three antibodies we did not observe C3b deposition (UKpn1, UKpn3, UKpn4), even at the highest tested antibody concentration (fig. 2b). Intriguingly, we observed that the binding of antibodies to the *Kpn*O2 surface did not correlate with their capacity to activate complement (fig. 2a, 2b). These data suggest that the binding of IgG1 to the surface of *K. pneumoniae* does not automatically lead to Fc-mediated activation of the complement system.

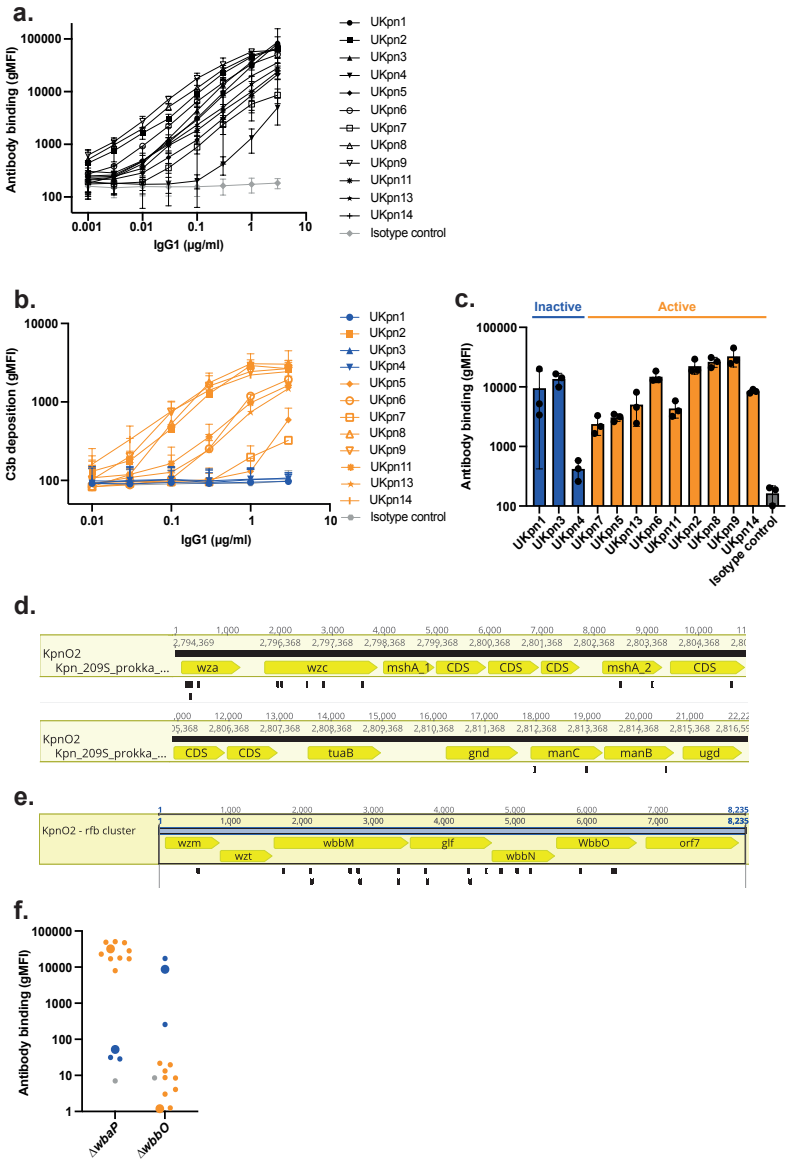

Figure 2| Monoclonal antibodies targeting O2-antigen but not capsule drive complement activation on *Kpn*O2

(a) *K. pneumoniae KpnO2* was incubated with a concentration range of different anti-*Kpn*O2 IgG1 antibodies. Antibody binding was detected by flow cytometry using anti-hu-IgG-AF647. **(b)** Antibody-dependent C3b deposition on *Kpn*O2 pre-incubated with anti-*Kpn*O2 IgG1. After antibody binding, bacteria were incubated in 3% normal human serum (NHS) as a complement source, and C3b-deposition was detected using anti-hu-C3b-AF647 by flow cytometry. In orange the antibodies that induce and in blue the antibodies that do not induce C3b deposition. **(c)** Bars represent antibody

binding data in the condition were 0.3 µg/ml IgG1 was added, ordered based on C3b deposition as measured in (b). **(d&e)** Transposon mutants that are not recognized by UKpn1 **(d)** or UKpn2 **(e)** were single cell sorted. The barcode of the selected mutants was sequenced to determine the location of the transposon insertions. Mutants that were no longer bound by UKpn1 had transposon insertions in genes involved in capsule synthesis **(d)**. Overview of the capsule locus with in black the location of the transposon insertions. For UKpn2 transposon insertions were found in the *rfb* locus in the transposon mutants that were no longer recognized by UKpn2 **(e)**. **(f)** Anti-*Kpn*O2 binding to capsule (Δ*wbaP*) and O-antigen (Δ*wbbO*) deletion mutants of *Kpn*O2. Strains were incubated with 1 µg/ml IgG1, and antibody binding was detected by flow cytometry using anti-hu-IgG-AF647. In blue the antibodies that do not stimulate complement activation and in orange antibodies that activate the complement system. Larger dots indicate UKpn1 (blue) and UKpn2 (orange). **(a-c, f)** Flow cytometry data are represented by geometric mean fluorescent intensity (gMFI) values of bacterial populations. Data represent mean ± standard deviation of three independent experiments **(a-c)** and a single experiment **(f)**.

We wondered whether the functional differences between the antibodies could be explained by differences in their target specificity. To identify the bacterial surface targets of the antibodies, we generated a transposon library in *Kpn*O2R using barcoded transposons [24,25]. We hypothesized that antibody binding would be lost for mutants where the transposon disrupts a gene that is involved in surface expression of the antibody target. The transposon library was exposed to either a complement-activating (UKpn2) or a non-activating (UKpn1) antibody, and transposon mutants that were no longer bound by the antibodies were isolated using single-cell sorting of live bacterial cells. We found that approximately 0.5-1% of the transposon mutants were no longer recognized by the antibodies (supplementary fig. 3a). Barcode sequencing of the sorted UKpn1-negative mutants revealed that sixteen unique transposons had inserted in six different genes involved in capsule synthesis (fig. 2d). Furthermore, sequencing of UKpn2-negative mutants identified twenty unique transposon insertions in five different genes in the *rfb* locus involved in biosynthesis of the O-antigen polysaccharide [26] (fig. 2e). To confirm these results, we used the lambda-red recombination system to specifically delete the *wbaP* (capsule glycosyltransferase) and *wbbO* (encoding the O-antigen synthesis galactosyltransferase) genes. Indeed, we observed that *Kpn*O2 *ΔwbaP* and *ΔwbbO* deletion mutants were no longer bound by UKpn1 and UKpn2, respectively (fig. 2f). We analyzed the binding of the other *Kpn*O2-specific antibodies to the *ΔwbaP* and *ΔwbbO* mutants. This revealed that all complement activating antibodies recognized the O-antigen, whereas the inactive antibodies all target the capsule (fig. 2f). Additional binding experiments revealed that anti-capsule antibodies recognize other clinical *K. pneumoniae* strains containing the KL110 capsule locus (supplementary fig. 3b). Furthermore, the anti-O-antigen antibodies specifically

recognized the O2-antigen, except for antibody UKpn14, which was also cross-reacted with an OL104-antigen expressing strain (supplementary fig. 3c).

Various O2-antigen subtypes can be expressed, based on genetic variation within the O locus, as well as the presence of accessory genes. The most common are the O2a and O2afg [14]. O2afg strains have, in addition to the O2a locus, a *gmlABC* gene cluster involved in modifying the O2-antigen [14,26]. While all O2-specific antibodies bound O2a strains, we found that UKpn6 and UKpn7 did not recognize O2afg strains (supplementary fig. 3d). This indicated that the epitopes of UKpn6 and UKpn7 in the O2a antigen are shielded by the O2afg modification. To further specify the difference in the epitopes of UKpn2 and UKpn6, we exposed the *Kpn*O2 transposon library to UKpn2 and UKpn6, and sorted UKpn2-negative mutants that were still bound by UKpn6 (supplementary fig. 3e). Transposon sequencing revealed five unique transposon insertions in the gene *orf7* [27]that is located directly downstream of the *rfb* operon (supplementary fig. 3f). This suggests that the galactosyltransferase encoded by *orf7* has a role in O2a biosynthesis that is crucial for binding of UKpn2, but not for UKpn6. In conclusion, we reveal that the target is critical for the identified antibodies to activate the complement system on *K. pneumoniae*.

Antibodies that target the O1 antigen differ in their potential to drive complement activation

To characterize the antibodies identified against the *Kpn*O1 strain, we first assessed antibody binding to *Kpn*O1. The antibody concentration to obtain clear binding varied more than 100-fold between the purified antibodies (fig. 3a). Measuring antibody-dependent C3b deposition revealed that 13 of the 17 antibodies activated the complement system on *Kpn*O1 (fig. 3b). Some antibodies efficiently induce C3b deposition at 0.01 µg/ml, whereas others required a 100-fold higher concentration. We observed that antibody biding to *Kpn*O1 did not correlate with the antibody's capacity to induce C3b deposition (fig. 3c), similar to what was observed for *Kpn*O2. Next, we aimed to identify the target of the anti-*Kpn*O1 antibodies. Since the anti-*Kpn*O2 antibodies were all directed against either the O-antigen or the capsule polysaccharide, capsule (Δ*wbaP*) and O-antigen (Δ*wbbO*) deficient mutants of *Kpn*O1 were generated. We observed that all antibodies still bound to *Kpn*O1 mutants lacking the *wbaP* capsule gene (supplementary fig. 4). In contrast, antibody binding to the Δ*wbbO* mutant was abrogated, suggesting that all antibodies against *Kpn*O1 targeted the O-antigen (fig. 3d).

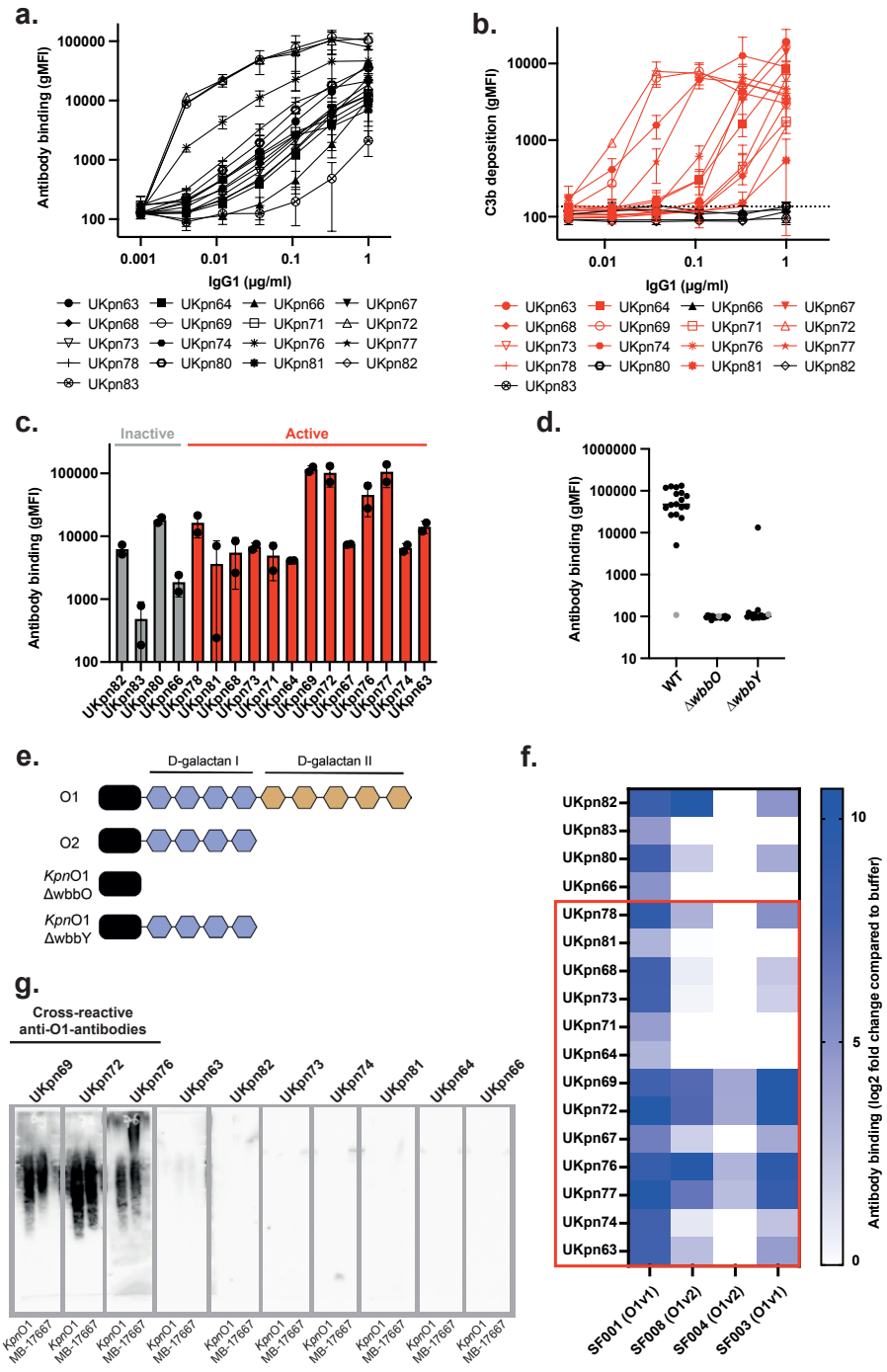
a.
Antibody binding (gMFI)
100000
10000
1000
100
0.001
0.01
0.1
1
IgG1 (µg/ml)
UKpn63 UKpn64 UKpn66 UKpn67
UKpn68 UKpn69 UKpn71 UKpn72
UKpn73 UKpn74 UKpn76 UKpn77
UKpn78 UKpn80 UKpn81 UKpn82
UKpn83
b.
C3b deposition (gMFI)
10000
1000
100
0.01
0.1
1
IgG1 (µg/ml)
UKpn63 UKpn64 UKpn66 UKpn67
UKpn68 UKpn69 UKpn71 UKpn72
UKpn73 UKpn74 UKpn76 UKpn77
UKpn78 UKpn80 UKpn81 UKpn82
UKpn83
c.
Inactive
Active
Antibody binding (gMFI)
100000
10000
1000
100
UKpn82 UKpn83 UKpn80 UKpn66 UKpn78 UKpn81 UKpn68 UKpn73 UKpn71 UKpn64 UKpn69 UKpn72 UKpn67 UKpn76 UKpn77 UKpn74 UKpn63
d.
Antibody binding (gMFI)
1000000
100000
10000
1000
100
10
WT
ΔwbbO
ΔwbbY
e.
D-galactan I
D-galactan II
O1
O2
KpnO1 ΔwbbO
KpnO1 ΔwbbY
f.
UKpn82
UKpn83
UKpn80
UKpn66
UKpn78
UKpn81
UKpn68
UKpn73
UKpn71
UKpn64
UKpn69
UKpn72
UKpn67
UKpn76
UKpn77
UKpn74
UKpn63
SF001 (O1v1)
SF008 (O1v2)
SF004 (O1v2)
SF003 (O1v1)
10
5
0
Antibody binding (log2 fold change compared to buffer)
g.
Cross-reactive anti-O1-antibodies
UKpn69
UKpn72
UKpn76
UKpn63
UKpn82
UKpn73
UKpn74
UKpn81
UKpn64
UKpn66
KpnO1 MB-17667

Figure 3| Antibodies against *Kpn*O1 recognize the O1 antigen and differ in capacity to drive complement activation

(a) *K. pneumoniae Kpn*O1 was incubated with a titration of anti-*Kpn*O1 IgG1. IgG1 binding was detected by flow cytometry using anti-hu-IgG-AF647. **(b)** Antibody-dependent C3b deposition on *Kpn*O1 pre-incubated with anti-*Kpn*O1 IgG1. After antibody binding, bacteria were incubated in 1% *Kpn*O1 ΔNHS as a complement source, and C3b-deposition was detected using anti-hu-C3b-AF647 by flow cytometry. Complement activating antibodies in red, and non-activating antibodies in black. **(c)** Bars represent antibody binding at 0.3 µg/ml IgG1 to *Kpn*O1, ordered based on signal strength of C3b deposition. Complement activating antibodies in red, and non-activating antibodies in black. **(d)** *Kpn*O1 wild-type, O-antigen (Δ*wbbO*) and D-galactan II (Δ*wbbY*) mutant strains were incubated with 1 µg/ml IgG1 followed by detection with anti-hu-IgG-AF647 using flow cytometry. **(e)** Schematic representation of the LPS O1- and O2-antigen polysaccharide. Both the O1- and O2-antigen consist of repeating D-galactan-I moieties in blue that attach to the LPS core saccharide in black, but the most distal part of O1-antigen consists of D-galactan-II repeats in orange. Deletion of the WbbO glycosyltransferase leads to the loss of the complete O-antigen, whereas deletion of the WbbY glycosyltransferase only leads to the loss of the distal D-galactan-II part of the O-antigen [14]. **(f)** O1-antigen expressing strains were incubated with 1 µg/ml IgG1 followed by detection with anti-hu-IgG-AF647 using flow cytometry. Relative antibody binding was calculated by dividing the signal by the buffer control. Depicted data show the log2 difference compared to the control. **(g)** Representative western blot developed using different anti-*Kpn*O1 IgG1. *Kpn*O1 and an additional clinical strain expressing the O1-antigen (MB-17667) were lysed, and the proteins in the lysate were digested. The samples were loaded on an SDS-PAGE gel and blotted onto a transfer membrane. The membrane was incubated with the *Kpn*O1 antibodies followed by goat anti-hu-IgG-HRP. Bands were visualized using ECL. The cross-reactive antibodies of (f) are indicated **(a-c)** Isotype controls are depicted in grey. Flow cytometry data are represented by geometric mean fluorescent intensity (gMFI) values of bacterial populations. Data represent mean ± standard deviation of two independent experiments. **(d)** A representative experiment of two independent experiments is shown.

Genes involved in the synthesis of the O-antigen are encoded by same locus in O1-antigen and O2-antigen strains [14]. However, O1-antigen strains express two additional genes (*wbbYZ*), which are involved in attaching D-galactan-II (O1) on top of a D-galactan-I (O2) segment at the distal part of the O-antigen to form a O1-antigen cap (fig. 3e) [14]. Upon specific deletion *wbbY*, we observed that 16 out of 17 antibodies could no longer bind to *Kpn*O1 (fig. 3d). Strikingly, we found that UKpn69 could still bind to *Kpn*O1 Δ*wbbY* strain, although with reduced capacity, suggesting suggests that UKpn69 has some affinity for D-galactan-I as well (fig. 3d). This shows that all the identified anti-*Kpn*O1 antibodies targeted the O1-antigen polysaccharide on *Kpn*O1. We next analyzed whether anti-*Kpn*O1 antibodies recognized different O1 strains. This revealed that most antibodies only react with *Kpn*O1 but not with other O1 strains (fig. 3f). In contrast, four O1 antibodies (UKpn69, UKpn72, UKpn76 and UKpn77) cross-reacted with all tested O1 strains (fig. 3f). Analysis of antibody binding to bacterial

lysates showed that only these antibodies recognized the O1 antigen outside the context of the bacterial cell membrane (fig. 3g). This supports the idea that different epitopes within the O1-antigen might be recognized. Altogether, these data show that identified O1 antigen specific antibodies differ in their capacity to drive complement.

Antibody-driven C3b deposition results in effective phagocytosis and killing of *Kpn*O2 and *Kpn*O1 by human neutrophils

Several identified antibodies stimulate C3b-deposition on *K. pneumoniae*, which can stimulate phagocytosis by human neutrophils. We tested the capacity of freshly isolated neutrophils to phagocytose GFP-labelled *Kpn*O2 or *Kpn*O1 in the presence of antibodies and ΔNHS as a complement source. As expected, anti-O2- and anti-O1-antibodies that stimulated C3b deposition also induced phagocytosis in a dose-dependent manner (fig. 4a, 4b). In line with the C3b deposition results, complement-mediated phagocytosis of *Kpn*O2 was only observed for the anti-O2-antigen antibodies UKpn2 and UKpn6, but not for the capsule targeting antibodies, UKpn1 and UKpn3 (fig. 4a). Similarly, only the complement activating anti-O1-antigen antibodies UKpn64 and UKpn72 induced phagocytic uptake of *Kpn*O1 by human neutrophils (fig. 4b). Neutrophil activation and phagocytosis of *K. pneumoniae* can result in killing of bacteria. To test if anti-*K. pneumoniae* antibodies induced neutrophil-mediated killing, we transformed a *lux*-reporter vector into *Kpn*O2 and *Kpn*O1 that induces luminescence when the bacteria are metabolic active [28]. In the presence of serum, UKpn2 and UKpn6 were able to stimulate neutrophil induced killing of *Kpn*O2 in a dose-dependent manner, whereas anti-capsule antibodies UKpn1 and UKpn3 did not promote killing of *K. pneumoniae* by neutrophils (fig. 4c). Similarly, we observed that UKpn64 and UKpn72 stimulated neutrophil killing of *Kpn*O1 (fig. 4d). Complement activation by UKpn2 and UKpn6 in serum in the absence of neutrophils slightly lowered the metabolic activity of *Kpn*O2 (fig. 4e). Although this effect was less compared to the condition where neutrophils were present (fig. 4c), it indicates that MAC-mediated killing might play a role. For UKpn72 and UKpn64 the neutrophil independent effect on metabolic activity was more pronounced suggesting that both antibodies can induce MAC-mediated killing (fig. 4f). For UKpn2 and UKpn72, we observed that bacterial viability increases again at higher concentrations. To summarize, we showed that antibody-dependent complement deposition leads to phagocytic uptake and killing of *K. pneumoniae.*

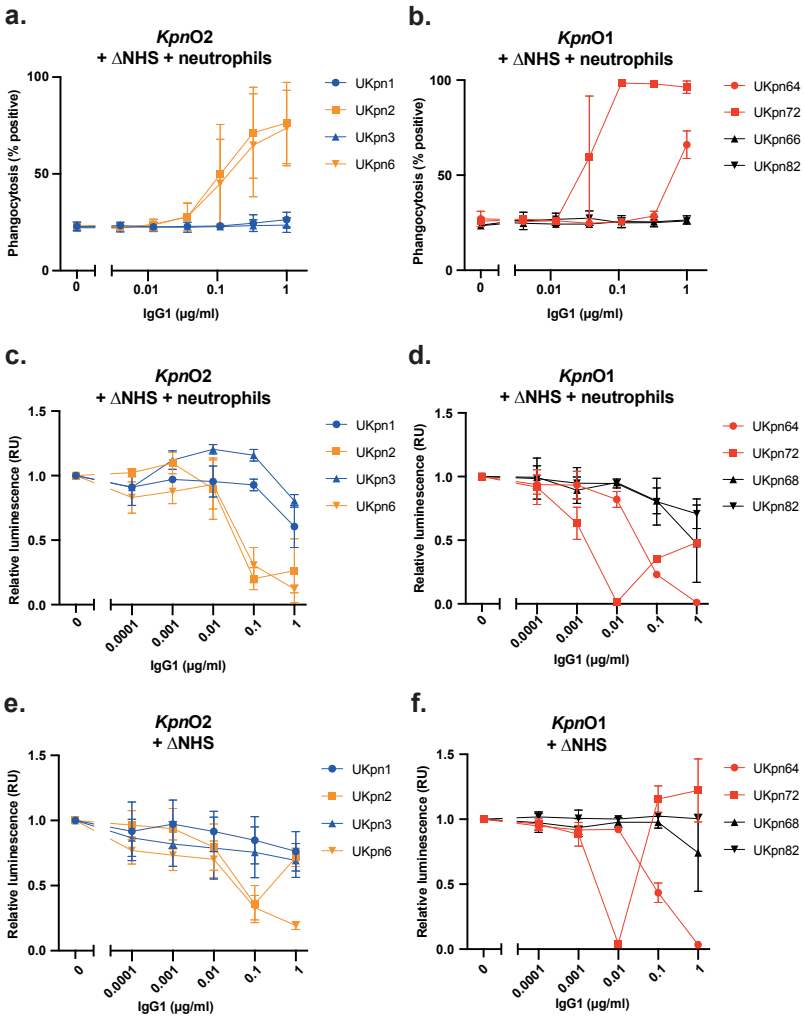

Figure 4| Complement activating monoclonal antibodies promote killing of *K. pneumoniae* by neutrophils and MAC

(a&b) Antibody-dependent phagocytosis of *K. pneumoniae* *Kpn*O2 (a) and *Kpn*O1 (b). GFP expressing bacteria were incubated in the presence of antibody and 3% ΔNHS (*Kpn*O2) or 0.5 ΔNHS (*Kpn*O1) as a source of complement. Isolated human neutrophils were allowed to phagocytose opsonized bacteria for 15 minutes at 37°C, after which the percentage of GFP-positive neutrophils was determined by flow cytometry. **(c-f)** Lux-expressing *K. pneumoniae* were incubated with antibodies and ΔNHS. Luminescence of *Kpn*O2 (c&e) and *Kpn*O1 (d&f) at 2 x 10^5 bacteria/ml was determined in 8% ΔNHS (*Kpn*O2) or 1% ΔNHS (*Kpn*O1) in the presence (c&d) or absence (e&f) of 2 x 10^6 neutrophils/ml. The luminescence was determined after 240 minutes at 37°C as a proxy for viability. The luminescent signal is depicted as the relative value compared to the control without antibody. **(a-f)** Data represent mean ± standard deviation of two independent experiments.

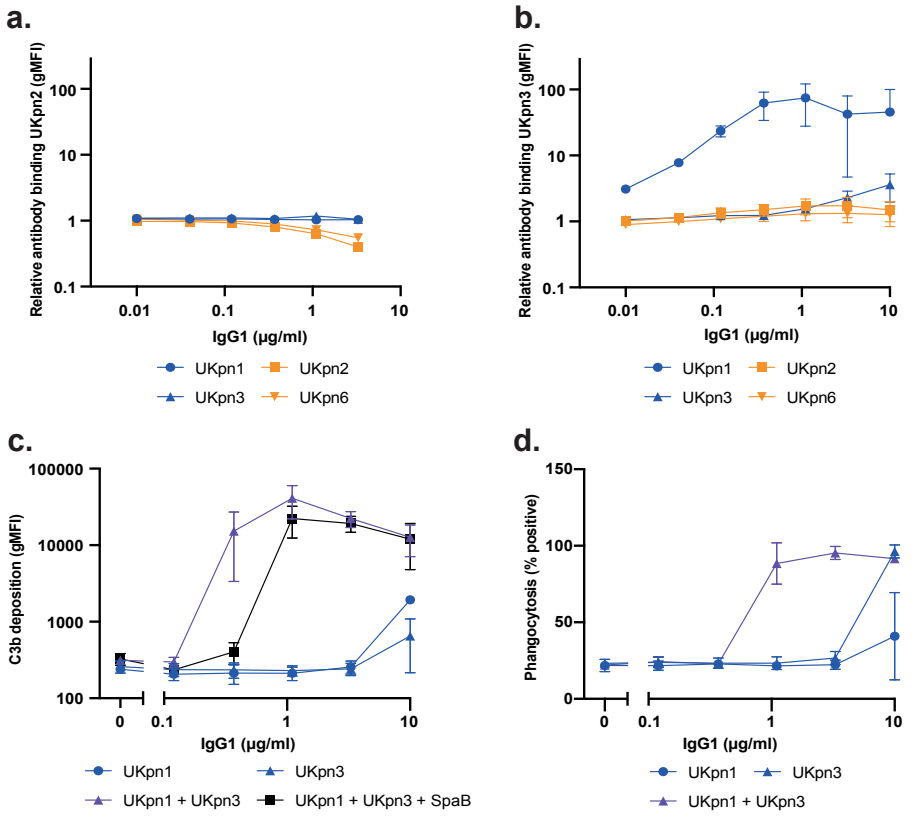

Figure 5| Combining capsule targeting antibodies improves complement activation on *Kpn*O2

(a&b) *K. pneumoniae KpnO2* was incubated with 0.1 µg/ml directly labelled UKpn2-AF488 (anti-O2) or UKpn3-AF647 (anti-capsule). A concentration range of antibodies UKpn1, UKpn2, UKnp3 or UKpn6 was added to the labeled antibodies. UKpn2-AF488 (**a**) and UKpn3-AF647 (**b**) binding was detected by flow cytometry. The relative antibody binding was calculated by dividing geometric fluorescent intensity (gMFI) with the gMFI of fluorescent antibody only. **(c)** Antibody-dependent C3b deposition on *Kpn*O2 pre-incubated with UKpn1, UKpn3 or UKpn1-UKpn3 combined, in the absence or presence of 10 µg/ml SpA-B. After antibody binding, bacteria were incubated in 3% normal human serum (NHS) as a complement source, in the absence or presence of 10 µg/ml SpA-B. C3b-deposition was detected using anti-hu-C3b-AF647 by flow cytometry. Data represent the geometric mean fluorescent intensity (gMFI) values of bacterial populations. **(d)** *Kpn*O2-GFP was pre-incubated with UKpn1, UKpn3 or UKpn1-UKpn3 combined in 3% NHS. Isolated human neutrophils were allowed to phagocytose opsonized bacteria, after which the percentage of GFP-positive neutrophils was determined by flow cytometry. **(a-d)** Data represent mean ± standard deviation of two independent experiments.

Combining anti-capsular antibodies enables complement activation

Finally, we wondered whether combining different antibodies targeting surface antigens would affect complement activation on *K. pneumoniae*. We focused on *Kpn*O2, as we have both O-antigen and capsule binding antibodies targeting this strain. To determine antibody binding, anti-capsule antibodies UKpn1 and UKpn3 and anti-O2-antigen antibodies UKpn2 and UKpn6 were fluorescently labelled. *Kpn*O2 was incubated with a fixed concentration fluorescent antibody in combination with increasing concentrations of unlabeled antibody. We observed competition in antibody binding between UKpn2 and UKpn6, indicating they bind a similar epitope, or epitopes that are in close proximity of each other (fig. 5a, supplementary fig. 5a). To our surprise, mixing the two anti-capsule antibodies did not lead to competition, but showed synergistic binding, as binding of fluorescent UKpn3 was strongly enhanced in the presence of UKpn1 (fig. 5b, supplementary fig. 5b). We next determined whether the synergistic binding of these capsule antibodies also enhanced complement activation. The two individual capsular antibodies only showed slight C3b deposition at the higher concentrations, however, the combination of both antibodies boosted complement activation efficiency more that 30-fold (fig. 5c). This enhanced C3b deposition also led to increased phagocytosis by neutrophils (fig. 5d).

We hypothesized that the synergistic effects might be due to Fc-Fc interactions between the anti-capsule antibodies that promoted IgG1 hexamerization on the bacterial surface. To test this, we added the SpA-B protein, which prevents Fc-mediated hexamerization of IgG1 antibodies [29]. The addition of SpA-B reduced C3b deposition induced by the anti-capsular antibodies, but did not fully block complement activation, indicating that enhanced hexamerization was not the driving factor of the observed synergistic effect (fig. 5d). On the other hand, SpA-B did efficiently inhibit the C3b-depositon induced by the anti-O2-antigen antibody UKpn2, indicating that the role of Fc-Fc interactions in complement activation differs between anti-*K. pneumoniae* antibodies with different surface targets (supplementary fig. 5c). These results show that the combination of antibodies targeting the capsule can enhance complement activation and phagocytosis of *K. pneumoniae*.

Discussion

In this study we describe a novel approach to identify human monoclonal antibodies targeting bacterial surface antigens. Using this method, we identified novel antibodies directed against surface antigens of *K. pneumoniae* and studied the differences in their complement activation potential. Combined, our data suggest that antibody-dependent complement activation is dependent on the surface target and that some but not all antibodies can act synergistically.

To better understand antibody-dependent complement activation on bacteria, we here aimed to identify and characterize a large and diverse panel of anti-*K. pneumoniae* antibodies. Although the binding of an antibody to the target surface is the first key step in the complement cascade, binding alone does not automatically trigger complement activation. For instance, on tumor cells, it was shown that not all antibodies have the capacity to form hexameric platforms[30]. For *K. pneumoniae*, it was not known which molecular determinants drive antibody-dependent complement activation. In part, this was due to the lack of a diverse panel of antibodies that recognize the same bacterial strain, and for which the information on the molecular target, binding capacity and complement functionality was known. Using our new method, we identified 29 unique human antibody clones directed against two clinical *K. pneumoniae* strains, *Kpn*O2 and *Kpn*O1. Functional analyses revealed that the ability to activate the complement system was influenced by the antigen target.

For the O2 strain, we found 12 antibodies targeting the O2-antigen and 3 against the capsule (KL110). Although the binding of antibodies against the O2-antigen and capsule was comparable, we found that all anti-O2-antigen antibodies were able to activate the complement system, whereas the anti-capsule antibodies were inactive. As the capsule polysaccharide is a highly abundant structure that consists of repeating motives, it has a high antigen density. Therefore, anti-capsule antibodies might be spaced too far apart to form hexamers. The importance of clustering of anti-capsule antibody for complement activation has previously been shown on *Streptococcus pneumoniae*, where wild-type IgG1 antibodies were not able to activate complement but introducing clustering enhancing mutations strongly promoted complement activation [31]. Interestingly, when combining two anti-capsule antibody clones, we observed that these antibodies synergized in binding and complement activation. We hypothesized that this synergy might have been caused by Fc-interactions between

IgG1 antibodies required for hexamerization and complement activation[1,32]. However, the addition of SpA-B, which prevents these interactions [29] could not fully inhibit the synergistic effects observed. This could indicate that complement activation by these antibodies does not depend on the previously reported hexamerization mechanisms for IgG1 [1,32], but might be dependent on different interactions between the antibodies. The possibility also remains that C1 might interact with anti-capsule antibodies that are not forming hexameric complexes.

For the O1 strain, all 17 antibodies recognized the O1-antigen. In contrast to the O2-targeting antibodies, not all anti-O1-antigen antibodies were able to activate complement. Our data suggest that the four most potent antibodies (UKpn69, UKpn72, UKpn76 and UKpn77) recognized a conserved epitope within the O1 antigen. Only these four antibodies were able to cross-react with all four tested O1 strains and could recognize the O1-antigen outside the context of the bacterium.

For all discovered complement-activating antibodies, we observed that C3b deposition on the surface of *K. pneumoniae* induced complement-mediated phagocytosis and killing by human neutrophils. It has previously been shown that anti-O1- and O2-antigen antibodies can induce opsonophagocytosis, and are protective in a murine infection model [15]. Altogether, these studies highlight the importance of complement-dependent phagocytosis in immune defense against *K. pneumoniae*. Since many clinical *K. pneumoniae* strains are MAC resistant[33], opsonophagocytic killing of *K. pneumoniae* using antibodies might be a very important defense mechanism.

In this study we present an approach to identify, sequence, and characterize novel anti-bacterial antibodies using a method to stain human B cells with intact bacteria. The presented method has several advantages compared to the more traditional methods in which bacterial antigens are first isolated and then used to stain B cells. First, as bacteria express a myriad of surface antigens, the use of intact bacteria allows the identification of antibodies against multiple surface antigens. Whereas previous studies were focused on identifying antibodies targeting the O-antigen [15,23], this is the first study describing human monoclonal antibodies recognizing the capsule of *K. pneumoniae*. A second advantage is that it allows the identification of antibodies that recognize antigens in the context of the whole bacterium. The importance of the bacterial context in antibody binding has previously been shown for antibodies against the O-antigen of *K. pneumoniae*, which were able to recognize the isolated

O-antigen but did not bind to bacteria expressing that same O-antigen [15]. *Vice versa*, we identified antibodies that were able to bind the O1-antigen on *K. pneumoniae* but did not recognize O1-polysaccharide outside the bacterial context. Identification of these antibodies might have been impossible using purified O1-antigen. The bacterial context could especially be important for surface antigens such as outer membrane proteins that display only a small part of their overall structure at the bacterial surface. A third advantage relates to efficiency; producing and purifying isolated antigens can be a laborious and costly process, especially for hydrophobic membrane proteins. Therefore, using entire bacteria in B cell selection is an interesting alternative to identify novel antibodies.

Next to these advantages, the presented method also has several challenges. Although we aimed to find antibodies against a large variety of surface antigens, we primarily found antibodies targeting the LPS O-antigen, as well as several anti-capsule antibodies. That only a limited number of antibody targets were identified might be due to our selection method, which relies on B cells binding bacterial surface antigens via their B cell receptors (BCR). It is plausible that only the O-antigen and capsule can be reached by BCRs, as other surface structures might be shielded by the O-antigen and capsule[12,19,20]. To overcome this limitation, B cell selections with O-antigen and capsule deficient strains could be performed. Finally, it is possible that healthy individuals primarily have B cells expressing antibodies targeting the O-antigens. Both the O1- and O2-antigen are expressed by a large number of *K. pneumoniae* strains, increasing the chances that a person encounters these antigens. However, for more diverse antigens, such as the capsule, this chance is smaller. This might be the reason that we did not identify antibodies directed to the capsule of *Kpn*O1. To overcome this problem, screening B cells isolated from patients that recovered from a bacterial infection using their associated strains is an interesting approach to identify a wider variety of antibodies.

Finally, since the antigenic targets of our antibodies were initially unknown, an additional strategy was required to identify the antigens of the antibodies. Here we used a transposon screening approach, which allowed us to screen for loss of antibody binding against many different *K. pneumoniae* mutants simultaneously to identify genes associated with the antibody targets. This revealed that, although most of identified antibodies recognized the O-antigen, the exact molecular epitopes recognized by the different antibodies varied. For example, we found several transposon mutants

that no longer bound UKpn2 while retaining UKpn6 binding. These mutants were all affected in the gene *orf7*, indicating that UKpn2 binding critically depends on *orf7* expression. The function of *orf7* is still unknown, but it is predicted to encode for a galactosyltransferase [27], and our data suggests that it may be involved in modifying the O-antigen. Additionally, we observed that UKpn6 and UKpn7 were able to recognize strains expressing the O2a-antigen, but not O2afg-expressing strains. The structure of O2a- and O2afg-antigen is similar, but the O2afg-antigen contains additional 1-4 linked α-D-Galp side groups [34]. This could suggest that UKpn6 and UKpn7 recognize an epitope on O2a that is shielded on O2afg. Furthermore, we observed that UKpn14 bound to the O2-antigen expressing *K. pneumoniae* strains, as well as to a strain that contained the OL104 locus. This was surprising, as OL104 locus shares sequence similarity with O3- and O5-loci and is therefore predicted to use mannose as the base sugar instead of galactose found in O2-antigens [35].

In conclusion, this work aids in the discovery of novel antibodies against bacteria and development of novel therapies to treat *K. pneumoniae* infections. Next to identifying novel antibodies, our work also shows that combining different antibodies can lead to strong and synergistic enhancement of complement activation. This will not only broaden our current understanding of complement activation on bacterial cells but might also be crucial for the development of potent antibody-based therapies.

Methods

Reagents

Normal human serum (NHS) was prepared as described before[36]. In short, blood was drawn from healthy volunteers, allowed to clot, and centrifuged to separate serum from the cellular fraction. Serum of 15-20 donors was pooled and stored at -80 °C. Bacterium depleted NHS (ΔNHS) was prepared as previously described [33]. Briefly, ice cold NHS was incubated with bacteria to allow bacterium specific antibodies to bind. Bacteria were pelleted and ΔNHS was collected. Three depletion rounds were performed followed by a filtration step. RPMI (ThermoFisher) supplemented with 0.05% human serum albumin (HSA, Sanquin), further referred to as RPMI buffer, was used in all experiments, unless otherwise stated. Phosphate-buffered saline (PBS) was prepared in house, unless otherwise stated. OxEA imaging buffer [37] consisted of PBS supplemented with 50 mM β-mercaptoethylamine hydrochloride (30078, Sigma-

Aldrich), 3% (v/v) OxyFluor™ (SAE0059, Sigma-Aldrich) and 20% (v/v) sodium DL-lactate solution (L1375, Sigma-Aldrich), pH 8.0-8.5 (NaOH). MACS buffer consisted of PBS supplemented with 0.5% heat-inactivated fetal calf serum (S181H, Biowest) and 2 mM EDTA (03610, Fluka). B cell culture medium consisted of IMDM (P04-20050, PAN Biotech) and 10% heat-inactivated fetal calf serum (S181H, Biowest). Flow cytometry staining buffer consisted of DPBS (PBS-1A, Capricorn) supplemented with 3% heat-inactivated fetal calf serum (S181H, Biowest). Lysis buffer consisted of RNAse free water supplemented with 10 mM Tris pH 8 (10708976001, Roche) and 1 U / µl RNAsin plus RNAse Inhibitor (N2613, Promega) at pH 8.

Bacterial strains

Klebsiella pneumoniae Kp209[38] was kindly provided by Axel Janssen (University Medical Centre Utrecht, The Netherlands; University of Lausanne, Switzerland) and will be referred to as *KpnO2*. Clinical *K. pneumoniae* strains, including *KpnO1,* were kindly provided Jelle Scharringa, Jannetta Top and Ad Fluit (University Medical Centre Utrecht, The Netherlands). An overview of strains used in this study is included in supplementary table 1. The O-antigen and capsule types (O-type and K-type, respectively) of the *K. pneumoniae* strains were determined based on previously published genome sequences using Kaptive v0.7.3 [14,39,40].

Bacterial growth

Unless stated otherwise, *K. pneumoniae* was cultured on Lysogeny broth (LB) 1.5% agar plates at 37 °C. Single colonies were picked and cultured overnight in LB medium at 37 °C while shaking. The following day the bacteria were subcultured by diluting the overnight culture 1:100 in fresh medium and grown to OD_{600}= 0.4-0.5 at 37 °C while shaking. Bacteria were washed twice with RPMI buffer by centrifugation at 10,000 g for 2 minutes and resuspended to OD_{600}= 0.5 in RPMI buffer.

Fluorescent labelling of bacteria via click-chemistry

Fluorescent labelling of *K. pneumoniae* was based on the labelling method for *E. coli* as previously described [41]. A 1:100 subculture containing 2 µM KDO-N_3 (kindly provided by Pieter de Saint Aulaire and Tom Wennekes, Utrecht University, The Netherlands) was cultured shaking for 16 hours at 37 °C. Bacteria were washed twice with ice cold DPBS + 3%FCS, γirradiated (10 kGy, Synergy Health, Ede, the Netherlands) and stored at 4 °C. The γirradiated bacteria were incubated with 50 µM DBCO-PEG_4-ATTO-488 (CLK-052-05, Jena Bioscience) or DBCO-Cy5 (777374, Sigma-Aldrich) or DBCO-Cy3

(777336, Sigma-Aldrich) for 24 hours shaking at 4 °C. Bacteria where then washed twice with DPBS + 3% FCS and counted by flow cytometry (MACSQuant, Milteny Biotech). Fluorescent labelling was assessed by flow cytometry (MACSQuant, Milteny Biotech or FACSVerse, BD Bioscience).

Generation of *K. pneumoniae*-GFP, *K. pneumoniae*-lux, and *K. pneumoniae* deletion mutants

K. pneumoniae was subcultured to OD_{600}=0.6-0.8 in 50 ml LB medium, washed twice with 50 ml ice cold miliQ water, and washed twice with 25 ml ice cold 10% glycerol. Bacteria were resuspended in 1 ml 15% glycerol and stored at -80 °C in 50 µl aliquots. 50 µl electrocompetent *K. pneumoniae* was mixed with plasmid or PCR product and transformed using a Gene Pulser Xcell electroporation system (Bio-Rad) in a 0.2 cm cuvette (voltage at 2500V, capacitance at 25 µF, and resistance at 200 Ω). Electroporated bacteria were cultured in 500 µl S.O.C. medium (15544034, Invitrogen) for 60 minutes at 37 °C, plated on LB agar plates containing the appropriate antibiotics and cultured overnight at 37 °C.

Knockouts were generated using the lambda red method [42]. In brief, primers were designed with 5060 bp flanking regions up and downstream of the target gene. The flanking sequences were fused to primers for amplification of a gentamycin resistance cassette. Purified PCR products were electroporated into electrocompetent *K. pneumoniae* cells containing the pREDKI vector [43]. Gentamycin resistant colonies were analyzed for successful deletion of the gene by PCR. To generate *K. pneumoniae* expressing GFP or the lux operon pULTRA-GFP [44] or pUC18-mini-Tn7T-Gm-lux [28] was used for electroporation. Transformed strains were selected for using 30 µg/ml kanamycin or gentamycin for pULTRA-GFP and pUC18-mini-Tn7T-Gm-lux, respectively.

dStorm Microscopy

µ-Slide glass bottom coverslips (80827, Ibidi) were coated with poly-L-lysine solution (P4707, Sigma-Aldrich). Bacteria that were fluorescently labeled via click-chemistry were washed three times in PBS, fixed in 2% PFA (04018-1, Polysciences) + 0.2% glutaraldehyde (G5882, Sigma-Aldrich) and incubated overnight on the coverslip. Immediately before imaging, coverslips were washed three times in PBS and samples were immersed in OxEA imaging buffer. dSTORM imaging was performed using a Nanoimager S Mark II (ONI) at 32 °C at an angle of 52 °, using a 488 nm and 640 nm laser at 50% laser power. 10.000 frames were acquired per sample with an exposure

time of 30 ms. Images were corrected for drift and filtered using the CODI cloud analysis platform (www.alto.codi.bio, ONI).

B cell isolation

Peripheral blood mononuclear cells (PBMCs) were isolated from buffy coats (E2824R00, Sanquin) using Ficoll-Paque Plus (GE17-1440-02, Cytiva) density gradients (390 g; 20 minutes). Remaining erythrocytes were lysed using cold miliQ for 30 seconds, whereafter 10x PBS was added. PBMCs were washed by centrifugation (296 g, 10 minutes) using MACS buffer. Human B cells were isolated from PBMCs using the untouched B cell Isolation Kit II, human (130-091-151, Miltenyi Biotec) by manual separation according to manufacturer's instructions using Pre-Separation Filters (30 µm, 130-041-407, Miltenyi Biotec). Isolated B cells were cryopreserved in B cell culture medium supplemented with 10% dimethylsulfoxide (DMSO, 1.02952, Sigma-Aldrich) and 40% heat-inactivated fetal calf serum (S181H, biowest) at -80 °C in a Mr. Frostry freezing container (5100-0001, Thermo Scientific). Cryopreserved B cells were thawed by added them to B cell culture medium pre-heated to 37 °C, and washed twice by centrifugation (296 g, 10 minutes, 37 °C). Viable B cells were counted using a TC20 Automated Cell Counter (Bio-Rad) with trypan blue (1450013, Bio-Rad), resuspended to 2 x 10^6 cells/ml and incubated for 2 hours at 37 °C and 5% CO2.

***K. pneumoniae* specific B cell stain and single cell sorting**

Isolated B cells were washed twice by centrifugation (296 g, 10 minutes) and resuspended in flow cytometry staining buffer containing combinations of detection antibodies and fluorescently labelled bacteria. Analysis of the dual bacterium staining was analyzed on a FACSVerse instrument using mouse anti-hu-CD19-BV510 (302242, BioLegend) at 1:25, mouse anti-hu-CD27-PE-Cy7 (560609, BD) at 1:200, *KpnO2*-ATTO-488 and *KpnO2*-Cy5 was used. Single B cell sorting was performed on different instruments. For the sort using the FACSMelody (BD) instrument mouse anti-hu-CD19-BV510 (302242, BioLegend) at 1:25, mouse anti-hu-IgG-BV421 (562581, BD) at 1:50, *KpnO2*-ATTO-488 & *KpnO2*-Cy3 was used. For the sort using the MA900 (Sony) instrument mouse anti-hu-CD19-PE-Cy7 (560728, BD) at 1:200, mouse anti-hu-IgG-BV421 (562581, BD) at 1:50, *KpnO2*-ATTO-488 and *KpnO2*-Cy5 was used. For the sort using the Influx cell sorter (BD) instrument mouse anti-hu-CD19-BV510 (302242, BioLegend) at 1:25, mouse anti-hu-IgG-PE-Cy7 (561298, BD) at 1:400, *KpnO1*-ATTO-488 and *KpnO1*-Cy5 was used. Bacteria of each fluorescent label were added at a living-B-cell-to-bacterium ratio of 2-to-1, unless stated otherwise. B cells

were incubated for 30 minutes, washed twice by centrifugation (296 g, 10 minutes), and resuspended in flow cytometry staining buffer. At least five minutes before sorting or measuring the samples in the flow cytometer, Sytox AADvance (R73137, Invitrogen) death cell marker was added at 1:40. *K. pneumoniae*-specific B cells were selected based on the following criteria: single cells, Sytox AADvance$^-$, CD19$^+$, IgG$^+$, and double-bacterium-positive. *K. pneumoniae*-specific B cells were sorted into 96-well PCR-plates (N8010560, Applied Biosystems) containing 10 µl lysis buffer using a FACSMelody (BD), MA900 (Sony) or Influx cell sorter (BD) instrument. PCR-plates were sealed (4306311, Applied Biosystems) and stored at -80 °C until further use.

Antibody cloning and expression

Lysed single B cells were thawed to amplify VH and VL regions using the OneStep RT-PCR kit (Qiagen). Procedure was performed according to manufacturer's protocol with a primer mixture to amplify heavy, kappa and lambda variable sequences (Supplementary table 2, primer list, each primer at 20 nM). To each well 15 µl master mix was added and RT-PCR was performed by incubation for 30 minutes at 50 °C, 15 minutes at 95 °C, followed by 40 cycles of 1 minute at 95 °C, 1 minute at 55 °C and 1 minute at 72 °C. A second PCR was performed for the amplification of the heavy and light chains separately using 1 µl of the RT-PCR and a mixture of primers containing sequence overhangs required for cloning. The PCR was performed by incubation for 30 seconds at 98 °C, followed by 40 cycles of 10 seconds at 98 °C, 20 seconds at 57 °C and 30 seconds at 72 °C using HF Phusion DNA polymerase (Thermo Scientific).

For cloning the heavy and light chain amplicons into the expression vectors, 1 µl 5-fold diluted heavy chain PCR product and 1 µl 5-fold diluted light chain PCR product were mixed with 2 µl of HiFi DNA assembly (NEB) mixture and 1 µl of pcDNA containing the constant region sequences of hu-IgG1, hu-Kappa and hu-Lambda (pFUSE-CHIg-hG1, pFUSE2-CHIg-hK, and pFUSE2-CLIg-hL2, respectively, Invitrogen). The mixture was incubated for 1 hour at 50 °C followed by transformation to competent *E. coli* Top10 cells. Transformation was equally divided and added to 1.5 ml LB containing either kanamycin or ampicillin for selection of the heavy chain and light chain expression vectors, respectively. After overnight incubation at 37 °C while shaking, the culture was diluted 1:100 in fresh LB medium containing kanamycin or ampicillin and cultured overnight. Plasmids were isolated using the PureLink™ *Pro* Quick96 Plasmid Purification Kit (K2110, ThermoFisher) and heavy chain and light chain plasmid were transfected into EXPI293F cells [45]. After a 5-day culture, supernatant was harvested

and tested for *K. pneumoniae*-specific antibodies using flow cytometry. For expression supernatants that contained antibodies binding to *K. pneumoniae*, the corresponding *E. coli* Top10 transformation cultures containing the heavy and light chain expression vectors were plated to select single colonies to obtain clonal plasmids. Plasmids were isolated from single colonies and the VH and VL sequences were analyzed using Sanger sequencing. Clonal plasmids were used for antibody production in EXPI293F cells followed by purification. Antibodies were purified using a HiTrap protein A column using the AktA Pure (GE Healthare) as previously described [46]. After capture antibodies were eluted according to the manufacturer's instructions. Collected antibodies were dialyzed overnight against PBS at 4 °C, and stored at -80 °C.

IgG1 sequence analysis

IgG genes usage was determined using the IgBlast web tool (Release 1.20.0, NCBI, https://www.ncbi.nlm.nih.gov/igblast/index.cgi) with standard settings. The heavy and light chain sequences were compared to germline sequences with the highest homology, and used to determine the number of somatic hypermutations, from the start of the fragmenting region 1 (FR1) to the end of the FR3. Deletions and insertions were counted as one mutation. Clonally related sequences were identified on bases of the *IGHV* CDR3 sequence. Translated sequence alignments were created using Genious R9 (v9.1.6)

Antibody deposition

Bacteria (OD_{600}= 0.05) were incubated with IgG1 antibodies diluted in RPMI buffer for 30 minutes at 4 °C under shaking conditions and washed twice by centrifugation with RPMI buffer. Unless stated otherwise, bacteria were resuspended in 1 µg/ml goat anti-hu-IgG-AF647 (2040-31, SouthernBiotech) or 1 µg/ml goat anti-hu-IgG-AF488 (2040-3, SouthernBiotech) for 30 minutes at 4 °C while shaking. Bacteria were washed twice with RPMI buffer and fixated in 1.5% paraformaldehyde in PBS for five minutes. Binding was assessed by flow cytometry.

Complement deposition

Freshly cultured bacteria (OD_{600}= 0.05) were incubated with antibody diluted in RPMI buffer with or without 10 µg/ml SpA-B (produced inhouse[29]) (30 minutes, 4 °C, 600rpm), and washed twice by centrifugation (5 minutes, 4 °C, 2424 g). Bacteria were resuspended and incubated in NHS diluted in RPMI buffer with or without 10 µg/ml SpA-B (30 minutes, 600rpm, 37 °C). After washing twice, bacteria were incubated

with mouse anti-C3b-AF647 (bH6, produced inhouse[36]) (30 minutes, 4 °C, 600rpm), washed twice again and fixated with 1.5% PFA. Fluorescence was detected via flow cytometry.

Conjugation of fluorophores to antibodies

To fluorescently label antibodies, Alexa Fluor 488 NHS Ester (A20000, Invitrogen) or Alexa Fluor 647 NHS Ester (A20006, Invitrogen) was used according to the manufacturer's protocols. Unbound label was removed by buffer exchange into PBS using Zebra Spin desalting columns (40K, Thermo Scientific), and the degree of labeling was measured. Antibodies were stored at 4 °C.

Transposon screening for antibody target identification

The barcoded Tn5 transposon library in *K. pneumoniae* Kp209_CSTR (here referred to as *Kpn*O2R) was previously described [33]. Coupling of the barcoded transposon to the genomic location was performed using Tnseq [24,25]. Not all barcodes could be allocated indicating that deeper sequencing of the transposon library would yield additional hits. The transposon library was stored at -80 °C. To select for loss-of-binding mutants, the library was thawed on ice, 10-fold diluted ant cultured to mid-log (OD_{600}=0.6). Bacteria were washed by centrifugation in RPMI buffer and resuspended to OD_{600}= 0.02 for UKpn1, and OD_{600}= 0.05 for UKpn2 and UKpn6. Bacteria were incubated with 10 µg/ml antibody conjugated with AF488 or AF647 for 30 minutes at 4 °C. Bacteria were washed twice by centrifugation in RPMI buffer and analyzed using a Sony MA900 cell sorter. Transposon mutant bacteria that stained negative for the tested antibodies were single cell sorted into 96 wells plates containing LB medium with 30 µg/ml kanamycin. Surviving bacterial clones were rechallenged with the antibodies to confirm that the mutant lacks the epitope required for antibody binding. Barcodes of the validated clones were amplified via colony PCR using Barseq primers. The PCR products were purified and sequenced by Sanger sequencing to identify the barcode of the selected mutant. Transposon insertion sites were visualized in Genious R9 (v9.1.6)

Bacterial lysate western blots

Single bacterial colonies were scraped of agar plates, washed by centrifugation in PBS (2 minutes 19,000 g), resuspended to OD_{600}= 1.0, and heat-inactivated at 56 °C for one hour. 1 ml heat-inactivated bacteria were pelleted and lysed using Laemmli buffer containing 0.7 M β-mercaptoethanol at 95 °C for 10 minutes. The proteins

in the samples were digested using 400 µg/ml proteinase K for 1.5 hours at 60 °C. Proteinase K was inactivated at 95 °C for 5 minutes, and 5 µl sample was ran over a NuPAGE gel (4%-12% BisTris, NP0323BOX, Invitrogen) for 30 minutes at 300 V. LPS was transferred to a 0.2 µm PVDF membrane (Bio-Rad) using a Transblot Turbo Transfer system (Bio-Rad). Membranes were blocked overnight at 4 °C using 4% Elk (dried skim milk, Campina), washed and incubated with 1 µg/ml antibody in 1% Elk for 1 hour at room temperature. After washing goat anti-hu-IgG-HRP (1:10,000, 2040-05, SouthernBiotech) in 1% Elk was added and incubated for 1 hour at room temperature. After washing, the membranes were developed with Pierce ECL Western Blotting Substrate (Thermo Scientific) and images in a LAS4000 Imagequant (GE Healthcare).

Phagocytosis and killing of *K. pneumoniae* by human neutrophils

Human neutrophils were isolated by density gradient as previously described [47]. Concentration of freshly cultured GFP or Lux expressing *K. pneumoniae* (OD_{600}= 0.5) was determined via flow cytometry (MACSQuant, Miltenyi Biotech). For phagocytosis, 7.5 x 10^5 GFP-expressing bacteria were incubated with antibody and ΔNHS diluted in RPMI buffer with or without 10 µg/ml SpA-B (produced inhouse [29]). After incubation for 15 minutes at 37 °C, while shaking (750 rpm), 7.5 x 10^4 human neutrophils were added, and incubated for another 15 minutes at 37 °C while shaking. Fixation of the samples was performed using 1.5% PFA and phagocytosis was measured via flow cytometry. Metabolic activity was used as proxy for viability of *K. pneumoniae* using Lux-expressing bacteria [28]. To measure viability, 2 x 10^4 Lux-expressing bacteria and 2 x 10^5 neutrophils were incubated in the presence antibody and ΔNHS diluted in RPMI buffer with or without 10 g/ml SpA-B at 37 °C, shaking every minute. Luminescence was measured in a microplate reader (CLARIOstar, BMG Labtech).

Flow cytometry

Flow cytometry was performed using a FACSVerse instrument (BD), acquiring 10,000 events per condition, unless stated otherwise. Flow cytometry data was analyzed in FlowJo V.10. B cells were gated based on forward and side scatter, death cell marker, and CD19 signal. Bacteria and neutrophils were gated based on forward and side scatter.

Data analysis and statistical testing

Unless stated otherwise data collected as three biological replicates and analyzed using GraphPad Prism version 9.4.1 (458). Statistical analyses are further specified in the figure legends.

References

1. Diebolder, C. A. *et al.* Complement is activated by IgG hexamers assembled at the cell surface. *Science* **343**, (2014).
2. Abendstein, L. *et al.* Complement is activated by elevated IgG3 hexameric platforms and deposits C4b onto distinct antibody domains. *Nat. Commun.* **14**, (2023).
3. Sun, D. *et al.* Real-time imaging of interactions of neutrophils with *Cryptococcus neoformans* demonstrates a crucial role of complement C5a-C5aR signaling. *Infect. Immun.* **84**, (2015).
4. Metzemaekers, M., Gouwy, M. & Proost, P. Neutrophil chemoattractant receptors in health and disease: double-edged swords. *Cellular and Molecular Immunology* **17**, (2020).
5. Denk, S. *et al.* Complement C5a-induced changes in neutrophil morphology during inflammation. *Scand. J. Immunol.* **86**, (2017).
6. Magill, S. S. *et al.* Multistate point-prevalence survey of health care–associated infections. *New England Journal of Medicine* **370**, (2014).
7. European Centre for Disease Prevention and Control. *Antimicrobial resistance in the EU/EEA (EARS-Net) - Annual Epidemiological Report 2021*. https://atlas.ecdc.europa.eu/ (2022).
8. Lin, Z., Yu, J., Liu, S. & Zhu, M. Prevalence and antibiotic resistance of *Klebsiella pneumoniae* in a tertiary hospital in Hangzhou, China, 2006–2020. *Journal of International Medical Research* **50**, (2022).
9. Bush, K. *et al.* Tackling antibiotic resistance. *Nature Reviews Microbiology* **9**, 894–896 (2011).
10. Laxminarayan, R. *et al.* Antibiotic resistance-the need for global solutions. *The Lancet Infectious Diseases* **13**, 1057–1098 (2013).
11. Murray, C. J. *et al.* Global burden of bacterial antimicrobial resistance in 2019: a systematic analysis. *The Lancet* **399**, 629–655 (2022).
12. Merino, S., Camprubi, S., Alberti, S., Benedi, V. J. & Tomas, J. M. Mechanisms of *Klebsiella pneumoniae* resistance to complement-mediated killing. *Infect. Immun.* **60**, 2529–2535 (1992).
13. Alberti, S. *et al.* C1q binding and activation of the complement classical pathway by *Klebsiella pneumoniae* outer membrane proteins. *Infect. Immun.* **61**, (1993).
14. Lam, M. M. C., Wick, R. R., Judd, L. M., Holt, K. E. & Wyres, K. L. Kaptive 2.0: updated capsule and lipopolysaccharide locus typing for the *Klebsiella pneumoniae* species complex. *Microb. Genom.* **8**, (2022).
15. Pennini, M. E. *et al.* Immune stealth-driven O2 serotype prevalence and potential for therapeutic antibodies against multidrug resistant *Klebsiella pneumoniae*. *Nat. Commun.* **8**, 1–12 (2017).
16. Fang, C. T., Chuang, Y. P., Shun, C. T., Chang, S. C. & Wang, J. T. A novel virulence gene in *Klebsiella pneumoniae* strains causing primary liver abscess and septic metastatic complications. *Journal of Experimental Medicine* **199**, (2004).
17. Lin, J. C. *et al.* High prevalence of phagocytic-resistant capsular serotypes of *Klebsiella pneumoniae* in liver abscess. *Microbes Infect.* **6**, (2004).
18. Álvarez, D., Merino, S., Tomás, J. M., Benedí, V. J. & Albertí, S. Capsular polysaccharide is a major complement resistance factor in lipopolysaccharide O side chain-deficient *Klebsiella pneumoniae* clinical isolates. *Infect. Immun.* **68**, (2000).
19. Domenico, P., Tomas, J. M., Merino, S., Rubires, X. & Cunha, B. A. Surface antigen exposure by bismuth dimercaprol suppression of *Klebsiella pneumoniae* capsular polysaccharide. *Infect. Immun.* **67**, 664–669 (1999).
20. Salo, R. J. *et al.* Salicylate-enhanced exposure of *Klebsiella pneumoniae* subcapsular components. *Infection* **23**, 371–377 (1995).

21. Domenico, P., Salo, R. J., Cross, A. S. & Cunha, B. A. Polysaccharide capsule-mediated resistance to opsonophagocytosis in *Klebsiella pneumoniae*. *Infect. Immun.* **62**, (1994).
22. Boyd, A. R. & Orihuela, C. J. Dysregulated inflammation as a risk factor for pneumonia in the elderly. *Aging and Disease* **2**, (2011).
23. Rollenske, T. *et al.* Cross-specificity of protective human antibodies against *Klebsiella pneumoniae* LPS O-antigen. *Nature Immunology* **19**, 617–624 (2018).
24. Shiver, A. L., Culver, R., Deutschbauer, A. M. & Huang, K. C. Rapid ordering of barcoded transposon insertion libraries of anaerobic bacteria. *Nature Protocols* **16**, (2021).
25. Wetmore, K. M. *et al.* Rapid quantification of mutant fitness in diverse bacteria by sequencing randomly bar-coded transposons. *mBio* **6**, 1–15 (2015).
26. Clarke, B. R. *et al.* Molecular basis for the structural diversity in serogroup O2-antigen polysaccharides in *Klebsiella pneumoniae*. *Journal of Biological Chemistry* **293**, (2018).
27. Szijártó, V. *et al.* Both clades of the epidemic KPC-producing *Klebsiella pneumoniae* clone ST258 share a modified galactan O-antigen type. *International Journal of Medical Microbiology* **306**, (2016).
28. Damron, F. H. *et al.* Construction of mobilizable mini-Tn7 vectors for bioluminescent detection of Gram-negative bacteria and single-copy promoter lux reporter analysis. *Appl. Environ. Microbiol.* **79**, (2013).
29. Cruz, A. R. *et al.* Staphylococcal protein A inhibits complement activation by interfering with IgG hexamer formation. *Proc. Natl. Acad. Sci. USA* **118**, (2021).
30. Oostindie, S. C. *et al.* DuoHexaBody-CD37®, a novel biparatopic CD37 antibody with enhanced Fc-mediated hexamerization as a potential therapy for B-cell malignancies. *Blood Cancer J.* **10**, (2020).
31. Aguinagalde Salazar, L. *et al.* Promoting Fc-Fc interactions between anti-capsular antibodies provides strong immune protection against *Streptococcus pneumoniae*. *Elife* **12**, (2023).
32. Strasser, J. *et al.* Unraveling the macromolecular pathways of IgG oligomerization and complement activation on antigenic surfaces. *Nano Lett.* **19**, (2019).
33. Van der Lans, S. P. A. *et al.* Colistin resistance mutations in *phoQ* can sensitize *Klebsiella pneumoniae* to IgM-mediated complement killing. *Scientific Reports* **13**, 12618 (2023).
34. Kelly, R. F., Perry, M. B., Maclean, L. L. & Whitfield, C. Structures of the O-antigens of *Klebsiella* serotypes O2 (2a,2e), O2 (2a,2e,2h), and O2 (2a,2f,2g), members of a family of related D-galactan O-antigens in *Klebsiella spp*. *J. Endotoxin Res.* **2**, (1995).
35. Follador, R. *et al.* The diversity of *Klebsiella pneumoniae* surface polysaccharides. *Microb. Genom.* **2**, (2016).
36. Heesterbeek, D. A. *et al.* Bacterial killing by complement requires membrane attack complex formation via surface-bound C5 convertases. *EMBO J.* **38**, e99852 (2019).
37. Nahidiazar, L., Agronskaia, A. V., Broertjes, J., Van Broek, B. Den & Jalink, K. Optimizing imaging conditions for demanding multi-color super resolution localization microscopy. *PLoS One* **11**, (2016).
38. Janssen, A. B. *et al.* Evolution of colistin resistance in the *Klebsiella pneumoniae* complex follows multiple evolutionary trajectories with variable effects on fitness and virulence characteristics. *Antimicrob. Agents Chemother.* **65**, (2021).
39. Wyres, K. L. *et al.* Identification of *Klebsiella* capsule synthesis loci from whole genome data. *Microb. Genom.* **2**, (2016).
40. Wick, R. R., Heinz, E., Holt, K. E. & Wyres, K. L. Kaptive web: User-Friendly capsule and lipopolysaccharide serotype prediction for *Klebsiella* genomes. *J. Clin. Microbiol.* **56**, (2018).
41. Heesterbeek, D. A. C. *et al.* Outer membrane permeabilization by the membrane attack complex sensitizes Gram-negative bacteria to antimicrobial proteins in serum and phagocytes. *PLoS Pathog.* **17**, (2021).
42. Datsenko, K. A. & Wanner, B. L. One-step inactivation of chromosomal genes in *Escherichia coli* K-12 using PCR products. *Proc. Natl. Acad. Sci. USA* **97**, (2000).

43. Yang, J. *et al.* High-efficiency scarless genetic modification in *Escherichia coli* by using lambda red recombination and I-SceI cleavage. *Appl. Environ. Microbiol.* **80**, (2014).

44. Mavridou, D. A. I., Gonzalez, D., Clements, A. & Foster, K. R. The pUltra plasmid series: A robust and flexible tool for fluorescent labeling of Enterobacteria. *Plasmid* **87–88**, (2016).

45. Zwarthoff, S. A. *et al.* Functional characterization of alternative and classical pathway C3/C5 convertase activity and inhibition using purified models. *Front. Immunol.* **9**, (2018).

46. Zwarthoff, S. A. *et al.* C1q binding to surface-bound IgG is stabilized by C1r2s2 proteases. *Proc. Natl. Acad. Sci. USA* **118**, e2102787118 (2021).

47. Bestebroer, J. *et al.* Staphylococcal superantigen-like 5 binds PSGL-1 and inhibits P-selectin-mediated neutrophil rolling. *Blood* **109**, (2007).

48. Van Den Bunt, G. *et al.* Dynamics of intestinal carriage of extended-spectrum beta-lactamase-producing enterobacteriaceae in the Dutch general population, 2014-2016. *Clinical Infectious Diseases* **71**, (2020).

Author contributions

S.P.A.vdL., P.F.K., S.H.M.R., B.W.B. conceived the project. M.F.L.vtW. performed mdTORM microscopy. P.F.K. and S.P.A.vdL optimized dual bacterium B cell staining and performed flow cytometry analyses. S.P.A.vdL, P.F.K. and R.M.M. performed B cell sorts. M.R., C.J.C.dH., L.M.S., and P.C.A. cloned expressed and generated antibodies. B.W.B, P.F.K., and S.P.A.vdL. performed sequences analysis. S.P.A.vdL, M.R. performed antibody binding experiments and C3b deposition. B.W.B. and S.B. performed the transposon screens and analysis. C.J.C.dH. and M.R. generated *K. pneumoniae* deletion mutants. M.R. performed the western blots. M.R. performed phagocytosis, opsonophagocytic killing and serum killing experiments. S.P.A.vdL. B.W.B., and S.H.M.R. wrote the manuscript.

Additional information

Acknowledgments

The authors would like to thank Axel Janssen, Jelle Scharringa, Jannetta Top and Ad Fluit for providing the *K. pneumoniae* used in this study, and Pieter de Saint Aulaire and Tom Wennekes for providing KDO-azide, and Pim van Hespen for his help with O- and K-type analysis using Kaptive v0.7.3.

Competing interests

The authors declare no competing interests.

Financial disclosure statement

This work was supported by the Netherlands Organization for Scientific Research (NWO) through a TTW-NACTAR Grant #16442 (to SvdL and SHMR). The funders had no role in the study design, data collection and analysis, or preparation of the manuscript

Supplementary information

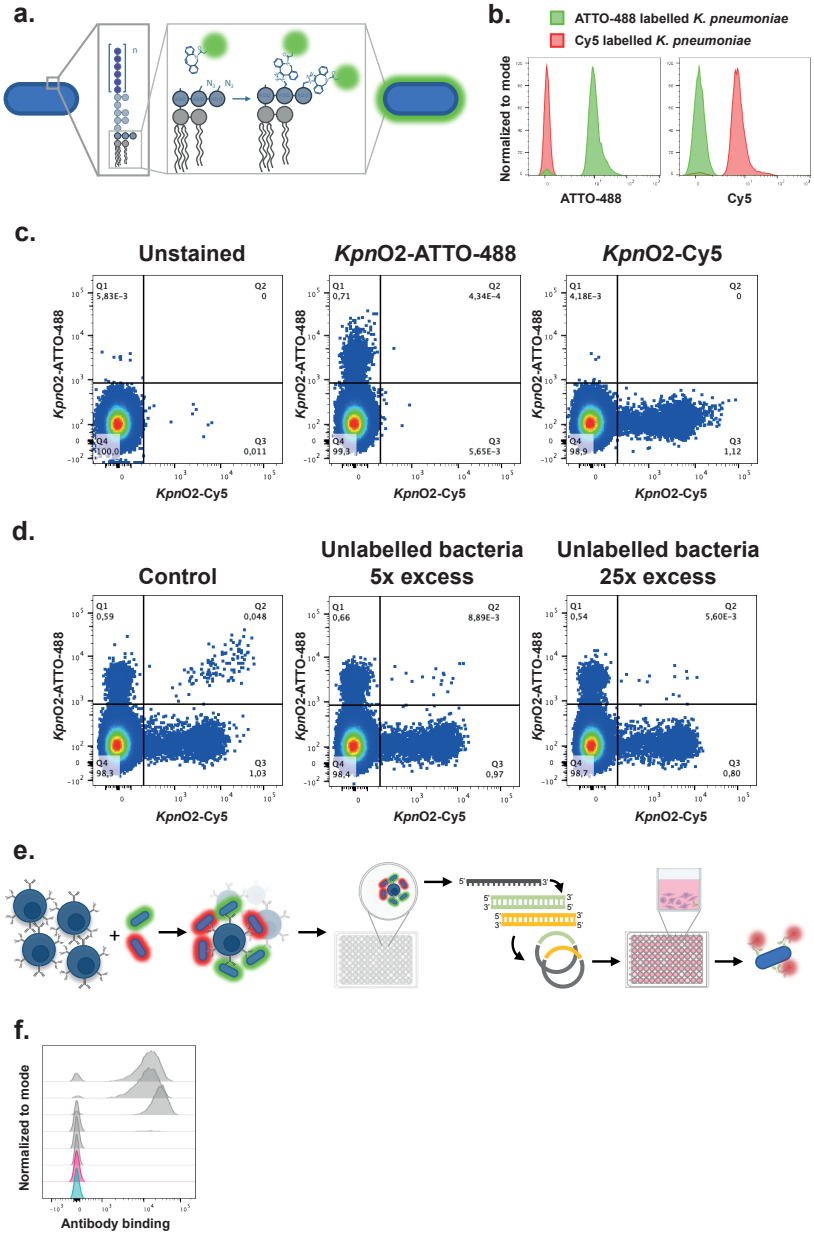

Supplementary figure 1

(a) Cartoon depicting fluorescent labeling of the outer membrane of *K. pneumoniae* via click-chemistry. *K. pneumoniae* was cultured overnight in the presence of KDO-azide (2 μM), which was metabolically incorporated into the LPS core. Cyclooctyne-labelled fluorophores (50 μM) were added, which "clicked" to the azide handles. **(b)**. Fluorescent labeling of *KpnO2* with cy5 or ATTO-488 was assessed via flow cytometry. Fluorescent intensity (gMFI) and number of events normalized to mode are depicted on the X- and Y-axis, respectively. **(c)** Human B cell isolated from healthy donors were incubated with *Kpn*O2-ATTO-488 or *Kpn*O2-Cy5 (MOI of 0.5 per fluorophore). B cells ($CD19^+$) that bound *Kpn*O2-ATTO-488 or *Kpn*O2-Cy5 were detected. **(d)** Human B cell isolated from healthy donors were incubated with *Kpn*O2-ATTO-488 and *Kpn*O2-Cy5 (MOI of 0.5 per fluorophore) with an excess of unlabeled *Kpn*O2. B cells ($CD19^+$) that bound both *KpnO2*-ATTO-488 and *KpnO2*-Cy5 were detected. **(e)** Cartoon depicting the process of *K. pneumoniae*-specific antibody identification. B cells were stained with differently fluorescently labelled *K. pneumoniae*, and B cells double positive for both fluorescent markers were single cell sorted. The variable regions of the heavy and light chain (VH and VL, respectively) were amplified by RT-PCR and cloned into IgG1 expression vectors. Antibodies were recombinantly expressed and tested for antibody binding to *K. pneunoniae*. **(f)** Expression supernatants were 10-fold diluted and incubated with *Kpn*O2 to screen for *Kpn*O2-specific antibodies. IgG1 binding was detected by flow cytometry using anti-hu-IgG-AF647. Exemplary histograms are depicted for the three supernatants with the strongest signal, supernatants without binding signal, empty vector IgG expression supernatants (magenta), and buffer control (teal). **(b&f)** Fluorescent intensity (gMFI) and number of events normalized to mode are depicted on the X- and Y-axis, respectively.

a.

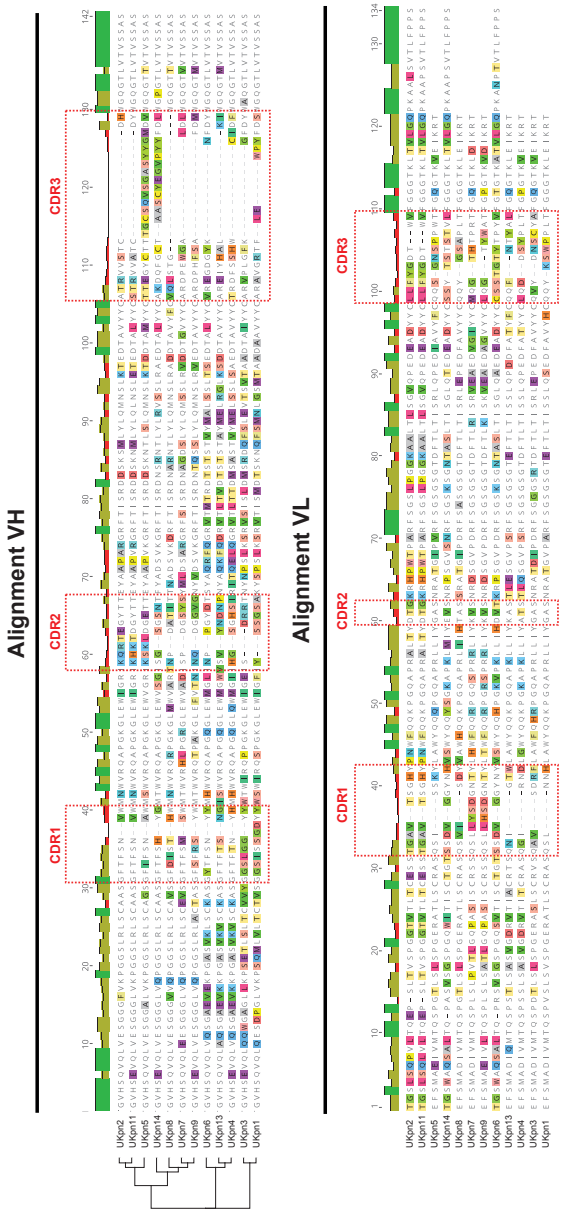

Supplementary figure 2

(a&b) Alignments of the variable regions of the heavy and light chains (VH and VL, respectively) of the unique *Kpn*O2 (a) and *Kpn*O1 (b) binding antibodies. Translated sequence alignment was generated using Genious R9 (v9.1.6). Location if the CDR regions determined using IgBlast web tool (Release 1.20.0)

b.

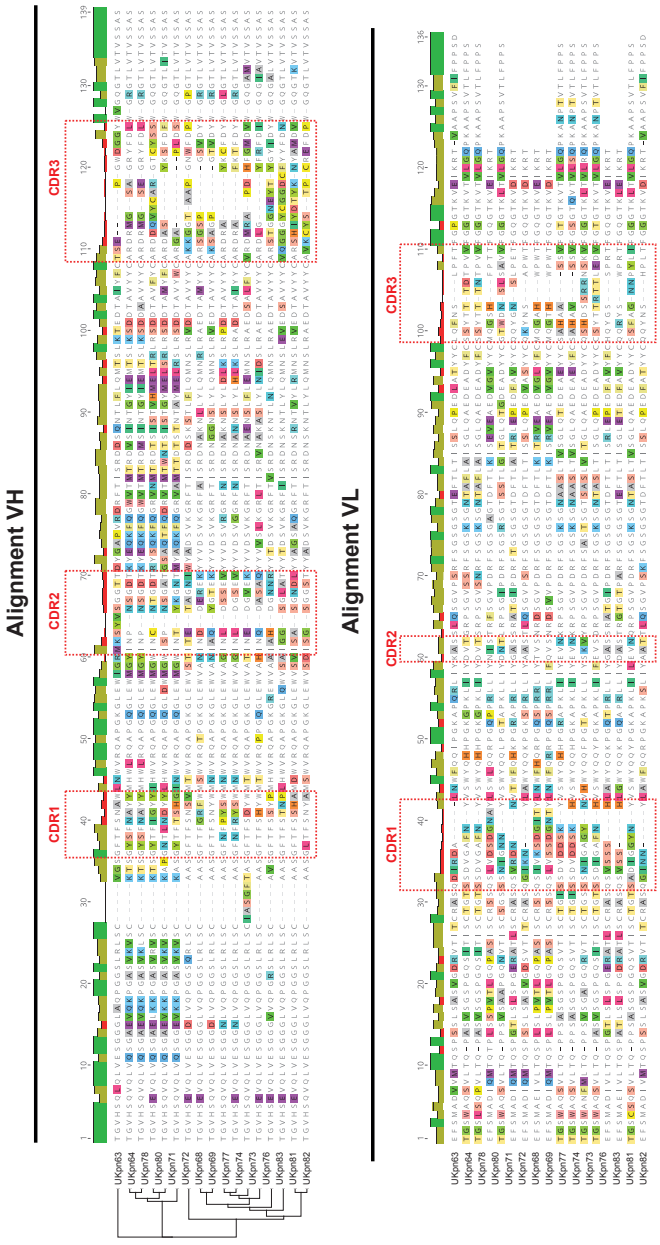

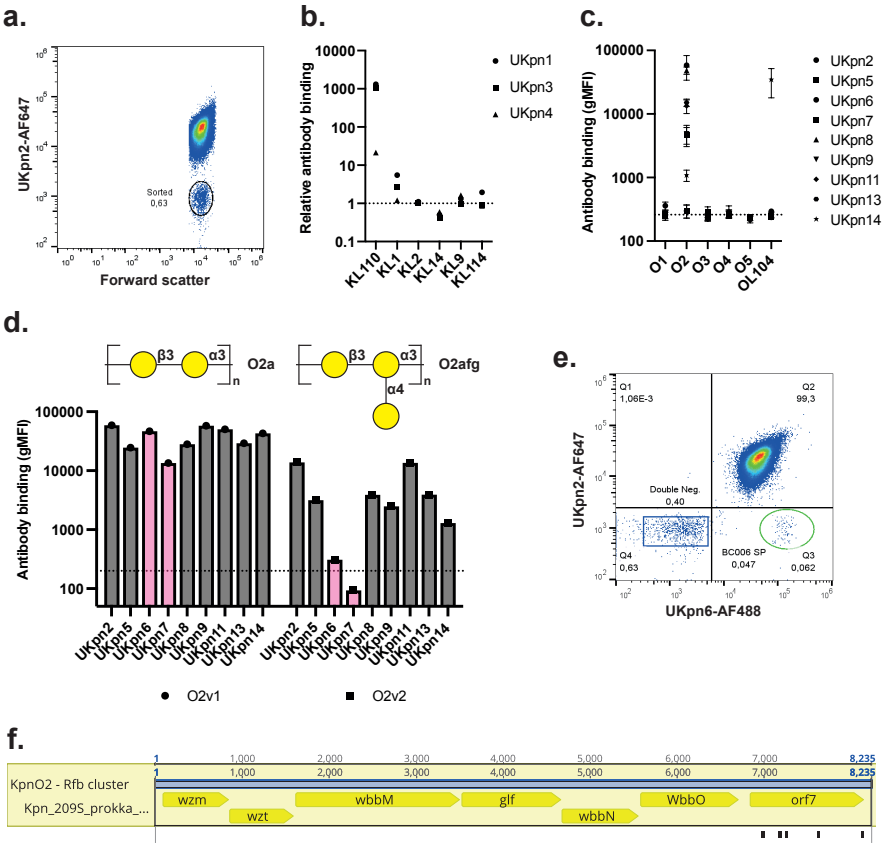

Supplementary figure 3

(a) To identify the antigenic targets of the anti-*Kpn*O2 antibodies, a transposon library of *Kpn*O2R (isogenic variant of *Kpn*O2 [33]) was incubated with fluorescently labelled UKpn2, and antibody binding was detected using flow cytometry. Bacteria that were not bound by the antibodies were single cell sorted. **(b)** Binding of UKpn1, UKpn3 and UKpn4 to clinical isolates expressing various capsule types. IgG1 binding was detected by flow cytometry using anti-hu-IgG-AF488. Flow cytometry data are represented as fold change of geometric mean fluorescent intensity (gMFI) values of bacterial populations over the background. **(c-d)** Binding of UKpn2, UKpn5-9, UKpn11, UKpn13 and UKpn14 to clinical isolates expressing various O-antigen types **(c)**, and to clinical isolates expressing either the O2a- or O2afg-antigen **(d)**. Bacteria were incubated with 1 µg/ml IgG1, and binding was detected by flow cytometry using anti-hu-IgG-AF647. Flow cytometry data are represented by geometric mean fluorescent intensity (gMFI) values of bacterial populations. Data represent mean ± standard deviation of two independent experiments. **(e)** A transposon library of *Kpn*O2R was incubated with UKpn2-AF647 and UKpn6-AF488, and antibody binding was detected using flow cytometry. Bacteria that were bound by UKpn6-AF488 but not by UKpn2-AF647 were single cell sorted (green gate). **(f)** The barcodes of single cell sorted transposon mutants were sequenced to determine location of the transposon inserts. Mutants that were longer bound by UKpn6-AF488 but not by UKpn2-AF647 had transposon insertions in *orf7*.

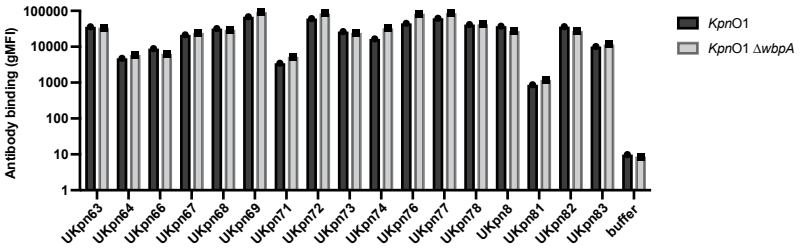

Supplemental figure 4

Anti-*Kpn*O1 IgG1 binding to the capsule deletion mutant of *Kpn*O1 (Δ*wbaP*). Bacteria were incubated with 1 µg/ml IgG1, and binding was detected by flow cytometry using anti-hu-IgG-AF647. Flow cytometry data are represented by geometric mean fluorescent intensity (gMFI) values of bacterial populations.

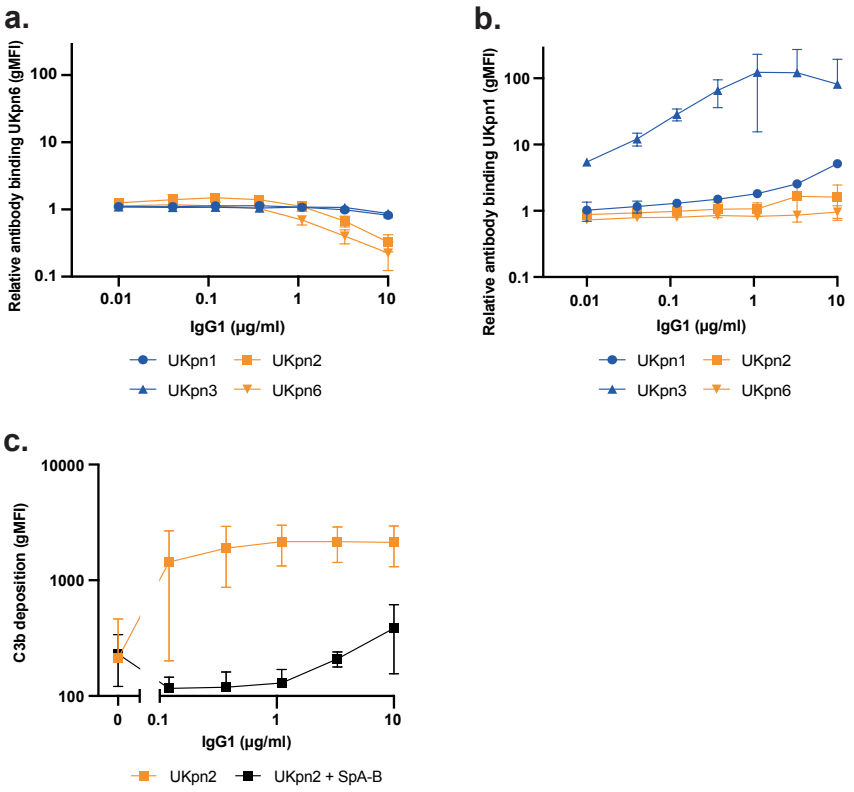

Supplementary figure 5

(a&b) *Kpn*O2 was incubated with 0.1 µg/ml directly labelled anti-O2-antigen UKpn6-AF647 (a) or anti-capsule UKpn1-AF647(b). A concentration range of antibodies UKpn1, UKpn2, UKnp3 or UKpn6 was added to the labeled antibodies. UKpn6-AF647 and UKpn1-AF647 binding was detected by flow cytometry. The relative antibody binding was calculated by dividing geometric fluorescent intensity (gMFI) with the gMFI of fluorescent antibody only. **(c)** Antibody-dependent C3b deposition on *Kpn*O2 pre-incubated with UKpn2 in the absence or presence of 10 µg/ml SpA-B. After antibody binding, bacteria were incubated in 3% normal human serum (NHS) as a complement source, in the absence or presence of 10 µg/ml SpA-B. C3b-deposition was detected using anti-hu-C3b-AF647 by flow cytometry. Data represent the geometric mean fluorescent intensity (gMFI) values of bacterial populations. **(a-c)** Data represent mean ± standard deviation of two independent experiments.

Supplementary table 1| Strains used in this study

Name	O-type	K-type	Selection marker	Reference
*Kpn*O2 (Kp209)	O2a	KL110		Janssen *et al.*, 2020[38]
*Kpn*O2 Δ*wbbO*	-	KL110	Gentamycin	This study
*Kpn*O2 Δ*wbaP*	O2a	-	Gentamycin	This study
*Kpn*O2 pULTRA-*gfp*	O2a	KL110	Kanamycin	This study
*Kpn*O2 pULTRA-*lux*			Gentamycin	This study
*Kpn*O2R (Kp209_CSTR) transposon library	O2a	KL110	Kanamycin	Van der Lans *et al.*, 2023[33]
*Kpn*O1 (UM-05-A#1)	O1	KL114		Verschuren *et al.*, unpublished
*Kpn*O1 Δ*wbbO*	-	KL114	Gentamycin	This study
*Kpn*O1 Δ*wbbY*	O2a	KL114	Gentamycin	This study
*Kpn*O1 Δ*wbaP*	O1	-	Gentamycin	This study
*Kpn*O1 pULTRA-*gfp*	O1	KL114	Kanamycin	This study
*Kpn*O1 pULTRA-*lux*	O1	KL114	Gentamycin	This study
UM-2A#3.1	O1	KL20		Verschuren *et al.*, unpublished
UM13B#1	O1	KL9		Verschuren *et al.*, unpublished
MB-17667	O1	KL30-D1		Van den Bunt *et al.*, 2020[48]
JS367*	O2afg	KL9		This study
MA-25932	O3b	KL60		Van den Bunt *et al.*, 2020 [48]
MA-49950	O4	KL17		Van den Bunt *et al.*, 2020 [48]
MA-44575	O5	KL10		Van den Bunt *et al.*, 2020 [48]
MA-18898	OL104	KL14		Van den Bunt *et al.*, 2020 [48]
K00059	O3a	KL110		Van den Bunt *et al.*, 2020 [48]
UM-05-B-#1	O2a	KL114		Verschuren *et al.*, unpublished
MC-04166	O2afg	KL136		Van den Bunt *et al.*, 2020 [48]

N0008	O3a	KL1	This study
MB-16059	O3b	KL2	Van den Bunt *et al.*, 2020 [48]

Supplementary table 2| RT-PCR primers

RT-PCR	
Heavy IgG	**Sequence**
H1_For_VH1	ACAGGTGCCCACTCCCAGGTGCAG
H1_For_VH3	AAGGTGTCCAGTGTGARGTGCAG
H1_For_VH4/6	CCCAGATGGGTCCTGTCCCAGGTGCAG
H1_For_VH5	CAAGGAGTCTGTTCCGAGGTGCAG
H1_Rev_int_CH1	GTTCGGGGAAGTAGTCCTTGAC
Kappa	
K1_For_Vκ1/2	ATGAGGSTCCCYGCTCAGCTGCTGG
K1_For_Vκ3	CTCTTCCTCCTGCTACTCTGGCTCCCAG
K1_For_Vκ4	ATTTCTCTGTTGCTCTGGATCTCTG
K1_For_Pan_Vκ	ATGACCCAGWCTCCABYCWCCCTG
K1_Rev_Cκ543	GTTTCTCGTAGTCTGCTTTGCTCA
K1_Rev_Cκ494	GTGCTGTCCTTGCTGTCCTGCT
Lambda	
λ1_For_Vλ1	GGTCCTGGGCCCAGTCTGTGCTG
λ1_For_Vλ2	GGTCCTGGGCCCAGTCTGCCCTG
λ1_For_Vλ3	GCTCTGTGACCTCCTATGAGCTG
λ1_For_Vλ4/5	GGTCTCTCTCSCAGCYTGTGCTG

Supplementary table 2| RT-PCR primers *(continued)*

λ1_For_Vλ6	GTTCTTGGGCCAATTTTATGCTG
λ1_For_Vλ7	GGTCCAATTCYCAGGCTGTGGTG
λ1_For_Vλ8	GAGTGGATTCTCAGACTGTGGTG
λ1_Rev_Cλ	CACCAGTGTGGCCTTGTTGGCTTG
2nd PCR	
Heavy IgG	
H2_For_AgeIC_VH1/5	GTTTCTGGTGGCTACTGCAACCGGTGTACATTCCGAGGTGCAGCTGGTGCAG
H2_For_AgeIC_VH3	GTTTCTGGTGGCTACTGCAACCGGTGTACATTCTGAGGTGCAGCTGGTGGAG
H2_For_AgeIC_VH3–23	GTTTCTGGTGGCTACTGCAACCGGTGTACATTCTGAGGTGCAGCTGTTGGAG
H2_For_AgeIC_VH4	GTTTCTGGTGGCTACTGCAACCGGTGTACATTCCCAGGTGCAGCTGCAGGAG
H2_For_AgeIC_VH4–34	GTTTCTGGTGGCTACTGCAACCGGTGTACATTCCCAGGTGCAGCTACAGCAGTG
H2_For_AgeIC_VH1–18	GTTTCTGGTGGCTACTGCAACCGGTGTACATTCCCAGGTTCAGCTGGTGCAG
H2_For_AgeIC_VH1–24	GTTTCTGGTGGCTACTGCAACCGGTGTACATTCCCAGGTCCAGCTGGTACAG
H2_For_AgeIC_VH3–33	GTTTCTGGTGGCTACTGCAACCGGTGTACATTCTCAGGTGCAGCTGGTGGAG
H2_For_AgeIC_VH3–9	GTTTCTGGTGGCTACTGCAACCGGTGTACATTCTGAAGTGCAGCTGGTGGAG
H2_For_AgeIC_VH4–39	GTTTCTGGTGGCTACTGCAACCGGTGTACATTCCCAGCTGCAGCTGCAGGAG
H2_For_AgeIC_VH6–1	GTTTCTGGTGGCTACTGCAACCGGTGTACATTCCCAGGTACAGCTGCAGCAG
H2_Rev_JH1/2/4/5	**GATGGGCCCTTGGTGCTAGC**TGAGGAGACGGTGACCAG
H2_Rev_JH3	**GATGGGCCCTTGGTGCTAGC**TGAAGAGACGGTGACCATTG
H2_Rev_JH6	**GATGGGCCCTTGGTGCTAGC**TGAGGAGACGGTGACCGTG
Kappa	
K2_For_Vκ1–5	GTAATCAGCACTTGCCTGGAATTCTCTATGGCTGACATCCAGATGACCCAGTC

Supplementary table 2| RT-PCR primers *(continued)*

K2_For_Vκ1–9	GTAATCAGCACTTGCCTGGAATTCTCTATGGCTGACATCCAGTTGACCCAGTCT
K2_For_Vκ1D–43	GTAATCAGCACTTGCCTGGAATTCTCTATGGCTGCCATCCGGATGACCCAGTC
K2_For_Vκ2–24	GTAATCAGCACTTGCCTGGAATTCTCTATGGCTGATATTGTGATGACCCAGAC
K2_For_Vκ2–28	GTAATCAGCACTTGCCTGGAATTCTCTATGGCTGATATTGTGATGACTCAGTC
K2_For_Vκ2–30	GTAATCAGCACTTGCCTGGAATTCTCTATGGCTGATGTTGTGATGACTCAGTC
K2_For_Vκ3–11	GTAATCAGCACTTGCCTGGAATTCTCTATGGCTGAAATTGTGTTGACACAGTC
K2_For_Vκ3–15	GTAATCAGCACTTGCCTGGAATTCTCTATGGCTGAAATAGTGATGACGCAGTC
K2_For_Vκ3–20	GTAATCAGCACTTGCCTGGAATTCTCTATGGCTGAAATTGTGTTGACGCAGTCT
K2_For_Vκ4–1	GTAATCAGCACTTGCCTGGAATTCTCTATGGCTGACATCGTGATGACCCAGTC
K2_Rev_Jκ1/4	GATGGTGCAGCCACCGTACGTTTGATYTCCACCTTGGTC
K2_Rev_Jκ2	GATGGTGCAGCCACCGTACGTTTGATCTCCAGCTTGGTC
K2_Rev_Jκ3	GATGGTGCAGCCACCGTACGTTTGATATCCACTTTGGTC
K2_Rev_Jκ5	GATGGTGCAGCCACCGTACGTTTAATCTCCAGTCGTGTC
Lambda	
λ2_For_Vλ1	GTTTCTGGTGGCTACTGCTACCGGTTCCTGGGCCCAGTCTGTGCTGACKCAG
λ2_For_Vλ2	GTTTCTGGTGGCTACTGCTACCGGTTCCTGGGCCCAGTCTGCCCTGACTCAG
λ2_For_Vλ3	GTTTCTGGTGGCTACTGCTACCGGTTCTGTGACCTCCTATGAGCTGACWCAG
λ2_For_Vλ4/5	GTTTCTGGTGGCTACTGCTACCGGTTCTCTCTCSCAGCYTGTGCTGACTCA
λ2_For_Vλ6	GTTTCTGGTGGCTACTGCTACCGGTTCTTGGGCCAATTTTATGCTGACTCAG
λ2_For_Vλ7/8	GTTTCTGGTGGCTACTGCTACCGGTTCCAATTCYCAGRCTGTGGTGACYCAG
λ2_Rev_Cλ	GTTGGCTTGAAGCTCCTCACTCGAGGGYGGGAACAGAGTG

Chapter 4

Combined flow cytometry- and mass spectrometry-based approach to characterize the immunoreactive antibody response against *Klebsiella pneumoniae* infections in kidney transplant recipients

Sjors P. A. van der Lans[1]*, Maurits A. den Boer[2]*, Hadia Hamdaoui[1], Maartje Ruyken[1], Albert Bondt[2], Pieter-Jan A. Haas[1], Arjan D. Van Zuilen[3], Bart W. Bardoel[1], Albert J.R. Heck[2], Suzan H.M. Rooijakkers[1]

[1]Department of Medical Microbiology, University Medical Center Utrecht, The Netherlands

[2]Biomolecular Mass Spectrometry and Proteomics, Bijvoet Center for Biomolecular Research, and Utrecht Institute of Pharmaceutical Sciences, Utrecht University, Utrecht, Netherlands

[3]Department of Nephrology and Hypertension, University Medical Center Utrecht, Utrecht, Netherlands

*Equal contribution

Partly published in Journal of Proteome Research DOI: 10.1021/acs.jproteome.3c00330

Abstract

Producing protective antibodies plays a crucial role in the immune defense against bacterial infections. Various antibodies can be generated that shape the overall polyclonal response. To gain better understanding of polyclonal antibody response to bacterial infections, we studied these responses in longitudinal plasma samples of two kidney transplant patients that developed a *K. pneumoniae* bloodstream infection post-transplantation. We found that both patients elicited antibodies against the infectious *K. pneumoniae* strains. Both *K. pneumoniae*-specific IgG, IgA, and IgM was generated and could be detected in patient plasma for several months. Using a combination of flow cytometry- and mass spectrometry-based analyses, revealed that several distinct IgG1 and IgA1 clones could be produced in response to the infections. The anti*K. pneumoniae* antibodies of both patients were able to activate the complement system, and those of one of the patients also enhanced antibody-depended phagocytosis of *K. pneumoniae* by human neutrophils in the presence of complement.

Introduction

Generating antibodies in response to bacterial infection is a vital part of the antibacterial immune response. Antibody generation is initiated after an invasive bacterium enters the body and is specifically recognized by B cells via surface expressed B cell receptors. This induces B cell activation, triggering various processes, including the formation of antibody-excreting plasmablasts. In response to an infection, multiple different B cells can be activated, leading to the production of various antibody clones that may target different antigens. Antigen specificity is determined by the variable regions of the Fab domain, which vary between antibody clones, allowing recognition of different antigens by different antibodies. Once an antibody binds its antigen on the bacterial surface, it can be recognized by the immune system via its Fc domain. Antibodies can be expressed as various isotypes, characterized based on the Fc domain usages. Each isotype interacts distinctively with specific parts of the immune system, thereby shaping the immune response. Antibodies belonging to the IgG and IgM isotypes are important for the immune protection against bacterial infections, as they recruit proteins of the classical pathway of the complement system to the bacterial surface. This leads to complement activation, subsequent deposition of various complement components on the bacterial surface, and the release of chemoattractants that can attract phagocytic cells, such as neutrophils. Neutrophils can recognize antibody- and complement-labelled bacteria via their Fc- and complement-receptors, which stimulates phagocytic uptake and subsequent clearance of the bacteria.

Historically, antibody responses have been investigated by assessing the total antibody titer in blood plasma directed towards intact bacteria or isolated antigens. However, antibody responses consist of various distinct antibody clones. These clones may have different affinities, targets and concentrations, and the clonal composition of the antibody repertoire thereby shapes the functionality of the complete antibody response. Recent developments in the field of proteomics now allow characterization of the soluble antibody repertoire at the protein level. Novel approaches enable antibody repertoire profiling by liquid chromatography mass spectrometry (LC-MS) analysis, providing a qualitative and quantitative snapshot of the antibody clonal repertoire present in a sample. The approach first identifies individual clones by their unique mass and retention time combination, after which for each of them the concentration is determined through intensity normalization against a spiked-in standard of recombinant monoclonal antibodies. Strikingly, such LC-MS repertoire

profiling experiments have revealed that that individual human antibody repertoires are highly unique, and furthermore, that they are much more restricted in composition than earlier B cell sequencing studies have suggested[1–3]. Typically, about 500 of the most abundant clones of an isotype are identified and quantified, explaining up to 95% of the total concentration[3]. Furthermore, these antibody repertoires appear largely stable over time in healthy individuals but can change rapidly during disease and infections. Previously, it has been demonstrated that multiple antibody clones of various concentrations are generated in response to SARS-CoV-2 infections[4]. However, the clonal composition of the viral-specific antibodies was assessed at a single timepoint, which did not permit to follow the antibody response in time.

Studying antibody responses to infections in time requires longitudinal sample sets that include a pre-infection sample. Unfortunately, these are rare, as most patients are sampled only once an infection has occurred. However, patients that have received a kidney transplant are sampled regularly as part of routine diagnostics. In addition, these patients are at increased risk of developing bacterial infections post-transplantation, due to a combination of renal remodeling and immunosuppressive therapy [5]. Among the leading causes of infections in kidney transplant recipients is the Gram-negative bacteria *Klebsiella pneumoniae*[5]. Here we studied the antibody response in two kidney transplant patients that developed a bloodstream infection with *K. pneumoniae* post-transplantation, using a combination of flow cytometry- and mass spectrometry-based analyses. Both patients elicited a specific antibody response, as the level of *K. pneumonia*-specific antibodies in plasma increased after the infection. Analysis of the antibody repertoire pre- and post-infection identified several antibody clones that were produced in response to the infection. Some of these clones were shown to be specific for *K. pneumoniae*, since depleting the samples using *K. pneumoniae* exclusively removed these clones from plasma. The antibody response generated functional antibodies, as antibodies of both patients were able to enhance complement activation on *K. pneumoniae.*

Results

Kidney transplant patients produce specific antibodies in response to *Klebsiella pneumoniae* infection

To study antibody responses to *K. pneumoniae* infections we made use of a cohort of kidney transplant recipient patients who participated in a biobank study to evaluate immunological developments post-transplantation. From this cohort, we retrospectively selected two patients that developed a confirmed *K. pneumoniae* bloodstream infection post-transplantation, and for whom a pre-transplantation and multiple post-transplantation plasma samples were available. These samples were collected over approximately a one-year period, and the date on which the pre-transplantation serum was collected was put at timepoint 1 as a reference. Within a month after the kidney transplantation took place, patient 1 developed a urinary tract infection with the ESBL-positive *K. pneumoniae* isolate M6193, which spread to the bloodstream where it could be detected several times during a three-month period (fig. 1a). The strain was detected twice more in the urine of patient 1, indicating that the strain might had colonized the urinary tract of this patient. Patient 2 developed a bloodstream infection 254 days post-transplantation, caused by *K. pneumoniae* isolate N1249, which originated from the urinary tract (fig. 1e).

To study whether circulating antibodies against *K. pneumoniae* could be detected in the plasma of the patients, antibody binding to the bacterial surface was quantified via flow cytometry. There was no antibody binding to M6193 in the pre-infection plasma of patient 1, but after infection, binding of IgG, IgA and IgM could be observed (fig. 1b-d). From day 117 onward the antibody binding increased a further 30-fold, 10-fold and 3-fold for IgG, IgA and IgM, respectively, towards day 240, and remained stable for the rest of the study (fig. 1b-d & supplementary fig. SI1). Plasma of patient 2 contained IgG, IgA and IgM antibodies against *K. pneumoniae* isolate N1249 prior to the bloodstream infection (fig. 1f-h). Binding levels of these pre-existing antibodies remained stable during the first 195 days after transplantation. After the bloodstream infection, the levels of antibodies binding to N1249 in plasma increased substantially (>100-fold, 30-fold and >30-fold for IgG, IgA and IgM, respectively) and remained stable for the remainder of the studied period (fig. 1f-h & supplementary fig. SI1).

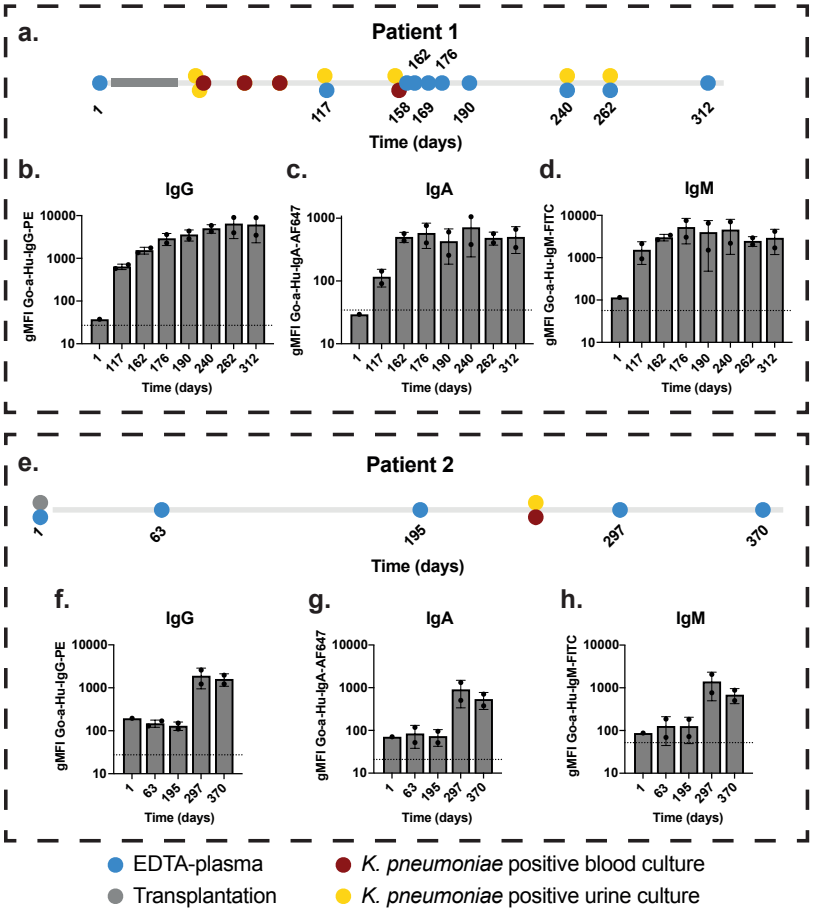

Figure 1| Kidney transplant patients produce specific antibodies in response to *Klebsiella pneumoniae* infections

(**a&e**). Timelines of sample collection and infections of patient 1 (a) and patient 2 (e). EDTA-plasma (blue) was collected from kidney transplant patients during diagnostic surveillance before the kidney transplantation (t=1) and in the post-transplantation period. *K. pneumoniae* M6193 and N1249 caused urinary tract and bloodstream infections in patient 1 and patient 2, respectively, during the post-transplantation period. Transplantation in grey, *K. pneumoniae* positive urine cultures in yellow and *K. pneumoniae* positive blood cultures in red. (**b-d & f-h**). Antibody binding to *K. pneumoniae* M6193 in plasma of patient 1 (b-d) and antibody binding to *K. pneumoniae* N1249 in plasma of patient 2 (f-h). Binding of IgG (b&e), IgA (c&g) and IgM (d&h) were measured in 0.1%, 0.3% and 0.3% plasma, respectively. Antibody binding was detected using anti-hu-IgG-PE, anti-hu-IgA-AF647 or anti-hu-IgM-FITC by flow cytometry. Flow cytometry data are represented by geometric mean fluorescent intensity (gMFI) values of bacterial populations. Data represent mean ± standard deviation of two independent experiments.

Next, we tested if the increase in antibody binding to *K. pneumoniae* was the result of a specific response to the infections, and not of an overall increase in antibody levels due to medical treatment or other influences. Therefore, antibody binding to *Staphylococcus aureus* was assessed, as virtually all individuals have antibodies recognizing *S. aureus*[6]. Both patients had stable levels of IgG, IgA and IgM targeting *S. aureus* Newman *Δspa Δsbi* over the course of the studied period, indicating that antibody levels against a non-klebsiella target remained unchanged (supplementary fig. SI2). In summary, we observe that two kidney transplant patients who underwent an infection with *K. pneumoniae* were able to elicit a specific antibody response against the invasive bacterial strain.

Kidney transplant patients can produce multiple different antibody clones in response to *K. pneumoniae* infection

We have seen that patients can respond to infections with *K. pneumoniae* by raising antibodies. As antibody responses are generally polyclonal, we aimed to get a more quantitative impression of the different antibody clones raised by the patients against the *K. pneumoniae* isolates. To this end, IgG1 and IgA1 intact Fab profiles were generated by mass spectrometry for each timepoint. All IgG1 and IgA1 antibodies were affinity-purified from patient plasma and selectively cleaved by hinge-directed proteases to generate single arm Fab fragments. The Fabs were measured by LC-MS to generate IgG1 and IgA1 clonal profiles. Some illustrative IgG1 Fab profiles of patient 1 have been published previously [7]. Each peak in the clonal profiles represents a unique identified Fab, and the height of the signal its relative abundance (fig. 2a&b). By spiking in monoclonal antibodies of known concentration and mass, the relative abundance could be converted to concentration of each antibody clone in the sample. Combined over all time points, we identified >950 unique IgG1 clones and >390 IgA1 clones per patient. We previously demonstrated that patient 1 suffered from monoclonal gammopathy of unknown significance (MGUS) [7]. This led to one very abundant IgG1 clone (termed M-protein; >1 mg/ml) to dominate in all the IgG1 profiles of patient 1[7].

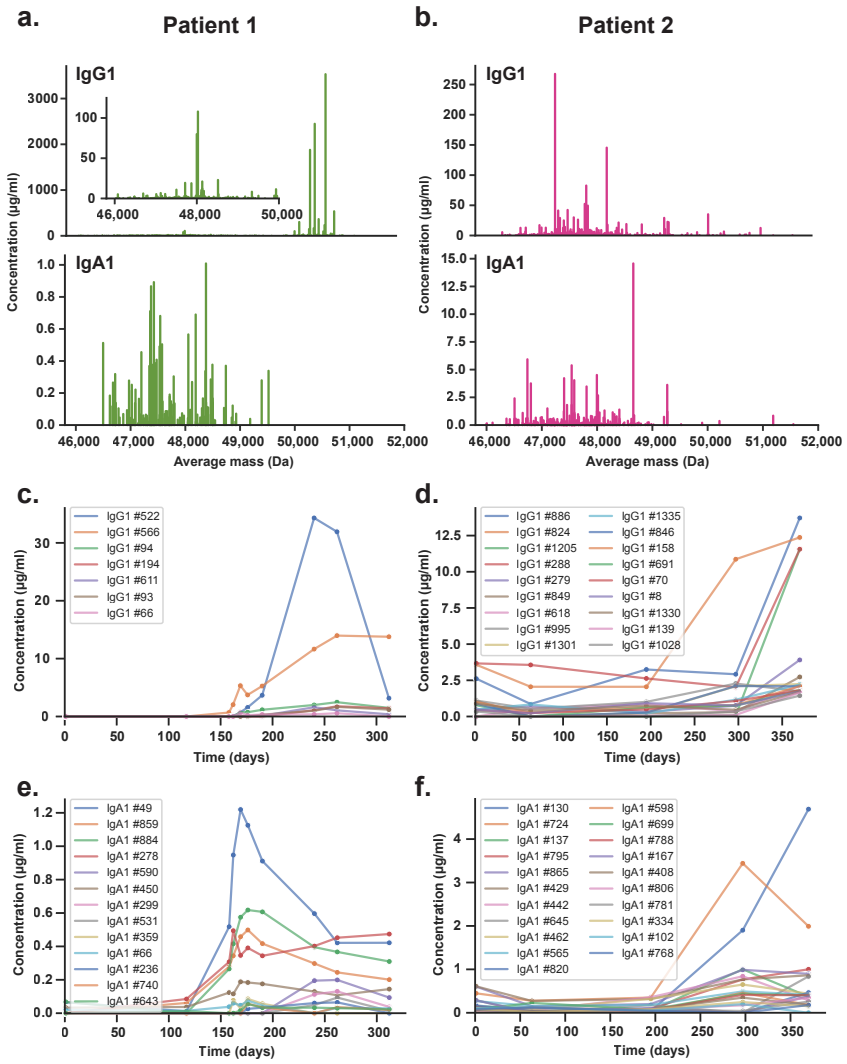

Figure 2| Kidney transplant patients produce multiple different antibody clones in response to *K. pneumoniae* infection

(a&b) Exemplary IgG1 and IgA1 clonal profiles of patient 1 (a) and patient 2 (b) in the pre-transplantation plasma. The IgG1 profile of patient 1 has previously been published (Peng 2023). Isolated single IgG1 and IgA1 Fab arms were measured via liquid chromatography mass spectrometry. Each bar represents an individual antibody clone of a certain mass (x-axis) and concentration (y-axis). The insert in the IgG1 profile of patient 1 shows the lower mass region in more detail. **(c-f)** Clonal identifications over time were related to flow cytometry binding data, to identify clones for which changes in concentration are synchronized with flow cytometry binding data (fig. 1). Several clones were suggested to be part of the response against the infectious *K. pneumoniae*. The concentration profiles for these IgG1 (c&d) and IgA1 (e&f) clones are shown for patient 1 (c&e) and patient 2 (d&e).

To determine which antibody clones in the total serum repertoire were generated in response to *K. pneumoniae* infection, we related the occurrence of clonal identifications over time to our flow cytometry binding data. In this way, we could identify clones that come up synchronously with the observed total binding levels, revealing which clones are likely to be part of the response against these bacteria. Using this approach, we could identify 7 IgG1 and 13 IgA1 clones in patient 1 that appear to be produced synchronously with total binding levels (fig. 2c&e). We could identify many more clones in patient 2, but as strong binding was observed at only two time points, the validity of these identifications was far more uncertain (fig. 2d&f).

To confirm that these antibody clones targeted *K. pneumoniae*, we assessed if they could specifically be depleted from plasma using *K. pneumoniae.* Plasma of patient 1 (t=190) was incubated with *K. pneumoniae* strain M6193 to allow for antibody binding, the bacteria were removed, and the depleted plasma was collected (fig. 3a). After 5 depletion cycles the level of IgG binding to M6193 was strongly reduced (fig. 3b). The antibody depletion was specific for M6193, as antibody binding to *S. aureus* was not affected (fig. 3c). To control for the effects of depletion non-specific antibodies, an IgG1 isotype control antibody was spiked in before the depletion. The IgG1 profiles of pre- and post-depletion samples were compared, revealing that the depletion procedure did not have an impact on the vast majority of the IgG1 clones. However, clones c522 and c566, which were previously identified as to be likely generated in response to the *K. pneumoniae* infection, were no longer present after the depletion (fig. 3d). The isotype control antibody was not affected by the depletion, indicating that only *K. pneumoniae* specific clones were removed. Together these data demonstrate that relating clonal-level antibody abundances to total bacterial binding levels in a longitudinal sample set allows for the identification of *K. pneumoniae* specific antibodies, and indicate that kidney transplant patients can produce multiple different antibody clones in response to *K. pneumoniae* infection.

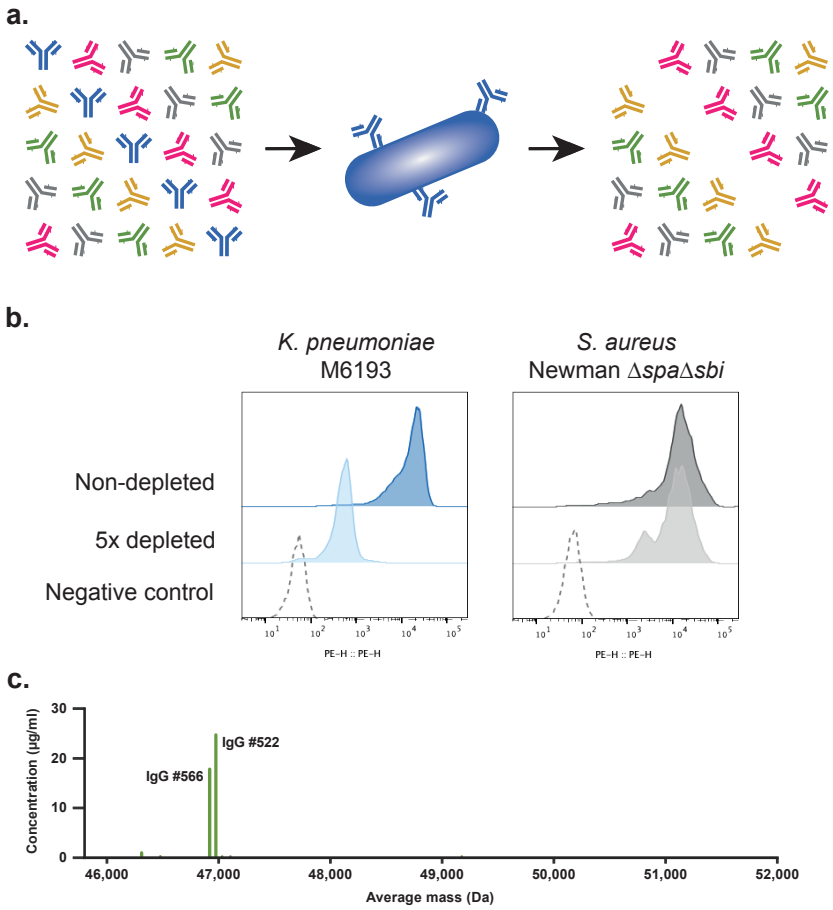

Figure 3| Identification of *K. pneumoniae*-specific antibody clones can be confirmed by specific antibody depletion

(**a**) Schematic representation of the method to deplete bacterium specific antibodies from plasma. Plasma was mixed with bacteria and incubated for 10 minutes at 4 °C to allow specific antibodies to bind. Bacteria were pelleted and discarded, and the depleted plasma was collected. (**b**) Total IgG binding to *K. pneumoniae* M6193 and *S. aureus* Newman *ΔspaΔsbi* in plasma of patient 1 (t=190), either non-depleted or five times depleted with M6193. IgG binding was measured in 0.1% plasma via flow cytometry using anti-hu-IgG-PE. Fluorescence intensity and the number of events normalized to the mode are depicted of the x- and y-axis, respectively. (**c**) IgG1 clonal profile of IgG1 Fab clones from patient 1 that were removed during plasma depletion using *K. pneumoniae* M6193. IgG1 was isolated from pre-and post-depletion plasma samples (t=190). IgG1 was enzymatically cleaved to generate single Fab arms, which were separated by liquid chromatography, and measured via mass spectrometry. After deconvolution, the signal intensity of individual Fab clones was normalized against spiked-in monoclonal reference antibodies of known concentrations. The pre- and post-depletion IgG1 clonal plasma profiles were compared, all clones that were present in both samples were omitted from the profile, leaving only the clones that were removed during the depletion.

Antibodies produced by kidney transplant patients are able to activate the innate immune system

Finally, we investigated whether the *K. pneumoniae*-specific antibodies produced in response to infections were able to trigger Fc-mediated effector functions, focusing on the complement system and neutrophils. To assess antibody-mediated complement activation, the *K. pneumoniae* strains were pre-incubated in patient plasma at 4 °C to allow antibody binding. After washing, the bacteria were incubated with normal human serum depleted of *K. pneumoniae* specific antibodies (ΔNHS) as a source of complement components. The ΔNHS concentrations were optimized per strain. Complement activation was determined by measuring the deposition of complement component C3b on *K. pneumoniae* strains by flow cytometry (fig. 4a&b). Incubation of M6193 with pre-infection plasma of patient 1 did not lead to C3b-deposition (fig. 4a), which is in line with the absence of antibody binding to M6193 in pre-infection plasma of patient 1 (fig. 1b-d). Post-infection plasma, where anti-M6193 antibodies were present, was able to induce antibody dependent C3b-deposition on this strain. Antibody-dependent C3b-deposition on N1249 occurred after incubation in both pre- and post-infection plasma of patient 2 (fig. 4b), which is in line with our finding that the pre-transplantation plasma already contains *K. pneumoniae*-binding antibodies (fig. 1f-h). We observed an increase in C3b-deposition when comparing pre- and post-transplantation samples, but no difference in C3b-deposition was detected between pre-infection (t=63; 195) and to post-infection (t=297; 370) samples taken after the transplantation. This indicates that pre-existing N1249-binding antibodies present in the pre-infection plasma of patient 2 were able to activate the complement system.

Antibodies can induce phagocytosis of bacteria by neutrophils. This can be either directly by engaging Fc-receptors (FcR) on neutrophils, and indirectly by stimulating deposition of complement components, which are recognized by complement receptors on neutrophils. To tested if the *K. pneumoniae*-specific antibodies in the patients' plasma could induce phagocytosis by human neutrophils, the strains were fluorescently labelled, incubated in cold patient plasma to allow antibody binding. FcR-mediated phagocytosis was measured by incubating the opsonized bacteria with neutrophils and determining bacterial uptake by flow cytometry. For both patients, phagocytosis was slightly increased in post-infection plasma compared to pre-infection plasma, suggesting that the anti-*K. pneumoniae* antibodies might be able enhance FcR-mediated phagocytosis (fig. 4c). Finally, we measured phagocytosis in the presence of complement by incubating the opsonized *K. pneumoniae* strains

with neutrophils and ΔNHS as a complement source. No difference was observed between opsonizing M6193 with pre- or post-infection plasma from patient 1 (fig. 4d). In contrast, antibodies in the post-infection plasma of patient 2 strongly increased complement-dependent phagocytosis of N1249 (fig.4d). Together this data shows that antibodies produced by patients in response to *K. pneumoniae* infection can activate the human complement system and phagocytosis by human neutrophils.

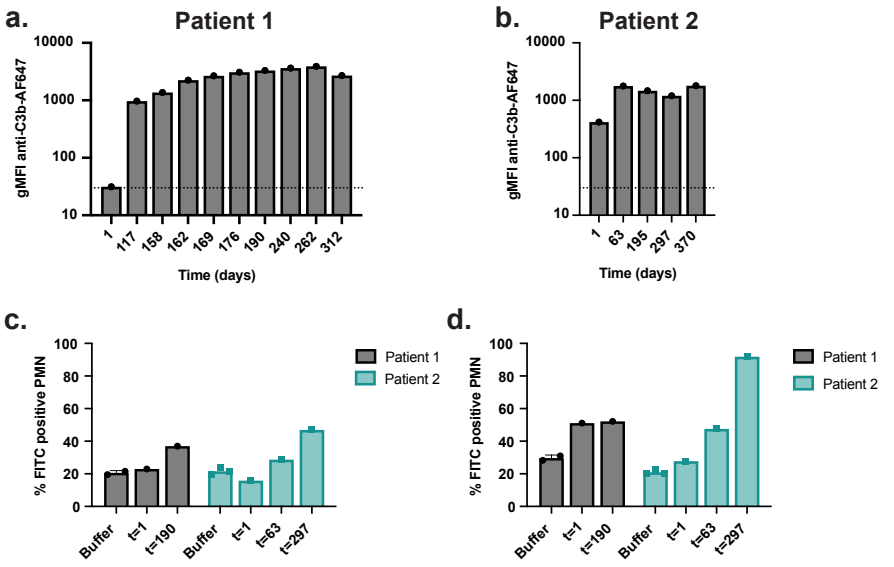

Figure 4| *K. pneumoniae* targeting antibodies produced by kidney transplant patients can activate the complement system and induce phagocytosis

(**a&b**) Antibody-dependent C3b deposition on (a) *K. pneumoniae* M6193 pre-incubated with 0.1% heat-inactivated plasma of patient 1 and (b) *K. pneumoniae* N1249 pre-incubated with 3% heat-inactivated plasma of patient 2. After antibody binding, bacteria were incubated in normal human serum depleted of *K. pneumoniae* specific antibodies as a complement source (ΔNHS; 0.3% and 2% for patient 1&2, respectively). C3b-deposition was detected using anti-hu-C3b-AF647 by flow cytometry. Flow cytometry data are represented by geometric mean fluorescent intensity (gMFI) values of bacterial populations. (**c&d**) Antibody-dependent phagocytosis of *K. pneumoniae* M6193 and N1249 opsonized with 2% heat inactivated plasma of patient 1 and patient 2, respectively. Opsonized fluorescently (FITC) labelled bacteria were incubated with isolated human neutrophils in the (c) absence or (d) presence of 3% ΔNHS as a complement source. The percentage of FITC-positive neutrophils was determined by flow cytometry.

Discussion

Generating protective antibodies is a vital part of the immune defense against invading bacteria. During antibody responses, various antibody clones can be generated. To gain a better understanding of the clonal composition of antibody responses during bacterial infections, we studied the antibody responses in two kidney transplant patients that developed a bloodstream infection with *K. pneumoniae* post-transplantation using a combination of flow cytometry- and mass spectrometry-based analyses. Both patients elicited an antibody response against their respective infectious *K. pneumoniae* isolates, generating IgG, IgA and IgM antibodies that could be detected in patient plasma for several months post-infection. Combining flow cytometry and mass spectrometry data revealed that several distinct IgG1 and IgA1 clones were produced in response to infection by both patients. The concentration of these clones increased after the infection and varied between distinct clones. The anti*K. pneumoniae* antibodies of both patients were able to activate the complement system, and those of one of the patients also enhanced antibody-dependent phagocytosis of *K. pneumoniae* by human neutrophils in the presence of complement.

In the past, antibody responses were primarily studied by determining the total antibody titer against pathogens or isolated antigen. However, during polyclonal antibody responses, different antibody clones are generated that together shape the overall response. Recently it became possible to assess the clonal composition of the human antibody repertoire by mass spectrometry [1–3]. While the feasibility of antigen-specific repertoire profiling has already been demonstrated, enriching antibodies using whole bacteria remains challenging [4]. To identify individual antibody clones that target infectious bacteria, we therefore related changes in abundance of individual clones over time to antibody binding *K. pneumoniae* in longitudinal plasma sample sets of patients that suffered from *K. pneumoniae* infections. This resulted in a list of clones that were potentially generated in response to the infection. The model predicted many more clones to be linked to the infection for patient 2 then for patient 1. However, the validity of these identifications was uncertain, as only two post-infection timepoints where available for patient 2. Due to the lack of additional datapoints, fluctuations in antibody concentration of clones that are unrelated to the infection might lead to incorrect identification of these clones. We could verify that the specificity of two of the IgG1 clones identified for patient 1 by depleting bacterium specific antibodies from plasma, which removed only these distinct clones but left other clones untouched. We

could verify that the specificity of the identified clones by depleting bacterium specific antibodies from plasma, which removed only these distinct clones but left other clones untouched. Strikingly, the plasma depletions seemed very specific, and might be used as a stand-alone approach to identify surface-specific antibodies in the future. Previously work has already shown that it is possible to generate antigen-specific IgG1 profiles, by immunocapturing antibodies targeting the SARS-CoV-2 spike protein from convalescent patient plasma at a single timepoint[4]. Here we used intact bacteria instead of an isolated antigen, which potentially allows the agnostic identification of antibodies targeting various surface antigens. The previous work on into the response against SARS-CoV-2 has demonstrated that the number of specific antibody clones that were generated during IgG1 responses against the SARS-CoV-2 spike protein varied strongly between patients, with some individuals only producing three antibody clones, whereas other generate as much as 281 (median of 39.5 clones per patient)[4]. This suggests that a larger number of antibody clones were generated in response to SARS-CoV-2 comparted to *K. pneumoniae*. However, only a small number of the anti-spike protein clones had a concentration above 0.5 µg/ml, which was the detection limit in our study. It is possible that many more antibody clones were generated in response to *K. pneumoniae* but that these could not be detected. Furthermore, the clonal analysis was limited to IgG1 and IgA1, leaving the clonal composition of other antibody isotypes unexplored.

Antibodies produced in response to the *K. pneumoniae* bloodstream infection could be detected in patient plasma for several months after the infections were resolved. The amount of antibody binding to *K. pneumoniae* only varied slightly during this period, and we observed that the concentration of most of the individual clones remained relatively stable. It has been reported that antibody repertoires can change rapidly under environmental influences including infections [2,3]. However, in the absence of such events, the antibody repertoires were found to be stable for periods extending that of antibody half-lives, as we observed as well. This indicates that the kidney transplant patients developed long-lived plasma cells that continuously produce these antibodies. Previous studies on long-term antibody responses in other solid organ transplant patient cohorts have reported mixed results, as both cases of rapidly declining and long-lasting responses have been observed[8,9]. How the antibody responses these two patients compare to antibody responses against *K. pnuemoniae* in healthy individuals or nonimmunosuppressed patients remains to be determined. However, this might be

difficult as this would require pre-infection samples, which are generally not available for healthy individuals.

We observed that the antibodies produced by both patient in response to the *K. pneumoniae* infections were able to induce antibody-dependent complement activation and C3b-deposition in normal human serum. The pre-existing N1249 binding antibodies in the plasma of patient 2 also induced C3b-deposition, but although antibody binding to N1249 increased post-infection, it did not lead to a further increase in C3b-deposition. The post-infection antibodies of patient 2 were able to slightly enhance phagocytosis directly, but in the presence of active complement, phagocytosis was much more efficient. This is in line with previous reports that showed phagocytosis greatly benefits from complement activation in *K. pneumoniae*[10–12]. In contrast, the increased C3b-deposition in post-infection plasma of patient 1 did not lead to increased phagocytosis. The dissimilarity observed could be due to variation between the *K. pneumoniae* strains, or be caused by differences in the antibody responses of both patients. Although this makes it difficult to compare the patient-isolate pairs, both patients were able to produces anti-*K. pneumoniae* antibodies that activated the immune system, suggesting that the infections might not have been the result of improper antibody responses but potentially other underlying factors.

Kidney disease affects an estimated 800 million people globally, and as many as 10 million patients require renal replacement therapy [13,14]. Although kidneys are the most transplanted solid organs, due to the high demand, patients often have to wait for several years before receiving a donor kidney [13]. Unfortunately, due to renal remodeling and immunosuppressive therapy, renal transplant recipients are at high risk of developing infections, which can lead to organ damage, loss of the kidney, or even death[5,8]. More than 10% of all kidney transplant recipients develop bacterial infections, of which between 5% and 50% are caused by *K. pneumoniae* [5,15]. Antibodies play an important role in the immune defense, but many solid organ transplant recipients have a reduced antibody response against viral infections and vaccination[8,9,16–19]. However, our results indicate that kidney transplant patients can elicit an antibody response to *K. pneumoniae* infections. Although the antibodies were able to activate the complement system *in vitro*, it remains unclear if these responses were also protective in the patients against invading *K. pneumoniae* strains. Here we only examined two patients, and it is not yet possible to make predictions for response to bacterial infections in the lager solid organ transplant recipient population, this study gives

an indication that kidney transplant patients are able to elicit an antibody response against bacterial infections.

Overall, we have shown that combining clonal antibody profiles with antibody binding data can be used to characterize the antibody response to bacterial infections, and that kidney transplant patients are able to generate antibodies that activate the immune system in response to *K. pneumoniae* infections.

Methods

Patient EDTA-plasma, serum and reagents

Patients that received a renal transplantation between 2015 and 2019 were asked to participate in a biobank study to evaluate immunological developments post-renal transplantation. The study was approved by the local Biobank Research Ethics Committee (protocol 15-019). Participants provided written informed consent to collect clinical data and EDTA-plasma samples pre- and post-transplantation, which were stored at -80 °C until use. From this larger cohort, two patients who developed a *K. pneumoniae* bloodstream infection post-transplantation were included in the current study. Normal human serum (NHS) was prepared as described before [20]. In short, blood was drawn from healthy volunteers after informed consent was obtained from all subjects. Approval was obtained from the medical ethics committee of the University Medical Center Utrecht, The Netherlands. Blood was allowed to clot, and centrifuged to separate serum from the cellular fraction. Serum of 15-20 donors was pooled and stored at -80 °C. Heat inactivation (Hi) of EDTA-plasma was achieved by incubating EDTA-plasma at 56 °C for 30 minutes. RPMI (ThermoFisher) supplemented with 0.05% human serum albumin (HSA, Sanquin), further referred to as RPMI buffer, was used in all experiments, unless otherwise stated.

Bacterial strains

The *Klebsiella pneumoniae* clinical isolates M6193 and N1249, infecting the renal transplant patients 1 and 2 respectively, were collected during routine diagnostics in the medical microbiology department in the University Medical Center Utrecht, The Netherlands. For the experiments with *Staphylococcus aureus*, the laboratory strain Newman was used with the *spa* and *sbi* genes inactivated to prevent non-specific IgG binding [6].

Bacterial growth

For all experiments, *K. pneumoniae* was cultured on Lysogeny broth (LB) 1.5% agar plates, and *S. aureus* on Todd Hewitt broth (TH) 1.5% agar plates, at 37 °C, unless stated otherwise. Single colonies were picked and cultured overnight in liquid LB or TH medium at 37 °C while shaking. The following day the bacteria were subcultured by diluting the overnight culture 1/100 in fresh medium and grown to OD_{600}= 0.4-0.5 at 37 °C while shaking. Bacteria were washed twice with RPMI buffer by centrifugation at 10,000 g for two minutes and resuspended to OD_{600}= 0.5 in RPMI buffer.

Antibody deposition

Bacteria (OD_{600}= 0.05) were incubated with heat-inactivated EDTA-plasma diluted in RPMI buffer for 30 minutes at 4 °C under shaking conditions. Bacteria were washed twice by centrifugation (5 minutes, 4 °C, 2424 g) with RPMI buffer, resuspended in 1 µg/ml goat antihuIgGPE (2040-09, SouthernBiotech), 1 µg/ml goat antihuIgAAF647 (2052-31, SouthernBiotech) and 2 µg/ml goat antihuIgMFITC (2020-02, SouthernBiotech) for 30 minutes at 4 °C while shaking. Bacteria were washed twice with RPMI buffer and fixated in 1.5% paraformaldehyde in PBS for at least five minutes. Binding was assessed by flow cytometry.

Generation of IgG1 and IgA1 profiles via Liquid Chromatography – Mass Spectrometry

Generation of IgG1 and IgA1 profiles was performed as previously described [1–3,7]. Briefly, IgG and IgA were captured from 1030 µl EDTA-plasma per condition using CaptureSelect FcXL or CaptureSelect IgA affinity matrix, respectively. After binding and washing, Fabs were released using IgdE or SialEXO + OgpA Ig proteases for IgG1 and IgA1, respectively. Collected Fabs were separated using reverse phase liquid chromatography, directly followed by intact-level mass spectrometry analysis. Two internal references (IgG1: trastuzumab and alemtuzumab, IgA1: 7D8-mIgA1 and 5D5-mIgA1) were spiked into the EDTA-plasma samples as internal controls. Raw data was processed by sliding window deconvolution using the ReSpect algorithm in BioPharma Finder version 3.2 (Thermo Fisher). Data analysis was performed using an in-house Python notebook as previously described [3,4].

Depletion of *K. pneumoniae*-specific antibodies from NHS and EDTA-plasma

Depletion of *K. pneumoniae*-specific antibodies from NHS was performed as previously described [21]. Briefly, freshly cultured bacteria (OD_{600}= 1.0) were incubated in ice cold

NHS (20% in RPMI buffer). After a 10-minute incubation on ice while shaking, bacteria were pelleted in a cooled centrifuge for 2 minutes at 10.000 g. The supernatant was collected as *K. pneumoniae* antibody depleted NHS. The depletion steps were performed trice in total. Antibody depletion was verified via flow cytometry. NHS depleted of *K. pneumoniae* specific antibodies will be further referred to as ΔNHS. Depletion of M6193-specific antibodies form heat-inactivated EDTA-plasma of patient 1 (t=190) was performed similar to NHS, with the differences that the depletion was performed using 100% EDTA-plasma and a total of five depletion rounds were performed. Specificity of the depletion was confirmed by measuring antibody binding to M6193 and *S. aureus* Newman *Δspa Δsbi* by flow cytometry.

Complement deposition

Freshly cultured bacteria (OD_{600}= 0.05) were incubated with heat-inactivated EDTA-plasma diluted in RPMI buffer (30 minutes, 4 °C, 600rpm), and washed twice by centrifugation (5 minutes, 4 °C, 2424 g). Bacteria were resuspended and incubated in ΔNHS diluted in RPMI buffer (30 minutes, 600rpm, at 37 °C). After washing twice, bacteria were incubated with mouse anti-C3b-AF647 (bH6, produced in house, Heesterbeek 2019) (30 minutes, 4 °C, 600rpm), washed twice again and fixated with 1.5% PFA. Fluorescence was detected via flow cytometry using a FACSVerse instrument (BD), acquiring 10,000 events per condition. Bacteria were gated based on forward and side scatter. Flow cytometry data was analyzed in FlowJo 10.9.0.

Phagocytosis of *K. pneumoniae* by human neutrophils

Human neutrophils were isolated by density gradient as previously described[22]. *K. pneumoniae* M6193 and N1249 were fluorescently labelled using fluorescein isothiocyanate (FITC). To this end, freshly cultured *K. pneumoniae* were washed twice by centrifugation (5 minutes, 4 °C, 2424 g) in 0.1 M $NaHCO_3$ pH 8.5, and incubated with 0.5 mg/ml FITC in 0.1 M $NaHCO_3$ pH 8.5 for 1 hour on ice. The labelled bacteria were washed three times by centrifugation (5 minutes, 4 °C, 2424 g) in RPMI buffer, and counted via flow cytometry (MACSQuant, Miltenyi Biotech).

For FcγR phagocytosis, 7.5 x 10^5 bacteria were incubated with heat-inactivated EDTA-plasma diluted in RPMI buffer. For FcγR+CR phagocytosis, this was supplemented with 3% ΔNHS diluted in RPMI buffer. After incubation (15 minutes, 37 °C, 750 rpm), 7.5 x 10^4 human neutrophils were added, and incubated for another 15 minutes at 37 °C while shaking. Samples were fixated with 1.5% PFA and phagocytosis was measured

via flow cytometry using a FACSVerse instrument (BD), acquiring 10,000 events per condition. Neutrophils were gated based on forward and side scatter. Flow cytometry data was analyzed in FlowJo 10.9.0.

Data analysis and statistical testing

Unless stated otherwise data collected as three biological replicates and analyzed using GraphPad Prism version 9.4.1 (458).

Author contributions

S.P.A.v.d.L., S.H.M.R., B.W.B., M.A.d.B and A.J.R.H. conceived the project. PJ.A.H. and A.D.v.Z. selected patients for the study. PJ.A.H. collected the bacterial isolates. S.P.A.v.d.L. and H.H. performed antibody deposition assays and plasma depletions with bacteria. M.A.d.B. and A.B. performed the mass spectrometry analyses. M.R. performed the complement deposition and phagocytosis assays. S.P.A.vdL., B.W.B. and S.H.M.R. wrote the manuscript. M.A.d.B., A.J.R.H and A.D.v.Z. proofread the manuscript.

Acknowledgments

This work was supported by the Netherlands Organization for Scientific Research (NWO) through a TTW-NACTAR Grant #16442 (to S.P.A.v.d.L., S.H.M.R., M.A.d.B and A.J.R.H.) The funders had no role in the study design, data collection and analysis, or preparation of the manuscript.

Competing interests

The authors declare no competing interests.

References

1. Bondt, A., Dingess, K. A., Hoek, M., van Rijswijck, D. M. H. & Heck, A. J. R. A direct MS-based approach to profile human milk secretory immunoglobulin A (IgA1) reveals donor-specific clonal repertoires with high longitudinal stability. *Front. Immunol.* **12**, (2021).
2. Dingess, K. A. *et al.* Identification of common and distinct origins of human serum and breastmilk IgA1 by mass spectrometry-based clonal profiling. *Cell Mol. Immunol.* **20**, (2023).
3. Bondt, A. *et al.* Human plasma IgG1 repertoires are simple, unique, and dynamic. *Cell Syst.* **12**, (2021).
4. van Rijswijck, D. M. H. *et al.* Discriminating cross-reactivity in polyclonal IgG1 responses against SARS-CoV-2 variants of concern. *Nat. Commun.* **13**, (2022).
5. Krawczyk, B., Wysocka, M., Michalik, M. & Gołębiewska, J. Urinary tract infections caused by *K. pneumoniae* in kidney transplant recipients – epidemiology, virulence and antibiotic resistance. *Frontiers in Cellular and Infection Microbiology* **12**, (2022).
6. Sibbald, M. J. J. B. *et al.* Synthetic effects of secG and secY2 mutations on exoproteome biogenesis in *Staphylococcus aureus*. *J. Bacteriol.* **192**, (2010).
7. Peng, W. *et al.* Direct mass spectrometry-based detection and antibody sequencing of monoclonal gammopathy of undetermined significance from patient serum: a case study. *J. Proteome Res.* **22**, 3022–3028 (2023).
8. Eckerle, I., Rosenberger, K. D., Zwahlen, M. & Junghanss, T. Serologic vaccination response after solid organ transplantation: a systematic review. *PLoS One* **8**, (2013).
9. Chavarot, N. *et al.* Decline and loss of anti–SARS-CoV-2 antibodies in kidney transplant recipients in the 6 months following SARS-CoV-2 infection. *Kidney International* **99**, (2021).
10. Kobayashi, S. D. *et al.* Antibody-mediated killing of carbapenem-resistant ST258 *Klebsiella pneumoniae* by human neutrophils. *mBio* **9**, (2018).
11. DeLeo, F. R. *et al.* Survival of carbapenem-resistant *Klebsiella pneumoniae* sequence type 258 in human blood. *Antimicrob. Agents Chemother.* **61**, (2017).
12. Krieger, A. K. *et al.* Porcine iucA+ but rmpA- *Klebsiella pneumoniae* strains proliferate in blood of young piglets but are killed by IgM and complement dependent opsonophagocytosis when these piglets get older. *Vet. Microbiol.* **266**, (2022).
13. Jager, K. J. *et al.* A single number for advocacy and communication-worldwide more than 850 million individuals have kidney diseases. *Nephrology Dialysis Transplantation* **34**, (2019).
14. Liyanage, T. *et al.* Worldwide access to treatment for end-stage kidney disease: A systematic review. *The Lancet* **385**, (2015).
15. Vidal, E. *et al.* Bacterial urinary tract infection after solid organ transplantation in the RESITRA cohort. *Transplant Infectious Disease* **14**, (2012).
16. Burack, D. *et al.* Prevalence and predictors of SARS-CoV-2 antibodies among solid organ transplant recipients with confirmed infection. *American Journal of Transplantation* **21**, (2021).
17. Magicova, M. *et al.* Humoral response to SARS-CoV-2 is well preserved and symptom dependent in kidney transplant recipients. *American Journal of Transplantation* **21**, (2021).
18. Korth, J. *et al.* Impaired humoral response in renal transplant recipients to SARS-CoV-2 vaccination with bnt162b2 (Pfizer-biontech). *Viruses* **13**, (2021).
19. Marion, O. *et al.* Safety and immunogenicity of anti-SARS-CoV-2 messenger RNA vaccines in recipients of solid organ transplants. *Annals of Internal Medicine* **174**, (2021).

20. Heesterbeek, D. A. *et al.* Bacterial killing by complement requires membrane attack complex formation via surface-bound C5 convertases. *EMBO J.* **38**, e99852 (2019).
21. Van der Lans, S. P. A. *et al.* Colistin resistance mutations in *phoQ* can sensitize *Klebsiella pneumoniae* to IgM-mediated complement killing. *Scientific Reports,* **13**, 12618 (2023).
22. Bestebroer, J. *et al.* Staphylococcal superantigen-like 5 binds PSGL-1 and inhibits P-selectin-mediated neutrophil rolling. *Blood* **109**, (2007).

Supplementary information

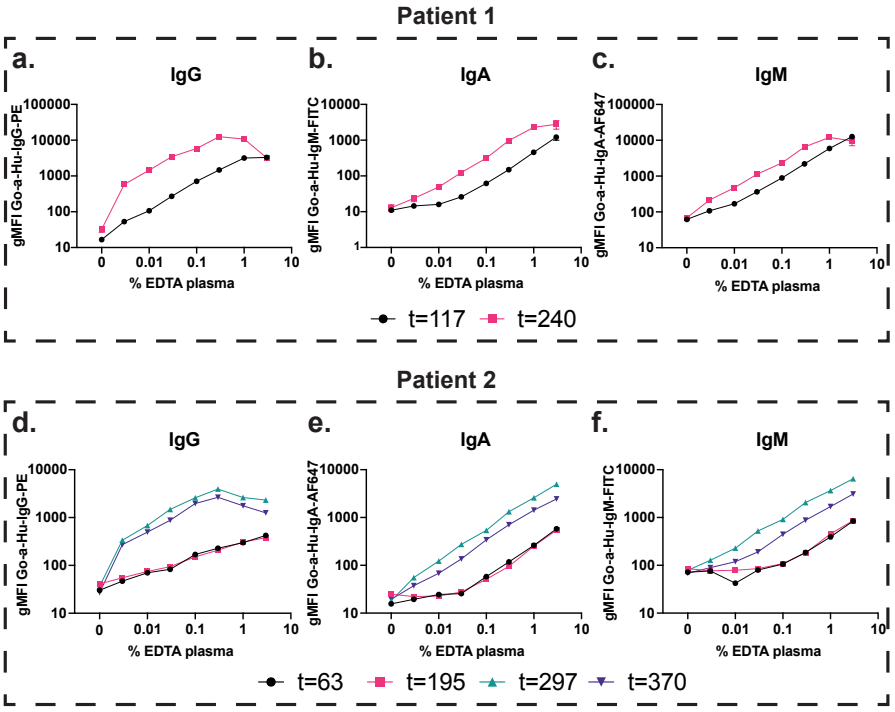

Supplementary figure 1

(**a-c**) Dose-response total IgG (a), IgA (b) and IgM (c) binding to M6193 in post-infection plasma of patient 1. (**d-f**) Dose-response total IgG (d), IgA (e) and IgM (f) binding to N1249 in pre-infection (t=63&195) and post-infection (t=297&370) plasma of patient 2. (**a-f**) Antibody binding was detected using anti-hu-IgG-PE, anti-hu-IgA-AF647 or anti-hu-IgM-FITC by flow cytometry. Flow cytometry data are represented by geometric mean fluorescent intensity (gMFI) values of bacterial populations.

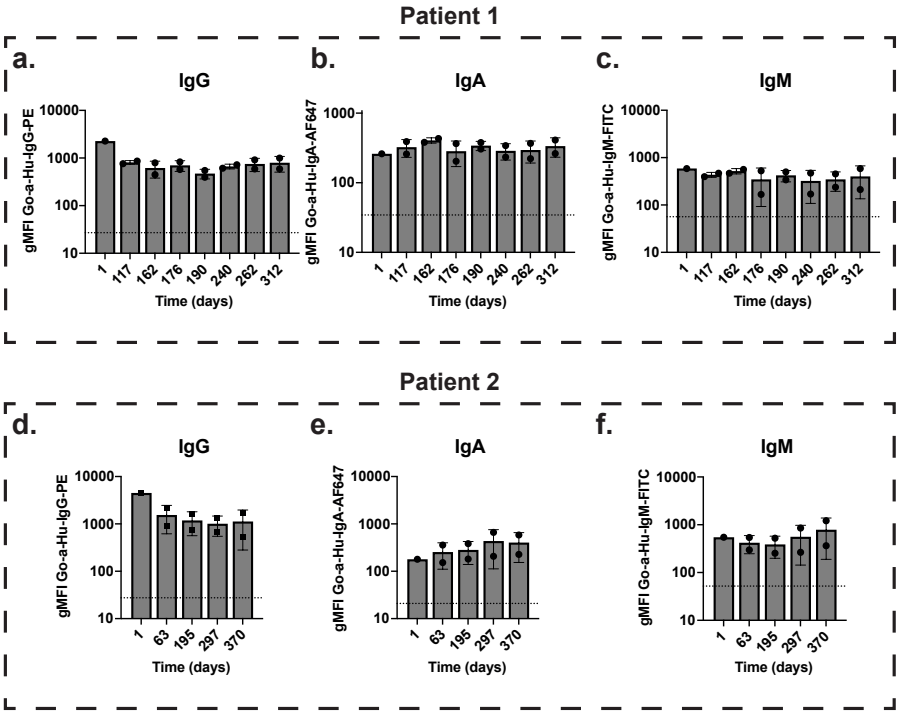

Supplementary figure 2

(**a-f**) Antibody binding to *S. aureus* Newman *ΔspaΔsbi* in the plasma of patient 1 (a-c) and patient 2 (df), respectively. Binding of IgG (a&d), IgA (b&e) and IgM (c&f) were measured in 0.1%, 0.3% and 0.3% plasma, respectively. Antibody binding was detected using anti-hu-IgG-PE, anti-hu-IgA-AF647 or anti-hu-IgM-FITC by flow cytometry. Flow cytometry data are represented by geometric mean fluorescent intensity (gMFI) values of bacterial populations. Data represent mean ± standard deviation of two independent experiments.

Chapter 5

General discussion: How antibodies and complement could be used to treat *Klebsiella pneumoniae* infections

Sjors van der Lans

The increasing prevalence of antibiotic resistant *Klebsiella pneumoniae* poses a major threat to global public health. *K. pneumoniae* is the third leading cause of antibiotic resistance associated deaths worldwide and treating infections with antibiotic resistant *K. pneumoniae* is challenging [1–3]. Due to the antibiotic resistance threat, the demand for novel antibacterial therapies is rising. A potential alternative for antibiotics could be the use of human monoclonal antibodies. In the past, antibodies have been effectively used to prevent and treat bacterial infections, either indirectly via vaccination or directly via intravenous immunoglobulin (IVIG) therapy [4]. More recently, monoclonal antibodies have been successfully introduced in the clinic to treat other diseases such as cancer [5,6]. Antibodies are highly specific and can exert protection against bacterial infections via several mechanisms such as neutralization of bacterial toxins or prevention of bacterial adhesion [7,8]. Importantly, antibodies that bind bacterial surface antigens have the potential to activate the complement system, which exerts various effector mechanisms. This makes antibody-mediated complement activation ideal for clearing bacterial infections. The use of complement-enhancing monoclonal antibodies might be a potential treatment option for infections caused by *K. pneumoniae* and other bacteria. However, this requires a thorough understanding of the interactions between antibodies, *K. pneumoniae* and the complement system. But there are several gaps in our current understanding. For instance, it is unclear which antigens should be targeted by antibodies, or what complement effector functions should be induced. In this thesis we explored how human antibodies activate the complement system on *K. pneumoniae*. For this, we used both polyclonal antibodies form healthy individuals and patients that suffered from *K. pneumoniae* infection as well as newly identified monoclonal antibodies recognizing various antigens.

The antigen matters

In this thesis, we have demonstrated that the antigenic target is an important determinant of antibody-dependent complement activation on Klebsiella. In chapter 3, we observed that anti-O2-antigen antibodies activated complement strongly, whereas anti-capsule antibodies binding to the same *K. pneumoniae* strain did not. We also found that the complement activation potential of anti-O1-antigen antibodies varied strongly between clones. This indicated that differences between epitopes on the same antigen can influence complement activation. Furthermore, in chapter 2 we showed that activation of the classical pathway via polyclonal antibodies critically depended on the recognition of a specific surface antigen that was available on a complement sensitive strain, but not on its complement resistant isogenic parental

strain. Unfortunately, we were unable to determine the target of the complement activating IgM in chapter 2.

Ideally, therapeutic monoclonal antibodies should target conserved surface antigens that are accessible throughout the entire bacterial infection cycle. For *K. pneumoniae*, these potentially include surface proteins such as outer membrane proteins, porins and transporter proteins [9]. However, targeting surface proteins could be complicated, as surface polysaccharides, such as the O-antigen and capsule, can prevent antibodies and complement from reaching these surface antigens [10–14]. Other potential targets could be antigens that are involved in virulence, such as siderophore receptors or adhesins [15–18]. In addition to activating the immune system, these antibodies might be able to block iron uptake, which is critical for the metabolism of *K. pneumoniae*, or prevent colonization by blocking bacterial tissue adhesion. Furthermore, targeting bacteria with complement activating antibodies during an infection is disadvantageous to the bacterium. Therefore, it will generate an adaptive pressure to alter or lose the antigen. In the case of virulence factors, this could result in a reduction in virulence of *K. pneumoniae* [19]. This is comparable to what we have observed in chapter 2, where development of colistin resistance increased the susceptibility of *K. pneumoniae* to MAC-mediated killing.

Next to surface proteins, the O-antigen and capsule are also potential targets for complement-enhancing antibodies. However, efficiently targeting of the capsule will be complicated as over seventy K-types have been described, without any preference for specific K-types among strains causing hospital acquired infections[20–23]. In contrast, hypervirulent *K. pneumoniae* causing community acquired infections almost exclusively express K1 or K2, making these K-types interesting antibody targets for this group of concerning *K. pneumoniae* strains[24–27]. The anti-capsule antibodies we identified were unable to induce complement activation (chapter 3). If this is the case for antibodies against other K-types remains to be determined, but the inability to activate the complement system might restricts their therapeutic use.

Several of the anti-O-antigen antibodies we identified were potent activators of the complement system and complement-mediated phagocytosis (chapter 3). As the majority of *K. pneumoniae* infections are caused by strains either expressing the O1, O2 or O3-antigen[20,28], targeting these O-antigens could already provide substantial benefit to the treatment of *K. pneumoniae* infections. Therefore, we believe that the

focus should be on developing multivalent therapies that utilized antibodies targeting these O-antigens.

Immunological effector functions

To use antibodies to treat bacterial infections, it is important that antibodies activate effector functions. Antibody-mediated complement activation can induce several effector functions, including complement-depended phagocytosis by neutrophils (chapter 3 & 4) and direct killing of bacteria via MAC formation (chapter 2 & 3). We observed that MAC formation can be very effective at killing *K. pneumoniae,* killing >99% of the bacterial population (chapter 2). However, many clinical *K. pneumoniae* strains are MAC resistant (chapter 2), whereas they can be killed by neutrophils (chapter 3). Neutrophils can recognize IgG-bound bacteria via Fc-receptors as well as complement opsonized bacteria via complement receptors, which is important for clearance of *K. pneumoniae* during infections [29,30]. Others and we have shown that antibody-induced complement-dependent phagocytosis of *K. pneumoniae* is more effective compared to phagocytosis induced by antibodies alone (chapter 4) [29–33]. Therefore, antibacterial therapeutic antibodies should be able to activate complement-mediated phagocytosis and killing of *K. pneumoniae* by neutrophils.

The ability of an antibody to exert certain effector functions is dependent on the Fc-region of the antibody isotype. For example, IgM is known to be a far more potent complement activator than IgG [34], and it might therefore be beneficial to use anti-*K. pneumoniae* IgM therapeutically. In chapter 2, we found that IgM of healthy individuals could induce MAC-mediated permeabilization of MAC-sensitive *K. pneumoniae* in serum, whereas IgG did not. However, on MAC-resistant *K. pneumoniae,* capsule could prevent IgM from binding bacterial surface antigens, which would complicate therapeutic use of IgM. In chapter 3, we have focused on IgG1 antibodies, but previous work in our group has indicated that IgG3 might be better suited as anti-bacterial therapeutic antibody. IgG3 is not only a more potent activator of the complement system, but could also be beneficial to uses against bacteria that specifically evade IgG1 [35 36].

Besides the isotype, antibody effector functions can be influenced by specific mutations in the Fc region. The complement activation potential of IgG1 antibodies can be increased by introducing hexamerization enhancing mutations [37,38]. These mutations might be beneficial for anti-capsule antibodies, as we observed that these had very

poor complement activating activity (chapter 3). Introducing hexamerization enhancing mutations in IgG1antibodies targeting the capsule of *S. pneumoniae,* could strongly improve complement activating capacity and protection in murine infection models [37,39].

Discovering potent antibodies

In this thesis, we used several approaches to identify novel antibodies against *K. pneumoniae*. In chapter 3, we used B cell receptor sequencing to successfully identify novel monoclonal antibodies targeting *K. pneumoniae.* The variety of surface antigens being targeted was limited to the O-antigen and the capsule. In the future we hope to find antibodies against additional antigens as well. We think that a major obstacle during B cell selection was shielding of surface structures by the O-antigen and capsule. This might be overcome by using mutant strains that lack the O-antigen and capsule. Other adaptations to the B cell selection could be the use of clinically relevant *K. pneumoniae* isolates to find antibodies against these strains. Furthermore, multiple *K. pneumoniae* could be combined in a B cell stain to identify more broad-reactive antibodies.

In the future it might be possible to identify anti-bacterial antibodies from serum directly via protein sequencing. This could circumvent some of the issues that arise when sorting B cells, such as shielding of surface structures by capsule and the O-antigen. In chapter 4, we used mass spectrometry techniques to identify antibody clones that recognized *K. pneumoniae* in serum directly. Although we could characterize the antibody responses to *K. pneumoniae* on a clonal level, but we were not able to sequence individual antibody clones. However, advances in *de novo* sequencing of antibody molecules via mass spectrometry [40] might make it possible to determine the sequences of anti-bacterial antibodies from serum directly. However, the major difficulty for anti-bacterial antibody discovery by mass spectrometry remains the limited detecting of low abundant antibodies, as we observed in chapter 4.

Using a different source of B cells might help to improve the antibody section process. Although we observed that healthy individuals possess both circulating antibodies and B cells targeting *K. pneumoniae* surface antigens (chapter 2 & 3), the specificity of antibodies will depend on the antigens that have previously been encountered by an individual (chapter 4). Healthy individuals have a high chance of encountering commonly expressed antigens, such as the O1- and O2-antigen. But this chance is lower for more diverse antigens such as capsule polysaccharides. Instead of using

B cells from healthy individuals, it can be beneficial to select B cells from convalescent patients using the infectious strain to identify more strain specific antibodies. This could be feasible as we have observed that patients suffering from *K. pneumoniae* infections are able to generate a strain specific antibody response (chapter 4). However, not all patient groups might be suited as a source of B cells, as underlying illnesses and treatments could influence B cell levels.

The limitations of anti-*K. pneumoniae* antibody therapy

There are several hurdles that may need to be overcome before an anti-*K. pneumoniae* monoclonal antibody therapy could be realized. *K. pneumoniae* is a well-recognized stealth pathogen, that prevents immune recognition *in vivo*, but our *in vitro* studies do not consider these defense mechanisms. However, they will influence the effectiveness of antibody therapies. For example, *K. pneumoniae* has been described to form biofilm during infection, which can prevent both antibodies and complement recognition, and hampers clearance by neutrophils[41–43]. In chapter 4, we observed that antibodies form infected patients were able to induce antibody-dependent complement activation on the infectious *K. pneumoniae in vitro* (chapter 4). However, the patients still suffered from infections, indicating that the presence of antibodies in the blood was not sufficient to clear the infection. Evading immune recognition leads to asymptomatic colonization of the urinary tract in many patients[44], which can lead to recurrent bloodstream infections similar to what we observed in chapter 4.

Furthermore, heterogeneity within *K. pneumoniae* populations may make it difficult to effectively target the entire bacterial population. It has been observed that the availability of surface antigens, such as fimbrial subunit MrkA, can be heterogeneous within a clonal population [45]. Additionally, when assessing antibody-mediated C3b deposition of *K. pneumoniae*, we frequently observed heterogeneous C3b-deposition within the bacterial population (fig. 1). It remains unclear why C3b was not deposited on certain bacteria even when they were bound by complement-activating antibodies (fig. 1). Although increasing the antibody or serum concentration did enhance the number of C3b-positive bacteria, part of the population remained C3b-negative. The level of heterogeneous C3b-deposition varied between *K. pneumoniae* strains, but heterogeneity was observed on all strains that have been tested. This was a surprising finding, as C3b was deposited homogeneously among the bacterial populations of other bacterial species we have tested, such as *S. aureus* and *E. coli*. It remains unclear what causes the heterogeneity, but we speculate that it might be due to the inability

of C1 to reach surface-bound antibodies on some of the bacteria. This could be due to differences in capsule expression between different bacteria, as capsule has been described to shield C1 from reaching surface structures [46]. It is not known whether heterogeneous C3b-deposition could occur *in vivo* during an infection, but it might prevent efficient clearance of the entire bacterial population in the body. Therefore, it would be important to investigate this phenomenon, as it may complicate the treatment of *K. pneumoniae* using complement-based therapies.

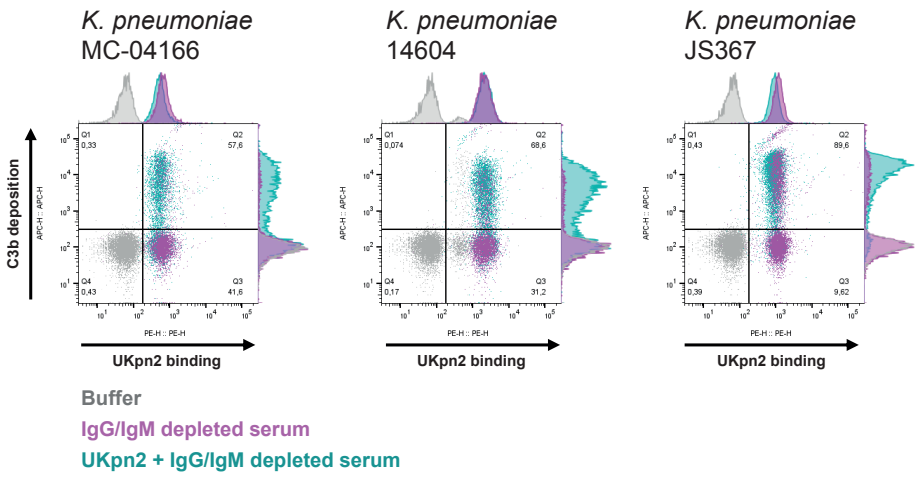

Figure 1| Heterogeneous C3b-deposition on *K. pneumoniae*

O2-expressing *K. pneumoniae* strains MC-04166, 14604, and JS367 were incubated at (37 °C, 30 minutes) in buffer (grey), or 3% IgG&IgM depleted normal human serum in the absence (magenta) or presence of 1 µg/ml anti-O2-antigen antibody UKpn2 (teal). Both C3b deposition and IgG deposition were measured using anti-hu-C3b-AF647 and anti-hu-IgG-PE, respectfully. UKpn2 binds homogeneous to all O2-expressing strains and induces C3b-deposition, although not on all bacteria within the population. Number in Q2 indicates the percentage C3b-positive events in UKpn2 + 1% IgG&IgM depleted normal human serum.

Lastly, during several of our assays we have observed that complement activating antibodies could also inhibit complement mediated functions, such as MAC-mediated killing (fig. 2). The more potently an antibody activated the complement system, the lower the concentration was at which the inhibition occurred. The mechanism behind this inhibition is unknown, but we speculate that these antibodies induce excessive deposition of complement components such as C3b. This could form a thick protein corona around the bacterium that prevents proper insertion of the MAC into the

bacterial outer membrane. We are not the first to report complement inhibition by antibodies, which has been observed for various bacterial species, both in infection models as well as in human patient studies[47]. It is important to keep this effect in mind when studying antibody-mediated complement activation *in vitro* during the development of antibody-based therapies to treat bacterial infections. As we have observed that an antibody can both activate and inhibit complement-dependent effector functions, depending on the antibody concentration, it is important to study monoclonal antibodies in dose-response assays. Although the inhibitory effect could be due to *in vitro* experimental conditions, it might also occur *in vivo*. Several studies have suggested that inhibitory antibodies produced by patients had a negative effect on the bacterial infection[48,49]. Complement inhibition by antibodies could therefore have important implications for antibody-based treatments of infections, as inhibition by antibodies could worsen the infection. Unfortunately, not much is known yet about the mechanisms that cause complement inhibition by antibodies. There are indications that the target might play a role, LPS has often been reported as the target for complement inhibiting antibodies, although other antigens have been reported as well[47].

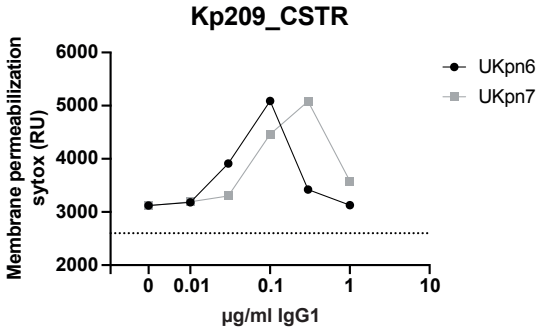

Figure 2| Inhibition of membrane permeabilization by complement activating antibodies
Inner membrane permeabilization of Kp209_CSTR in the presence of 1% bacterium depleted normal human serum (ΔNHS) and varying concentrations of anti-O2-antigen antibodies UKpn6 and UKpn7. Bacteria were incubated at 37 °C in the presence of 1 µM SYTOX green nucleic acid stain, and inner membrane permeabilization (SYTOX fluorescence intensity) was detected after 60 minutes in a microplate reader. Both UKpn6 and UKpn7 are able to induce membrane permeabilization in a dose-dependent manner that correlates with C3b-deposition (chapter 3). However, after a certain concertation of antibodies is reached, membrane permeabilization is inhibited. Dotted line indicates signal in the absence of IgG1 and ΔNHS.

Passive immunization or vaccination

Generating antibodies via vaccination is a proven and effective method to prevent and treat bacterial infections, and should be employed as much as possible. Besides being relatively low cost [50]and providing long-lasting protection, vaccination can induce the production of antibodies of different isotypes[51]. For example, IgM can play a crucial role in complement activation (chapter 2), but the recombinant production of IgM on an industrial scale has severe limitations, and IgM might be too unstable for therapeutic use[52]. Vaccination, however, could elicit production of protective IgM. Additionally, vaccination induces the generation of multiple antibody clones, similar to the antibody responses we have observed for infections with *K. pneumoniae* in chapter 4. The importance of generating various antibody clones was demonstrated in chapter 3. There we combined two anti-capsule antibody clones which strongly improved their complement activating potential. Synergistic protective complement activation has previously been shown to be important for *Streptococcus pneumoniae* and *Neisseria meningitidis* as well [53,54]. Furthermore, targeting multiple different antigens also makes it more complex for bacteria to escape the antibody response, as altering multiple surface antigens simultaneously would be difficult[55–57].

Anti-*K. pneumoniae* vaccines could be beneficial for patients who are at an increased risk of developing an infection in the future, and where there is enough time to elicit a protective antibody response, such as patients with planned surgery. But in those cases where vaccination is not feasible or sufficient, the use of therapeutic monoclonal antibodies provides a valid alternative. A major advantage of monoclonal antibodies over vaccines is that administered antibodies are immediately effective, whereas generating antibodies via vaccination takes days to weeks. This is important in cases of acute infections, such as neonatal sepsis, where the treatment should be acting fast [58]. Furthermore, patients that are unable to generate sufficient antibodies themselves might benefit from monoclonal antibody therapy. These might include patients receiving immunosuppressive therapy as well as patients with B cell or antibody deficiencies. In certain cases, such patients already receive intravenous immunoglobulins (IVIG) prophylactically to protect against infection [4], and monoclonal antibodies might be administered in addition to IVIG. One of the patient groups we expected to benefit from anti-*K. pneumoniae* antibody therapy were kidney transplant patients. These patients are at increased risk of developing infections with *K. pneumoniae* due to the combination of immunosuppressive therapy and a damaged urinary tract[59]. However, we observed that kidney transplant patients could produce *K. pneumoniae*-specific

antibodies in response to infections, indicating that the infection might not have been due to an impaired antibody response (chapter 4). Whether these patients might benefit form therapeutic antibodies remains unclear.

Patients that benefit from anti-*K. pneumoniae* monoclonal antibody therapy could either be treated prophylactically or therapeutically. When a patient has a high risk of developing a *K. pneumoniae* infection in the near future, for instance after surgery, antibodies might be administered prophylactically. However, as not all patients develop *K. pneumoniae* infections, it might be more practical to treat infections when they occur. Furthermore, to adequately use monoclonal antibodies, it is important to ensure that the infectious bacterium is targeted. These could be done by screening the bacterium prior to the treatment, and adjust the specific antibody administered to it. Alternatively, an antibody cocktail could be used that targets the majority of the clinically relevant *K. pneumoniae* strains.

Besides being immediately effective, the use of monoclonal antibodies can have several additional benefits compared to vaccination. For instances, antibodies can be thoroughly characterized to determine their effectiveness. In chapter 3 we have observed that some but not all antibodies targeting the O1-antigen are able to activate the complement system. By determining which antibodies activate the complement system beforehand ensures that complement activating antibodies are administered during treatment. However, it might be more difficult to steer the generation of immune activating antibodies by vaccination. Additionally, recombinantly produced antibodies can be modified to enhance their performance. Ideally, antibodies circulate for a relatively long time in the body, providing durable protection. This can be accomplished by introducing mutations that prolong the half-live of an antibody [60]. Furthermore, mutations could be introduced that improve Fc effector functions such as complement activation potential or Fc receptor interactions [37,61].

As the number of antibiotic resistant *K. pneumoniae* strains rises, infections with these bacteria becomes an increasing risk to human health. To be able to treat infections in the future it is important to understand the interaction between antibodies, *K. pneumoniae* and the complement system. The work presented in this thesis has broadened the current understanding of antibody-mediated complement activation on *K. pneumoniae*, and might benefit in the development of potent antibody-based therapies to treat *K. pneumoniae* infections.

References

1. Murray, C. J. *et al.* Global burden of bacterial antimicrobial resistance in 2019: a systematic analysis. *The Lancet* **399**, 629–655 (2022).
2. Bush, K. *et al.* Tackling antibiotic resistance. *Nature Reviews Microbiology* **9**, 894–896 (2011).
3. Laxminarayan, R. *et al.* Antibiotic resistance-the need for global solutions. *The Lancet Infectious Diseases* **13**, 1057–1098 (2013).
4. Jolles, S., Sewell, W. A. C. & Misbah, S. A. Clinical uses of intravenous immunoglobulin. *Clinical and Experimental Immunology* **142**, (2005).
5. Kretschmer, A., Schwanbeck, R., Valerius, T. & Rösner, T. Antibody isotypes for tumor immunotherapy. *Transfusion Medicine and Hemotherapy* **44**, (2017).
6. Puthenpurail, A., Rathi, H., Nauli, S. M. & Ally, A. A brief synopsis of monoclonal antibody for the treatment of various groups of diseases. *World. J. Pharm. Pharm. Sci.* **10**, (2021).
7. Dumas, E. K. *et al.* Toxin-neutralizing antibodies elicited by naturally acquired cutaneous anthrax are elevated following severe disease and appear to target conformational epitopes. *PLoS One* **15**, (2020).
8. Poolman, J. T. & Hallander, H. O. *Acellular pertussis* vaccines and the role of pertactin and fimbriae. *Expert Review of Vaccines* **6**, (2007).
9. Brinkworth, A. J. *et al.* Identification of outer membrane and exoproteins of carbapenem-resistant multilocus sequence type 258 *Klebsiella pneumoniae*. *PLoS One* **10**, (2015).
10. Merino, S., Camprubi, S., Alberti, S., Benedi, V.-J. & Tomas, J. M. Mechanisms of *Klebsiella pneumoniae* resistance to complement-mediated killing. *Infection and Immunity* **60**, (1992).
11. Ciurana, B. & Tomas, J. M. Role of lipopolysaccharide and complement in susceptibility of *Klebsiella pneumoniae* to nonimmune serum. *Infect. Immun.* **55**, (1987).
12. McCallum, K. L., Schoenhals, G., Laakso, D., Clarke, B. & Whitfield, C. A high-molecular-weight fraction of smooth lipopolysaccharide in *Klebsiella* serotype O1:K20 contains a unique O-antigen epitope and determines resistance to nonspecific serum killing. *Infect. Immun.* **57**, (1989).
13. Domenico, P., Tomas, J. M., Merino, S., Rubires, X. & Cunha, B. A. Surface antigen exposure by bismuth dimercaprol suppression of *Klebsiella pneumoniae* capsular polysaccharide. *Infect. Immun.* **67**, 664–669 (1999).
14. Salo, R. J. *et al.* Salicylate-enhanced exposure of *Klebsiella pneumoniae* subcapsular components. *Infection* **23**, 371–377 (1995).
15. Hsieh, P. F., Lin, T. L., Lee, C. Z., Tsai, S. F. & Wang, J. T. Serum-induced iron-acquisition systems and TonB contribute to virulence in *Klebsiella pneumoniae* causing primary pyogenic liver abscess. *Journal of Infectious Diseases* **197**, (2008).
16. Bachman, M. A. *et al. Klebsiella pneumoniae* yersiniabactin promotes respiratory tract infection through evasion of lipocalin 2. *Infect. Immun.* **79**, (2011).
17. Podschun, R., Sievers, D., Fischer, A. & Ullmann, U. Serotypes, hemagglutinins, siderophore synthesis, and serum resistance of *Klebsiella* isolates causing human urinary tract infections. *Journal of Infectious Diseases* **168**, (1993).
18. Schroll, C., Barken, K. B., Krogfelt, K. A. & Struve, C. Role of type 1 and type 3 fimbriae in *Klebsiella pneumoniae* biofilm formation. *BMC Microbiol.* **10**, (2010).
19. Castledine, M. *et al.* Parallel evolution of *Pseudomonas aeruginosa* phage resistance and virulence loss in response to phage treatment *in vivo* and *in vitro*. *Elife* **11**, (2022).

20. Lam, M. M. C., Wick, R. R., Judd, L. M., Holt, K. E. & Wyres, K. L. Kaptive 2.0: updated capsule and lipopolysaccharide locus typing for the *Klebsiella pneumoniae* species complex. *Microb. Genom.* **8**, (2022).

21. Follador, R. *et al.* The diversity of *Klebsiella pneumoniae* surface polysaccharides. *Microb. Genom.* **2**, (2016).

22. Mbelle, N. M. *et al.* Pathogenomics and evolutionary epidemiology of multi-drug resistant clinical *Klebsiella pneumoniae* isolated from Pretoria, South Africa. *Sci. Rep.* **10**, (2020).

23. Zhang, Z. Y. *et al.* Capsular polysaccharide and lipopolysaccharide O type analysis of *Klebsiella pneumoniae* isolates by genotype in China. *Epidemiol. Infect.* **12**, (2020)

24. Chung, D. R. *et al.* Emerging invasive liver abscess caused by K1 serotype *Klebsiella pneumoniae* in Korea. *Journal of Infection* **54**, (2007).

25. Fung, C. P. *et al.* A global emerging disease of *Klebsiella pneumoniae* liver abscess: Is serotype K1 an important factor for complicated endophthalmitis? *Gut* **50**, (2002).

26. Shon, A. S., Bajwa, R. P. S. & Russo, T. A. Hypervirulent (hypermucoviscous) *Klebsiella pneumoniae*: A new and dangerous breed. *Virulence* **4**, (2013).

27. Yu, W. L. *et al.* Comparison of prevalence of virulence factors for *Klebsiella pneumoniae* liver abscesses between isolates with capsular K1/K2 and non-K1/K2 serotypes. *Diagn. Microbiol. Infect. Dis.* **62**, (2008).

28. Pennini, M. E. *et al.* Immune stealth-driven O2 serotype prevalence and potential for therapeutic antibodies against multidrug resistant *Klebsiella pneumoniae*. *Nat. Commun.* **8**, 1–12 (2017).

29. Satlin, M. J. *et al.* Emergence of carbapenem-resistant Enterobacteriaceae as causes of bloodstream infections in patients with hematologic malignancies. *Leuk. Lymphoma* **54**, (2013).

30. Valdez, J. M., Scheinberg, P., Young, N. S. & Walsh, T. J. Infections in patients with aplastic anemia. *Semin. Hematol.* **46**, (2009).

31. Kobayashi, S. D. *et al.* Antibody-mediated killing of carbapenem-resistant ST258 *Klebsiella pneumoniae* by human neutrophils. *mBio* **9**, (2018).

32. DeLeo, F. R. *et al.* Survival of carbapenem-resistant *Klebsiella pneumoniae* sequence type 258 in human blood. *Antimicrob. Agents Chemother.* **61**, (2017).

33. Serushago, B. A., Mitsuyama, M., Handa, T., Koga, T. & Nomoto, K. Role of antibodies against outer-membrane proteins in murine resistance to infection with encapsulated *Klebsiella pneumoniae*. *J. Gen. Microbiol.* **135**, 2259–2268 (1989).

34. Kauffman, R. C. *et al.* Impact of immunoglobulin isotype and epitope on the functional properties of *Vibrio cholerae* o-specific polysaccharide-specific monoclonal antibodies. *mBio* **12**, (2021).

35. Zwarthoff, S. A. *et al.* C1q binding to surface-bound IgG is stabilized by C1r2s2 proteases. *Proc. Natl. Acad. Sci. USA* **118**, e2102787118 (2021).

36. Cruz, A. R. *et al.* Staphylococcal protein A inhibits complement activation by interfering with IgG hexamer formation. *Proc. Natl. Acad. Sci. USA* **118**, (2021).

37. Diebolder, C. A. *et al.* Complement is activated by IgG hexamers assembled at the cell surface. *Science* **343**, (2014).

38. de Vor, L. *et al.* Monoclonal antibodies effectively potentiate complement activation and phagocytosis of *Staphylococcus epidermidis* in neonatal human plasma. *Front. Immunol.* **13**, (2022).

39. Aguinagalde Salazar, L. *et al.* Promoting Fc-Fc interactions between anti-capsular antibodies provides strong immune protection against *Streptococcus pneumoniae*. *Elife* **12**, (2023).

40. Peng, W. *et al.* Direct mass spectrometry-based detection and antibody sequencing of monoclonal gammopathy of undetermined significance from patient serum: a case study. *J. Proteome Res.* **22**, 3022–3028 (2023).

41. Struve, C., Bojer, M. & Krogfelt, K. A. Identification of a conserved chromosomal region encoding *Klebsiella pneumoniae* type 1 and type 3 fimbriae and assessment of the role of fimbriae in pathogenicity. *Infect. Immun.* **77**, (2009).

42. Rosen, D. A. *et al.* Molecular variations in *Klebsiella pneumoniae* and *Escherichia coli* FimH affect function and pathogenesis in the urinary tract. *Infect. Immun.* **76**, (2008).

43. Vidal, E. *et al.* Bacterial urinary tract infection after solid organ transplantation in the RESITRA cohort. *Transplant Infectious Disease* **14**, (2012).

44. Gołębiewska, J. E. *et al.* Host and pathogen factors in *Klebsiella pneumoniae* upper urinary tract infections in renal transplant patients. *J. Med. Microbiol.* **68**, (2019).

45. Wang, Q. *et al.* Anti-MrkA monoclonal antibodies reveal distinct structural and antigenic features of MrkA. *PLoS One* **12**, (2017).

46. Albertí, S. *et al.* Interaction between complement subcomponent C1q and the *Klebsiella pneumoniae* porin OmpK36. *Infect. Immun.* **64**, (1996).

47. Torres, V. V. L., Coggon, C. F. & Wells, T. J. Antibody-dependent enhancement of bacterial disease: Prevalence, mechanisms, and treatment. *Infect. Immun.* **89**, (2021).

48. Coggon, C. F. *et al.* A novel method of serum resistance by *Escherichia coli* that causes urosepsis. *mBio* **9**, (2018).

49. Wells, T. J. *et al.* Increased severity of respiratory infections associated with elevated anti-LPS IgG2 which inhibits serum bactericidal killing. *Journal of Experimental Medicine* **211**, (2014).

50. Centers for Disease Control and Prevention (CDC). CDC Vaccine Price List. https://www.cdc.gov/vaccines/programs/vfc/awardees/vaccine-management/price-list/index.html (2023).

51. Tarkowski, M. *et al.* Anti-SARS-CoV-2 immunoglobulin isotypes, and neutralization activity against viral variants, according to BNT162b2-vaccination and infection history. *Front. Immunol.* **12**, (2021).

52. Chromikova, V., Mader, A., Steinfellner, W. & Kunert, R. Evaluating the bottlenecks of recombinant IgM production in mammalian cells. *Cytotechnology* **67**, (2015).

53. Gingerich, A. D. *et al.* Synergistic protection against secondary pneumococcal infection by human monoclonal antibodies targeting distinct epitopes. *The Journal of Immunology* **210**, (2023).

54. Natali, E. N. *et al.* Synergic complement-mediated bactericidal activity of monoclonal antibodies with distinct specificity. *FASEB Journal* **34**, (2020).

55. Chakraborty, C., Sharma, A. R., Bhattacharya, M. & Lee, S. S. A detailed overview of immune escape, antibody escape, partial vaccine escape of SARS-CoV-2 and their emerging variants with escape mutations. *Frontiers in Immunology* **13**, (2022).

56. Liu, D. & Shameem, M. Antiviral monoclonal antibody cocktails as a modern weapon in combating pandemics. *Therapeutic Delivery* **13**, (2022).

57. Moellering, R. C. Rationale for use of antimicrobial combinations. *Am. J. Med.* **75**, (1983).

58. Afroza, S. Neonatal sepsis- a global problem: an overview. *Mymensingh medical journal* **15**, (2006).

59. Krawczyk, B., Wysocka, M., Michalik, M. & Gołębiewska, J. Urinary tract infections caused by *K. pneumoniae* in kidney transplant recipients – epidemiology, virulence and antibiotic resistance. *Frontiers in Cellular and Infection Microbiology* **12** (2022).

60. Saunders, K. O. Conceptual approaches to modulating antibody effector functions and circulation half-life. *Frontiers in Immunology* **10**, (2019).

61. Kang, T. H. & Jung, S. T. Boosting therapeutic potency of antibodies by taming Fc domain functions. *Experimental and Molecular Medicine* **51**, (2019).

Closing pages

Nederlandse samenvatting

Het menselijk lichaam is continue in contact met miljarden bacteriën, die op onze huid en in ons darmstelsel leven. In gezonde mensen voorkomt het immuunsysteem dat bacteriën het lichaam kunnen binnendringen. Maar in situaties waarin het immuunsysteem verzwakt is, kan het gebeuren dat het immuunsysteem niet langer in staat is het lichaam te beschermen en kan er een bacteriële infectie ontstaan. Zo zijn mensen met een auto-immuunziekte, kanker of een getransplanteerd orgaan meer vatbaar voor infecties. Om bacteriële infecties te behandelen worden antibiotica gebruikt. Dit zijn medicijnen die bacteriën kunnen doden of hun groei voorkomen. Maar het veelvuldig gebruik van antibiotica kan leiden tot het ontwikkelen van antibioticaresistentie, waardoor bacteriën niet meer gevoelig zijn voor één of meerdere antibiotica. Hierdoor worden infecties met antibioticaresistente bacteriën moeilijk te behandelen, waardoor patiënten kunnen overlijden aan de gevolgen van de infectie.

Klebsiella pneumoniae

Één van de meest problematische antibioticaresistente bacteriën van het moment is *Klebsiella pneumoniae*. Deze bacterie is wereldwijd een van de grootste oorzaken van ziekenhuisinfecties en heeft in de afgelopen decennia een sterke stijging in antibioticaresistentie laten zien. Jaarlijks veroorzaakt *K. pneumoniae* nabij de zevenhonderdduizend antibiotica gerelateerde sterftegevallen. Om infecties met antibioticaresistentie *K. pneumoniae* te behandelen zijn er nieuwe therapieën nodig. Één van de mogelijkheden voor een nieuwe therapie is het gebruik van antilichamen die een specifiek onderdeel van het immuunsysteem, het complementsysteem, activeren.

Antilichamen

Antilichamen zijn eiwitten die in staat zijn om heel specifiek ziekteverwekkers, zoals bacteriën en virussen, te herkennen en vervolgens het immuunsysteem te activeren. De werking van antilichamen hangt samen met hun vorm. Het zijn Y-vormige moleculen met aan het einde van iedere arm een domein dat lichaamsvreemde stoffen (antigenen) kan herkennen. Door de samenstelling van dit bindingsdomein te variëren, kunnen verschillende antilichamen verschillenden antigenen herkennen en binden. De staart van het antilichaam wordt het Fc-domein genoemd. Wanneer een antilichaam een bacterie heeft gebonden, kunnen andere onderdelen van het immuunsysteem het Fc-domein herkennen en de afweerreactie in gang zetten. Het lichaam kan de

samenstelling van het Fc-domein van een antilichaam variëren. De verschillende varianten, isotypen genoemd, activeren het immuunsysteem verschillend.

Antilichamen worden geproduceerd door een bepaald type immuun cellen (B cellen) in reactie op infecties of vaccinatie. Het lichaam bevat een grote verscheidenheid aan unieke B cellen, ook wel B cel klonen genoemd. Elke B cel kloon produceert een uniek antilichaam, wat een monoklonaal antilichaam genoemd wordt (van het Griekse *monos*: één). Elk monoklonaal antilichaam herkent een specifiek antigen. Door de grote verscheidenheid aan B cellen en antilichamen kan het lichaam veel verschillende bacteriën, virussen en andere ziekteverwekkers herkennen. Tegen één bacterie kunnen verschillende monoklonale antilichamen gevormd worden, die verschillende bacteriële antigenen kunnen herkennen. Alle monoklonale antilichamen samen vormen een groep polyklonale antilichamen tegen een bacterie (van het Griekse *polus*: veel).

Het complementsysteem

De binding van antilichamen aan *K. pneumoniae* en andere bacteriën kan onder meer leiden tot de activatie van het complementsysteem. Het complement systeem is onderdeel van het aangeboren immuunsysteem en bestaat uit ongeveer dertig eiwitten die door de bloedbaan circuleren. Ze vormen samen een verdedigingsmechanisme waarin de verschillende complementeiwitten verschillende rollen vervullen. De eerste stam in de activatie van het complementsysteem is herkenning van de bacterie. Dit gebeurt onder meer doordat het complement C1-complex aan de Fc-staarten van bacteriegebonden antilichamen kan binden. Dit leidt tot de ingangzetting van een kettingreactie waarin verschillende complement componenten op het bacteriële oppervlak worden afgezet. Een belangrijk component is C3b, dat herkend kan worden door immuuncellen, zoals neutrofielen. Dit leidt tot activatie van deze immuuncellen, die vervolgens antibacteriële stoffen uitscheiden of de bacterie opnemen (fagocyteren) en intern doden. Daarnaast zorgt complementactivatie voor de vorming van het *membrane attack complex* (membraan aanvalscomplex of MAC), die een porie in het buitenste celmembraan van *K. pneumoniae* kan vormen. Hierdoor kan het complementsysteem *K. pneumoniae* direct doden.

Antilichaamtherapieën tegen *K. pneumoniae?*

In de afgelopen jaren zijn in het laboratorium gemaakte antilichamen therapeutisch succesvol ingezet voor het behandelen van verschillende ziekten, waaronder kanker en auto-immuunziekten. Antilichamen zijn lichaamseigen stoffen, en kunnen daardoor

veilig worden gebruikt zonder dat ze voor bijwerkingen zorgen. Omdat antilichamen in staat zijn het complementsysteem te activeren, zouden ze mogelijk ook gebruikt kunnen worden om infecties met *K. pneumoniae* te behandelen. Maar voordat complement activerende antilichamen gebruikt kunnen worden voor de behandeling van *K. pneumoniae* infecties, is er een grondige kennisbasis nodig van de interacties tussen antilichamen, *K. pneumoniae* en het complementsysteem. Zo is het bijvoorbeeld nog niet volledig bekend tegen welke antigenen antilichamen het best gericht kunnen zijn, of welke complementfuncties geactiveerd moeten worden.

In dit proefschrift hebben we ons tot doel gesteld om te onderzoeken hoe antilichamen het complement systeem op *K. pneumoniae* activeren. Dit hebben we gedaan met behulp van polyklonale antilichamen uit gezonden individuen en patiënten die een *K. pneumoniae* infectie hebben doorgemaakt. Daarnaast hebben we monoclonale antilichamen tegen verschillende *K. pneumoniae* antigenen geïdentificeerd en hun complementactivatie potentieel gekarakteriseerd.

Bevindingen

Antibioticaresistentie zorgt ervoor dat gangbare behandelingen van infecties niet meer mogelijk zijn. Daarnaast is het bekent dat antibioticaresistentie ervoor kan zorgen dat gevoeligheid van bacteriën voor bepaalde onderdelen van het immuunsysteem kan veranderen. In **hoofdstuk 2** hebben we onderzocht wat het effect is van het ontwikkelen van resistentie tegen het antibioticum colistine op de gevoeligheid van *K. pneumoniae* voor het *membrane attack complex* (MAC). Hiervoor hebben we gebruikt gemaakt van colistinegevoelige *K. pneumoniae* stammen die in een evolutieëxperiment in het laboratorium colistineresistent zijn geworden. Van deze stammenparen hebben we de gevoeligheid voor MAC bepaald, waaruit bleek dat twee van de drie colistineresistente stammen gevoeliger waren geworden voor MAC. Één van de stammenparen (Kp209 en Kp209_CSTR) hebben we uitvoeriger bestudeerd. Het bleek dat de colistineresistente stam (Kp209_CSTR) een mutatie had in het *phoQ* gen, waardoor het PhoQ eiwit actiever werd. Deze actievere vorm van PhoQ zorgde ervoor dat de stam zowel colistineresistent als MAC-gevoelig werd. Uitgebreide analyse van complementactivatie op Kp209_CSTR in menselijk bloedserum liet zien dat antilichamen van het IgM isotype cruciaal waren voor complementactivatie op deze stam. Opvallend genoeg bonden deze complementactiverende IgMs niet aan de colistinegevoelige stam, wat liet zien dat colistineresistentie herkenning van *K. pneumoniae* door het immuunsysteem kan beïnvloeden.

Om complementactivatie door antilichamen in detail te bestuderen zijn monoklonale antilichamen tegen verschillende antigenen nodig. In **hoofdstuk 3** hebben we een methode ontwikkeld om antilichamen tegen bacteriën te identificeren. Hierbij maakten we gebruik van geheugen B cellen, die de antilichamen die ze maken aan hun oppervlakte bevestigen als B cel receptoren (BCR). Met de BCRs kunnen geheugen B cellen antigenen aan zich binden. Om *K. pneumoniae* specifieke B cellen te identificeren hebben we *K. pneumoniae* fluorescent (lichtgevend) gelabeld en met menselijke B cellen gemengd. De B cellen die bacteriën bonden, hebben we één voor één gesorteerd met een cel-sorteermachine, om zo de antilichaaminformatie per B cel te verkrijgen. Hierna konden we de antilichamen in het laboratorium namaken en testen. We hebben verschillende *K. pneumoniae* stammen gebruikt (*Kpn*O1 en *Kpn*O2) en in totaal 29 unieke antilichamen gevonden. Alle zeventien antilichamen tegen *Kpn*O1 bonden aan het O1-antigen oppervlaktesuiker. Dertien van deze antilichamen waren in staat om het complementsysteem te activeren. Van de twaalf antilichamen tegen *Kpn*O2 bonden er negen aan het O2-oppervlakte suiker en drie aan de capsule van *Kpn*O2. Alle anti-O2-antilichamen konden het complementsysteem activeren, maar de anti-capsule antilichamen konden dat niet. Dit laat zien dat het antigen van belang is voor het complementactivatie potentieel van een antilichaam. De complementactiverende anti-O1 & O2-antigen antilichamen induceerde ook fagocytose door neutrofielen. Doordat we antilichamen tegen verschillende antigenen van *Kpn*O2 hebben gevonden, konden we antilichamen mengen en het effect hiervan op complementactivatie bestuderen. Hieruit bleek dat wanneer we twee inactieve anti-capsule antilichamen mengde, deze samen in staat waren het complement systeem te activeren. Dit toonde aan dat antilichamen samen kunnen werken om het immuunsysteem efficiënt te activeren.

K. pneumoniae veroorzaakt voornamelijk ziekenhuisinfecties in patiënten met een verzwakt immuunsysteem. Een belangrijke deel hiervan zijn patiënten die een niertransplantatie hebben ondergaan. Door de beschadigingen aan de urinewegen in combinatie met immuunsysteem onderdrukkende medicijnen die deze patiënten krijgen, zijn niertransplantatiepatiënten extra gevoelig voor *K. pneumoniae* infecties. Een van de redenen dat deze patiënten infecties ontwikkelen is dat ze niet goed in staat zijn om antilichamen te produceren in reactie op een infectie. In **hoofdstuk 4** hebben we de polyklonale antilichaamresponse in reactie op een *K. pneumoniae* infectie bestudeerd in twee niertransplantatiepatiënten. Hieruit bleek dat beide patiënten in staat waren om specifieke antilichamen tegen *K. pneumoniae* te genereren. Door

het combineren van *flow* cytometrie en massa spectrometrie waren we in staat om de polyklonale antilichaamresponse tot op het niveau van individuele monoklonale antilichamen in kaart te beregenen. Hieruit bleek dat er meerdere verschillende klonen van verschillende antilichaam isotype werden geproduceerd door de patiënten in reactie op de infectie.

De antilichamen van de patiënten waren in staat om het complementsysteem te activeren en complementafhankelijke fagocytose te initiëren. Ondanks de aanwezigheid van deze antilichamen in het bloed van de patiënten, ondergingen ze toch infecties met *K. pneumoniae,* wat aangeeft dat de aanwezigheid van antilichamen niet per se bescherming garandeert.

Ter conclusie

Het onderzoek gepresenteerd in dit proefschrift heeft laten zien dat de interactie tussen antilichamen, *K. pneumoniae* en het complementsysteem complex is. We hebben geleerd dat het antigen cruciaal kan zijn voor het complementactivatie potentiaal van antilichamen, dat het belangrijk is om complement gemedieerde fagocytose te induceren en dat het combineren van verschillende antilichamen complementactivatie sterk kan bevorderen. Dit proefschrift verbreedt de kennis over antilichaam gemedieerde complementactivatie op *K. pneumoniae* en kan mogelijk bijdragen aan het ontwikkelen van op antilichaam gebaseerde behandelingen van *K. pneumoniae* infecties.

Short English summary

The human body is in constant contact with bacteria and relies on the immune system to ward off infections. Weakened immune defenses make individuals susceptible to bacterial infections. Antibiotics can be used to treat infections but development of antibiotic resistance by bacteria makes treatment of infections increasingly difficult. Combatting infections with antibiotic resistant requires innovative therapies. Utilizing antibodies to activate the immune system emerges as a promising strategy but requires a thorough understanding of the interactions between bacteria, antibodies and the immune system. In this work we aimed to understand the complex interactions between antibodies, *K. pneumoniae* (presently one of the most problematic antibiotic resistant bacteria), and human the complement system (a network of proteins in the blood that plays a crucial role in the immune response).

Antibiotic resistance poses a challenge to conventional infection treatments and can alter bacterial sensitivity to components of the immune system. In **chapter 2**, the impact of developing resistance to the last-resort antibiotic colistin on the sensitivity of *K. pneumoniae* to the membrane attack complex (MAC) was investigated. Colistin-sensitive *K. pneumoniae* strains were evolved in the lab to become colistin-resistant, revealing that two out of three resistant strains became more sensitive to MAC. The in-depth analysis of one strain (Kp209_CSTR) identified an active PhoQ protein due to a mutation in the *phoQ* gene, rendering the strain both colistin-resistant and MAC-sensitive. Examination of complement activation in human blood serum highlighted the crucial role of IgM antibodies in activating complement on this strain, emphasizing how colistin resistance can influence immune recognition of *K. pneumoniae*.

To study complement activation by antibodies in detail, using monoclonal antibodies against various antigens is essential. In **chapter 3**, we developed a method to identify novel antibodies against bacteria. Memory B cells, which express the antibodies they produce on their surface as B cell receptors (BCR), were utilized. By labeling *K. pneumoniae* fluorescently and mixing them with human B cells, bacteria-binding B cells could be individually sorted using a cell sorter. Subsequently, their antibodies were recombinantly expressed and tested. Using different *K. pneumoniae* strains (*Kpn*O1 and *Kpn*O2), a total of 29 unique antibodies were found. All seventeen antibodies against *Kpn*O1 bound to the O1-antigen surface sugar, with thirteen activating the complement system. Among the twelve antibodies against *Kpn*O2, nine bound to

the O2-surface sugar, and three to the *Kpn*O2 capsule. While all anti-O2 antibodies could activate the complement system, the anti-capsule antibodies could not. This underscores the significance of the antigen for the complement activation potential of an antibody. Complement-activating anti-O1 & O2 antigen antibodies also induced phagocytosis by neutrophils. Mixing anti-capsule revealed that these efficiently activate the complement system in a collaborative.

K. pneumoniae primarily causes hospital infections, including in immunocompromised patients who have undergone a kidney transplantation. These patients are at high risk of developing infection due to urinary tract damage and immunosuppressive medications. In **chapter 4**, the polyclonal antibody response to *K. pneumoniae* infection was studied in two kidney transplant patients. We determined that both patients produced specific antibodies against infectious *K. pneumoniae*. Using flow cytometry and mass spectrometry analysis we investigated the polyclonal antibody responses in these patients on a clonal level. We found that both patients were able to elicit a specific antibody response to the infectious bacteria, consisting of various clones. Although the antibodies produced by both patients activated the complement system and initiated complement-dependent phagocytosis, the presence of antibodies did not guarantee protection, as the patients still suffered from *K. pneumoniae* infections.

The research presented in this work reveals the intricate interaction between antibodies, *K. pneumoniae*, and the complement system. Crucially, the antigen's role in the complement activation potential of antibodies was highlighted. It emphasized the significance of inducing complement-mediated phagocytosis and demonstrated that combining different antibodies significantly enhances complement activation. This thesis contributes to expanding knowledge on antibody-mediated complement activation in *K. pneumoniae*, holding potential implications for the development of antibody-based treatments for *K. pneumoniae* infections.

Dankwoord (Acknowledgements)

The greatest joy of my PhD has been the opportunity to meet, befriend and collaborate with so many amazing people. All of you have my greatest gratitude! And there are several people that have made the realization of this thesis possible, and I would like to thank in particular.

Suzan, ik ben je ontzettend dankbaar dat je me de kans hebt gegeven om dit fascinerende onderzoek te mogen doen in het allerleukste lab in Utrecht (en ver daarbuiten). Vanaf de eerste week van mijn stage (toen nog bij Alex en Nina) wist ik dat ik promotieonderzoek wilde doen bij de MMB. En ik ben na al die jaren nog steeds blij de kans te hebben gekregen. Niet dat mijn promotie altijd even gemakkelijk verliep maar jouw vertrouwen, positiviteit en goede zorgen heeft er mede voor gezorgd dat het project een succes is geworden. En zelfs in de recente periode waarin je het zelf moeilijk had, heb je me tot het uiterste gesteund. Daarvoor mijn grootste waardering. **Bart,** als er iemand diep betrokken is geweest bij mijn promotie, dan ben jij het. Het was ontzettend fijn dat ik altijd bij je terecht kon; om na te denken over experimenten, om te filosoferen over hypothesen, of om kleine dingentjes in het lab te bespreken. Zelfs wanneer je dag eigenlijk al overvol zat nam je nog de tijd voor me. Ik heb het ontzettend fijn gevonden om met je samen te mogen werken, heel erg bedankt! **Maartje**, zonder jou zou dit proefschrift zo goed als leeg zijn. Je hebt zo'n ongelofelijke hoeveelheid proeven voor het project gedaan (>200!), waarvan alleen het topje van de ijsberg hier uiteindelijk verschenen is. Zonder jou onvermoeibare inzet zou het project niet zo succesvol zijn geweest. Je bent een van de meest hardwerkende, gemotiveerde en vriendelijke personen die ik ken, en niet alleen essentieel geweest voor mijn promotie maar voor het lab in zijn geheel. Dankjewel! **Priscilla**, we zijn op dezelfde dag aan het grote B cel avontuur begonnen en ik heb zo ontzettend veel van je geleerd. Maar niet alleen dat, je bent ook gewoon een ontzettend gezellig persoon, en ik vind het onwijs gaaf dat we samen antilichamen hebben gevonden!

I would also like to thank prof. dr. **Leendert Trouw**, prof. dr. **Gestur Vidarsson**, prof. dr. **Rob Willems**, prof. dr. **Han Wösten** and dr. **Alex McCarthy** for critically reading my thesis. **Alex** and **Nina**, my adventures at the UMCU started with you. And now the circle is complete with the both of you being part of the opposition during my defense. **Alex**, my internship with you was amazing. Before I started with you, I was not sure whether to continue in sciences, but working together motivated me to go for a PhD position. And

I want to thank you for being great friend for all these years, and years to come. **Jos** en **Kok**, ontzettend bedankt voor jullie onuitputtelijke expertise. **Jos**, jouw scherpe vragen en eigenzinnige invalshoeken dreven mij, en vele met mij, om kritisch naar ons eigen onderzoek te kijken. Maar met een klein grapje wist je spanning weer te verleggen. **Kok**, als ik echt niet meer wist wat ik aan moest met mijn experimenten, dan was jij daar altijd nog met een oplossing. Of het nu kleine handigheidjes waren, of een hele andere aanpak, je advies heeft veel van mijn experimenten beter gemaakt. **Albert** en **Maurits**, bedankt voor de samenwerking de afgelopen jaren. Ondanks dat we geen antilichaam tegen *Klebsiella* hebben gesequenced, zijn er een aantal interessante bevindingen uit onze samenwerking gekomen. Één mooie publicatie is er al, en hopelijk volgen er nog. I had several great collaborations during my PhD. I would like to thank all those who contributed to the **NACTAR** project, in particular **Frank**, **Renoud**, **Janine**, **Erik**, **Loek**, **Michiel**, **Pieter-Jan** en **Titia**. **Manon**, **Ina**, **Kimberly** and **Willem**, thank you for your help and expertise that helped create chapter 2 of this thesis and a great publication. En **Axel**, bedankt voor je *Klebsiella* stammen, ze hebben hun dienst zeker bewezen!

Eva, 1 november 2018 zijn we allebei gestart en samen wegwijs geworden. Het was voor mij ontzettend fijn om iemand te hebben die zo ongeveer in hetzelfde schuitje zat. En nu zijn we allebei klaar! Ongelofelijk! Bedankt voor een fijne tijd. **Remy**, ik heb je eerst student leren kennen, en daarna later fijne collega. Gezellig samen een beetje mopperen het verkeerd gebruik van de assenschaal, en lol hebben in het lab. **Julia**, I was in doubt whether I should write to you in Dutch or Spanish so I settled for English. There never was a dull moment with you around, and I hope you keep wearing your fabulous earring! **Lisanne**, met jou was het nooit saai. Meestal wel in voor een grapje en een grol, en veel lol. Je bent een harde werker, en ik ben vaak onder de indruk geweest van de hoeveelheid werk die je verzetten. Daarnaast heb je een erg goede smaak, dus ik heb me laten inspireren door jou boekje voor het design mijn proefschrift. **Frerich**, wanneer er een WhatsAppberichtje van jou kwam, wist ik hoe laat het was: tijd voor een koffietje. Of een biertje! En ik heb ontzettend genoten van onze gesprekken over interessante taalkwesties, en *Klebsiella* natuurlijk. **Dani**, **Dennis** en **Seline**, toch wel de OC's (original complementologists) van het lab. Toen ik in het lab begon was complement een waar mysterie voor me, maar met jullie hulp ken ik het nu als mijn broekzak. En bedankt voor alle leuke momenten! **Elena**, **Goisia**, **Yuxi**, **Vincent**, **Angelio** and **Sergio**, thanks for instantly making me feel at home in the lab and at the MMB. **Kulsum** & **Marije**, thanks for all the nice moments we shared during the short time that we have been working in the lab together. **Còco** & **Lotte**, al ben

ik op het einde van mijn promotie naar de tweede verdieping gegaan, toch vond ik het erg leuk om met jullie op een kamer te hebben gezeten! And also a big thanks to **Leonardo**, **Rita**, **Astrid**, **Hendrik**, **Patrique**, **Coco**, **Marieke**, **Ninée**, **Matteo**, **Tristan**, **Barath**, **Ruben**, **Jesse**, **Janneke**, **Manon**, **Marco**, **Malbert** ,**Shu**, **Stephanie**, **Andras**, **Rob**, **Guus**, **Lidewij**, **Roos**, **Magda**, **Moniek**, **Ingrid**, **Ad**, **Jannetta**, all others in our group and at the MMB that have made these years very memorable. **Suzanne**, **Hadia**, en **Sebastiaan**, erg leuk dat jullie stage bij mij hebben willen lopen.

Carla, dit hoor je vast vaker, maar heel erg bedankt voor alle eiwitten en antilichamen die je voor me hebt gemaakt! En je bent een ontzettend leuk persoon om in het lab te hebben. **Piet**, bij jou denk ik aan twee dingen: een groot sportman, en een ontzettend secure werken. Wanneer ik een eppje met antilichamen van jou kreeg, wist ik zeker dat ze tiptop in orde waren. Ik ga je leuke woordgrapjes missen. **Erik**, de enige echte Eindhovenaar in het lab. Ondanks dat Brabant goed vertegenwoordigd is in de groep, was jij de enige die met mij de treinrit naar het Zuiden helemaal afmaakte. Ik ga onze gesprekken over bier, brouwen en proeven missen. **Lisette**, jij bent wat mij betreft Utrecht ten top! Bedankt voor al je hulp, de leuke momenten en gezellige borrels! **Anneroos** en **Adinda**, de tijd dat ik tegenover jullie in het lab zat, blijft een van de leukste dingen van werken bij de MMB. **Yvonne**, heel fijn dat je er altijd voor zorgde dat alles op rolletjes liep! **Jelle**, bedankt dat je er altijd was wanneer ik even nodig moest epibreren, voor alle gezellige momentjes, en voor het delen van je oneindige kennis over de natuur.

Paul, onze eerste kennismaking zal ik nooit vergeten. Het was iets in de trant van 'Oh, jij bent diegene die de PCR-agenda verprutst heeft'. Maar dat heeft de pret en de pig squeals niet mogen drukken.

Kaixo **Leire**, unibertsitateko nire gogokoena, uhmm, lagun gogokoena esan nahi dut. Ez, egia esanda, niretzat ohore bat da zure laguna izatea eta gure adiskidetasuna oso garrantzitsua da. Nire doktoradoaren azken urte ez da erraza izan eta, txokolate pixka bat partekatzea, txantxak egitea eta elkar bazkaltzea zoragarria izan da. Zorte handia dut zu lagun eta paraninf izateaz, eta mundu erdiak bananduko gaituen arren, beti egongo zara nire bihotzean! Aguuur! (Irune, eskerrik asko itzulpenagatik)

Julian, you are one of the smartest, kindest and most outgoing people I know! And not only that, but you are also a great scientist and performer! I will never forget the

great talks you have given, and the sexy graphs you have shared with the world! Many thanks for the many nice times we shared, and I look forward to the many to come.

Giel, vanaf het moment dat ik aan mijn promotie begon wist ik dat ik jou als mijn paranimf wilde. Als er iemand is die ik tijdens mijn verdediging aan mijn zijde wil hebben, dan ben jij dat. Onze vriendschap betekent heel veel voor me! Van samen koken, carnaval vieren of weekendjes weg met Sem en Inge, tot diepgaande gesprekken over de politiek, etymologie of essentie van het leven met een Duchesse de Bourgogne erbij, het kan allemaal! Maar ook met de moeilijker dingen kunnen we bij elkaar terecht! **Sem**, je bent de meest stijlvolle bioloog die ik ken! En een hele fijne vriendin, voor Inge en mij. Ik waardeer het enorm dat we het samen altijd zo fijn mogen hebben. Samen met jou Keezen maakt de avond altijd goed, want als team zijn wij (bijna) onverslaanbaar!

Mijn lieve jaarclub, **Firenze**, nu alweer negen jaar samen! **Giel**, **Jens**, **Feylin**, **Midas**, **Hespen**, **Ruben**, **Jelle**, **Hugo en Vork,** ontzettend bedankt voor alle mooie jaren clubeten tijdens mijn promotie. We hebben tijdens onze clubvorming heel bewust voor elkaar gekozen maar het blijft voor mij erg bijzonder dat we nu nog steeds zo betrokken bij elkaar zijn. Ik wil jullie daar allemaal ontzettend voor bedanken. En wat betreft dit proefschrift in het speciaal **Jens**, **Hespen**, **Ruben**, **Jelle** en **Feylin**. **Jens**, je ontwerpen voor de omslag en hoofdstukken zien er fenomenaal uit, ik had er niet blijer mee kunnen zijn. Bedankt voor alle tijd en energie die je erin hebt gestopt, ik waardeer het echt enorm. **Pim**, zonder jouw coding skills had ik Kaptive 2.0 nooit kunnen gebruiken, bedankt voor je hulp. **Ruben**, **Jelle** en **Feylin**, bedankt voor het verduidelijken van mijn Nederlandse samenvatting.

Jim en **Stefanie**, onze lieve vrienden! Ondertussen begint het zelfs al wat meer als familie te voelen, zeker nu wij jullie lieve **Lewis** ook steeds groter zien worden. De warmte en gastvrijheid die we bij jullie ervaren is ongekend. Stefanie, bedankt dat je zo'n fijne vriendin voor mij, en vooral ook voor Inge bent! Jim, ik hoop dat we samen nog veel mooie bodemschatten mogen vinden! Weet dat ik onze vriendschap enorm waardeer en ik jullie ontzettend graag zie!

Lieve **papa**, **mama**, **Liselot**, **Coos**, **Glenn**, **Theo**, **José**, **Luuk**, en **Evy**, ik kan me geen fijnere familie voorstellen, en ik wil jullie heel erg bedankt voor alle steun in al die jaren. Het is niet altijd even makkelijk voor me geweest, maar gelukkig stonden jullie altijd voor me klaar om me er doorheen te helpen. De ene keer met welgemeend advies, de

andere keer met een kom thee of een emmertje soep! Ik weet dat wat er ook gebeurt, ik op jullie kan vertrouwen!

Lieve **Inge**, ons leven is in de afgelopen vijf jaar ontzettend veranderd. In het begin van mijn promotie woonde ik nog in Bunnik en kwam je me elk weekend gezelschap houden. Gelukkig zijn we vrij snel naar Best verhuisd en kregen we al gauw gezelschap van **Tommie** en **Frits**. **Tommie** heeft een grote bijdrage geleverd aan dit proefschrift door me gezelschap te houden tijdens het schrijven en pareltjes zoals deze te tikken door over het toetsenbord te lopen: 8u09cscyt6-0puy9irt%$#####[];””.

Lieve **Inge**, zonder jouw steun had ik dit proefschrift mogelijk niet geschreven. Jij weet als geen ander dat er hele moeilijke perioden voor me bij zaten, en je was soms de enige aan wie ik liet zien hoe lastig ik het vond. Je bent er altijd voor me geweest en ik weet dat je er ook altijd voor me zal zijn. Gelukkig waren het niet alleen maar struggels. Ik wil je heel erg bedanken voor alle geweldige momenten die we samen al hebben meegemaakt. Ik vind het fantastisch dat we zo veel met elkaar kunnen lachen, zo veel waardering voor elkaar hebben en er samen een prachtig leven van maken. Lieve Inge, ik hou van jou.

About the author

Sjors van der Lans was born on January 20th 1995 in Eindhoven, The Netherlands. He graduated his pre-university education (Atheneum) in 2013 at the Eckartcollege in Eindhoven, and started his bachelor Biology in the same year at the Utrecht University. During his bachelor, he focused on molecular biology, microbiology, and evolution. After finishing his bachelor in 2016, Sjors continued is education at Utrecht University, enrolling in the Graduate School of Life Sciences master track Molecular and Cellular Life Sciences (MCLS). In 2016-2017, Sjors performed a research internship in the Lab of prof. dr. Han Wösten at Utrecht University, under the supervision of dr. Martin Tegelaar, studying hyphal growth in *Penicillium chrysogenum*. Sjors continued his training under the supervision of prof. dr. Nina van Sorge and dr. Alex McCarthy at the department of Medical Microbiology at the University Medical Center Utrecht. There he worked on unraveling the interactions between the β-protein *Streptococcus agalactiae* and leukocyte immunoglobulin-like receptors (LILRs) on neutrophils. After graduating, Sjors started his doctoral education in the group of prof. dr. Suzan Rooijakkers at the department of Medical Microbiology at the University Medical Center Utrecht. This doctoral research was part of the NWO NACTAR program, and was performed in collaboration with the group of prof. dr. Albert Heck (Utrecht University), Genmab B.V, and Hycult Biotechnology B.V. Sjors focused on understanding the interactions between human antibodies, *Klebsiella pneumoniae*, and the human complement system. Together with the research team in the UMCU, Sjors developed a new approach to efficiently identify novel human antibodies against bacteria, resulting in discovery of several potent antibodies against *K. pneumoniae.*

List of publications

Related to this thesis:

van der Lans, S.P.A., Janet-Maitre, M., Masson, F.M., Walker, K.A., Doorduijn, D.J., Janssen, A.B., van Schaik, W., Attrée, I., Suzan H. M. Rooijakkers, S.H.M., Bardoel, B.W. Colistin resistance mutations in *phoQ* can sensitize *Klebsiella pneumoniae* to IgM-mediated complement killing. *Sci. Rep.* **13**, 12618 (2023). DOI: 10.1038/s41598-023-39613-5

Peng, W., den Boer, M.A., Tamara, S., Mokiem, N.J., **van der Lans, S.P.A.**, Bondt, A., Schulte, D., Haas, P.-J., Minnema, M.C., Rooijakkers, S.H.M., van Zuilen, A.D., Heck, A.J.R., Snijder, J. Direct Mass Spectrometry-Based Detection and Antibody Sequencing of Monoclonal Gammopathy of Undetermined Significance from Patient Serum: A Case Study. *Proteome Res.* **22(9)**, 3022–3028 (2023) DOI: 10.1021/acs.jproteome.3c00330

van der Lans, S.P.A., Kerkman, P.F., Ruyken, M., de Haas, C.J.C., Baijens, S., Muts, R.M., Scheepmaker, L.M., Aerts, P.C., van 't Wout, M.F.L., Beurskens, F.J., Schuurman, J., Bardoel, B.W., Rooijakkers, S.H.M. Unbiased selection of B cell using intact bacteria identified novel antibodies against *Klebsiella pneumoniae* that synergistically stimulate a potent complement response. *Manuscript in preparation*

Other publications:

Tegelaar, M., **van der Lans G.P.A.**, Wösten H.A.B. Apical but not sub-apical hyphal compartments are self-sustaining in growth. *Antonie Van Leeuwenhoek* **113(5)**, 697-706 (2020). DOI: 10.1007/s10482-020-01383-9